University of Louisville

ThinkIR: The University of Louisville's Institutional Repository

8-2017

Mitochondrial Transcription Factor A's role in heart failure.

George H. Kunkel
University of Louisville

Follow this and additional works at: https://ir.library.louisville.edu/etd

Part of the Cellular and Molecular Physiology Commons

MITOCHONDRIAL TRANSCRIPTION

FACTOR A's ROLE IN HEART FAILURE

B{

George H. Kunkel

B.S., St. John's University

M.S., University of Louisville

A F issertation

Submitted to the faculty of

School of Medicine of vhe University of Louisville

In partial fulfillment of the requirements

for the degree of

Doctor of Philosophy in Physiology and Biophysics

"

""""""""Department of Physiology & Biophysics

University of Louisville

Louisville, Kentucky

August, 2017

MITOCHONDRIAL TRANSCRIPTION

FACTOR A's ROLE IN HEART FAILURE

By

George H. Kunkel

B.S., St. John's University

M.S., University of Louisville

A Dissertation Approved on

July 14th, 2017

by the following Dissertation Committee

_____

Suresh C. Tyagi, Ph.D., Mentor

_____

Dale A. Schuschke, Ph.D.

_____

Claudio Maldonado, Ph.D.

_____

Utpal Sen, Ph.D.

_____

Douglas Borchman, Ph.D

ii

DEDICATION

This dissertation is dedicated to my mother Ms. Marlene Espada and my brothers, Christopher and Nicholas Kunkel, for believing in me throughout my life.

This is also dedicated to the St. John's University McNair Scholar's program for mentoring and guiding me towards pursuing a graduate degree. The McNair Scholar's program has not only changed my life for the better but also continuous to propel thousands of undergraduate students, across the U.S., to pursue their full intellectual potential.

Most especially, I would like to thank my McNair Mentor Dr. Irvin Hirshfield, the McNair Scholars Director Ms. Asnath Gedeon, MA and Vice Provost Dr. Andre McKenzie for their unwavering support.

ACKNOWLEDGEMENTS

ABSTRACT

MITOCHONDRIAL TRANSCRIPTION

FACTOR A's ROLE IN HEART FAILURE

George H. Kunkel

July 14th, 2017

Background: An essential mitochondrial component, Mitochondrial Transcription Factor A (TFAM) is reduced within the failing heart. TFAM maintains regulatory functions of cardiomyocyte physiology and stability. Mitochondrial Transcription Factor A forms a mitochondrial nucleoid anti-oxidant structure and reduces pathophysiological abnormalities to structural and contractile proteins. Overall, this functions to physically stabilize mtDNA. Significant molecular changes such as a loss of TFAM drive pathophysiological concentrations of cytoplasmic Ca^{2+} and reactive oxygen species. Both of these factors induce proteolytic enzymes to degrade the physiological cardiomyocyte. In TFAMs absence, heart function deteriorates and hypertrophic expansion ensues: thereby changing the physiological myocardium to a pathological state. This alteration activates a remodeling cascade leading to cardiomyocyte decline. These maladaptive factors are major players in the pathological and time dependent formation of a failing myocardium.

Heart failure is a leading cause of death in the United States and a multitude of molecular therapeutics individually target Ca^{2+} transporters or inhibit oxidative enzymes. However, the role of TFAM in reducing pathological cardiac remodeling

maladaptive factors remains unclear. Furthermore, the purpose of this study is to assess TFAM's role in inhibiting ROS and Ca^{2+} driven cardiomyocyte remodeling factors.

Methods: In the first set of experiments, we studied the effect of TFAM overexpression vector and Crispr-cas9 knockdown on HL-1 cardiomyocytes. The cells were subjected to oxidative stress through hydrogen peroxide treatment and the analysis was compared to a standard control as well as control treatment groups; Lipofectamine and an empty vector. Molecular analysis of cardiomyocte remodeling factors Calpain1, MMP9 and NFAT4 and Ca^{2+} transporter SERCA2a was assessed via western blotting and immunocytochemistry. Statistical analysis was performed on graphpad prism software.

In the second set of experiments, we studied the effects of aortic banding on TFAM transgenic mice. Trans-aortic constriction surgery with a $27^{1/2}$g needle was performed on 8-10 week old mice. Prior to surgery, echocardiography ultrasound and blood pressure (coda tail cuff method) functional assays were performed and served as a baseline for post-surgical assessment. Eight weeks post-banding, ultrasound of aortic arch perfusion and turbulence were used to assess banding procedure. Cardiac hypertrophy, fibrosis and morphology were assessed via heart weight/body weight ratio, Mason Trichrome and Hematoxylin & Eosin Staining respectively. Molecular

analysis of cardiac remodeling factors; Calpain1, MMP9, NFAT4 and Ca^{2+} transporter SERCA2a were assessed via western blotting and immunohistochemistry.

Results: *In vitro* analysis of remodeling factors reveals that TFAM knockdown induces significant increases in maladaptive factors MMP9, Calpain1 and NFAT4. In HL-1 cardiomyocytes subjected to pathological concentrations of H_2O_2 (mimicking heart failure *in vivo* studies), TFAM overexpression mitigated hypertrophic stimulator and ROS inducer NFAT4 and decreased MMP9 expression. The TFAM transgenic animal model has reduced cardiac hypertrophy and morphology when compared to it's WT surgical counterpart. Molecular analysis shows that TFAM overexpression reduces ROS propagated proteases (MMP9) and hypertrophic factors (NFAT4) in cardiac remodeling. Additionally, it was observed that TFAM overexpression does not increase SERCA2a protein expression and Calpain1 remains high in the TFAM-TG TAC model.

Conclusion: This study reveals that TFAM overexpression plays a vital role in pressure overload heart failure by inhibiting NFAT4 and MMP9. The Ca^{2+} induced Calpain1 pathway is not mitigated by TFAM overexpression in the TAC pressure overload model, but additional Ca^{2+} transporters may be affected by TFAM overexpression. TFAM loss or overexpression shifts the homeostatic balance held within the physiological myocardium.

TABLE OF CONTENTS

LIST OF FIGURES

LIST OF TABLES

CHAPTER I

INTRODUCTION

Pumping around 72 times per minute or over 100,000 times per day for the average resting adult, the physiological heart is the strongest muscle in the human body. The heart's primary function is to enable deoxygenated blood from tissues to pick up oxygen from the lungs and return this newly oxygenated blood back to those tissues. Tissue oxygenation is dependent on a functional myocardium consisting of four working chambers. The first two chambers of the heart, the right atrium and the right ventricle, pump blood through the pulmonary circulatory system. After blood absorbs oxygen in the lungs, this oxygenated blood then cycles through the left atrium and left ventricle and progresses to the tissues via the systemic circulatory system.

To incessantly force blood to even the most distant extremities, the heart must generate a substantial amount of force. However, there are situations in which the workload becomes excessive. These situations are detected by medical professionals via changes in both perfusion and pressure dynamics. As the workload increases in intensity and the heart's normal capabilities grow inadequate, delivery to tissues become limited. To fulfill these new delivery requirements, the heart initiates compensatory adaptations such as hypertrophy, expansion, muscle mass build-up, and

enlargement. This restructuring of the entire heart muscle is denoted as cardiac remodeling. In a chronic situation, cardiac remodeling results in a condition in which the heart's ability to meet the body's demand for blood and oxygen progressively declines. One measure of the heart's ability to pump blood throughout the body is ejection fraction. This measure is defined as the percentage of blood leaving the left ventricle with each heartbeat. Once this value degenerates below 55%, this inefficiency is categorized as heart failure (HF).

HF results from a multitude of agents, including cardiovascular diseases (CVD). HF produced by CVDs is prevalent across the United States, affecting 5.7 million Americans, with a high fatality rate five years post onset (Fig. 1). Associated risk factors for heart failure include hypertension, obesity, high cholesterol, diabetes, and smoking (Shrout, Rudy, and Piascik 2017). Furthermore, a sedentary lifestyle, coupled with a lack of exercise, exacerbates the risk of developing heart failure (Mozaffarian et al. 2016; Pearson-Stuttard et al. 2017).

After the onset of heart failure, the body suffers the effects of cardiac inefficiency. These effects include edema, weight gain, and shortness of breath. Therapeutics such as diuretics, dietary restrictions, and oxygen therapy manage but do not ameliorate the progressive nature of heart failure. The root to intrinsically changing a pathological myocardium into a more efficient pumping organ remains at the molecular level.

Factors Influencing Pathological Cardiac Remodeling

MMPs

Heart failure is a multifaceted disease state encompassing a variety of significant changes to structural/contractile proteins and the extracellular matrix (Hammerling and Gustafsson 2014). The extracellular matrix of cardiomyocytes, or the cardiac matrix, serves as a physical scaffolding to support the structural and functional integrity of the myocardium. It provides a microenvironment for mechanical, cellular, and molecular activities and is crucial to supporting the physiological myocardium. MMPs and their respective TIMPs (tissue inhibitors of metalloproteinases) regulate matrix degradation, which affects cardiac fibrosis and performance (Mishra et al. 2013).

Cardiac fibrosis is the abnormal thickening of myofibers by increasing collagen density within the myocardial tissue. This is caused by increased proliferation of cardiac fibroblasts, which induces connective tissue up-regulation. Cardiac fibrosis leads to heart failure (Fan et al. 2012). Fibrotic regions within the injured myocardium create cardiac stiffening, decreasing ventricular elastance (Kawaguchi et al. 2003). The ratio of the two major fibrous macromolecules collagen and elastin found within the cardiac matrix affects myocardial force. Cardiac ECM collagen/elastin ratio changes in the course of cardiomyopathies such as heart failure, during which MMPs are significantly increased.

In myocardial tissue damage, enhanced oxidative stress leads to remodeling of the extracellular matrix. At pathological levels, reactive oxygen species (ROS)

concentrations induce apoptosis, myocyte hypertrophy, and interstitial fibrosis by activating matrix metalloproteases (MMPs) (Spinale et al. 1998; Siwik et al. 1999). MMPs degrade a wide spectrum of extracellular proteins that lead to remodeling of the matrix (Vu and Werb 2000). The degradation of extracellular proteins provides an abnormal microenvironment of matrix, in which the myocytes interact. The MMPs degrade collagen and elastin in the matrix. In heart failure, collagen is replaced faster than elastin, altering the collagen/elastin ratio (Tyagi 1998; Weber et al. 1994; Mujumdar, Smiley, and Tyagi 2001). Collagen deposition decreases the tensile strength of the ventricular walls, leading to dilated cardiomyopathy.

MMPs are zinc-dependent endopeptidases, capable of degrading the extracellular matrix (ECM), resulting in cardiac remodeling. This family of proteases has two well-studied members within the cardiac system: MMP2 and MMP9 play a role in heart failure. This family of proteases is recognized for its involvement in cardiac remodeling and atherosclerotic plaque formation. Mittal et al noted two genetic polymorphisms involved in the development of coronary artery disease, a factor in heart failure (HF) (Mittal et al. 2014). Molecular mechanisms that promote anabolic cascades involving MMP 2 & 9 are reduced with increased TIMP expression (Frati et al. 2015).

Polyakova et al. studied collagen metabolism and MMP/TMP activity. Analysis of failing human hearts revealed that specific MMPs are associated with particular types of heart failure. Although MMP 2 & 9 had increased levels in all cardiomyopic states (dilated, ischemic, and inflammatory), MMP9 had the highest

4

up-regulation in dilated cardiomyopathies (Polyakova et al. 2011; Chaturvedi et al. 2015). Conclusively, all forms of heart failure exhibited an increase in collagen deposition within the cardiac system, and cardiac fibrosis is noted as a factor in heart failure (Polyakova et al. 2011; Polyakova et al. 2004).

The Tyagi laboratory has demonstrated the significance of MMP9 and TIMP-3 in cardiac hypertrophy. Attenuation of MMP9 and TIMP3 was observed post-treatment of mitochondrial division inhibitor (Mdivi), which inhibited cardiac mitophagy in the transverse aortic constriction (TAC) pressure overload model. There was decreased expression of mitophagy markers, fibrotic deposition, and improved echocardiography. The therapeutic activity of Mdivi decreased the proteolytic effects of MMP9 by inhibiting abnormal mitophagy, resulting in decreased ROS (Givvimani et al. 2012). Future studies of MMP9's role in the degradative process of heart failure (HF) may show even more significant interplay than is currently known (Ali et al. 2012).

Calpains

Cardiac pathologies involving cardiac hypertrophy and cardiac dilation show increased extracellular and intracellular protease activity. Subcellular remodeling of the sarcolemma, sarcoplasmic reticulum, myofibrils, and mitochondria occur due to proteolytic degradation (Muller et al. 2012). Hemodynamic stress-induced myocardial remodeling is caused by increased calpain activity. The Galvez group evaluated calpain-induced cardiac tissue turnover from normal to pathological. Increased

5

proteolysis coincided with increased protein ubiquitination and up-regulation of protein turnover (Galvez et al. 2007). Stress-induced activation of calpain myocardial remodeling occurs via increased Ca^{2+} concentration, which activates the remodeling cascade. Proteases such as calpains molecularly degrade the cellular components of cardiomyocytes (Moshal, Metreveli, et al. 2008; Singh et al. 2004).

Calpains are a family of intracellular cytosolic cysteine proteases activated by Ca^{2+} and localized within the cytosol and mitochondria. The family's most prevalent members are μ-calpain and m-calpain. As heterodimers, the calpain family contains two domains: a catalytic (80kda) domain and a regulatory (30kda) domain. Binding of Ca^{2+} to the large subunit induces the activation of the protease function. Alternative splicing allows for variations in the calpain protein isoforms, leading to five different calpains present in the cardiovascular system: calpain 1, 2, 3, 4, & 5 (Suzuki et al. 2004b).

The endogenous inhibitor calpastatin regulates calpain within the myocardium to decrease the proteolytic activity in the physiological heart. Calpastatin contains four inhibitory domains that bind reversibly to calpain, inhibiting its activity (Suzuki et al. 2004a). Calpain inhibitors showing calpistatin-like inhibition significantly reduce calpain activity, though in HF excessive calpain expression exceeds the counteractivity (Yang et al. 2010; Parameswaran and Sharma 2012). Increased calpain levels directly influenced the Angiotensin II (Ang II)/Ang II receptor (ATR)/calpain/calpastatin (CaN) pathway, suggesting that protease up-regulation enriched AngII-induced cardiac remodeling (Yang et al. 2010). Calpain regulation is

6

also performed by Micro-RNA 181a-3p, which will target the 3' UTR of calpain 1. Exogenous inhibition through micro-RNAs are insufficient in reducing calpain 1 in the failing heart (Campos et al. 2014). Analysis of calpastatin deficient mice in comparison to wild type revealed a significant reduction in survival rate (Kudo-Sakamoto et al. 2014).

An imbalance of proteases and their inhibitors is present within the heart failure model (Müller and Dhalla 2012; Wei et al. 2012). Alterations in cytoskeletal and contractile proteins due to calpain protease up-regulation causes the degradation of proteins such as myosin, F-actin, and titin, resulting in a disorganized sarcomere (Ellis et al. 2010). The proteolytic activity of calpains leads to intracellular degradation of proteins such as Titin, an essential contractile protein of the sarcomere (Kunkel, Chaturvedi, and Tyagi 2015a).

Overall, calpains are prevalent in heart failure and cardiac remodeling. The protective role of calpain 4's inhibition was investigated in calpain 4 knockout mice subjected to hemodynamic stress by pressure overload, revealing that calpain 4 deficiency results in decreased calpain 1 & 2 protein levels. Pressure overload via TAC caused ventricular dilation, interstitial fibrosis, heart failure, and contractile dysfunction (Taneike et al. 2011). Ventricular hypertrophy is correlated with increased calpain activity (Takahashi et al. 2005). The literature suggests that overall degradation of both contractile and cytoskeletal proteins is mainly caused by calpain proteases, as seen in cardiac remodeling. We can speculate that intermolecular

signaling may occur between regional calpain isoforms, naturally causing a decrease in calpain 1 & 2.

Electrophysiological effects were analyzed during calpain inhibition, increasing Ca^{2+}-dependent late Na^+ current (INaL) decay. Inhibiting calpain 1 increased myocyte function/viability and reduced intracellular Ca^{2+} in primary cardiomyocytes (Undrovinas, Maltsev, and Sabbah 2013). Increased calpain 1 & 2 proteolysis stimulated calcineurin, forming a calmodulin-independent and constitutively active calcineurin. Human heart failure patients express calcineurin equally in both ventricles. Calcineurin activity was present in micro-Ca^{2+} concentrations, which would increase endogenous calpain expression (Wang et al. 2012).

Therapeutic agents targeting calpain inhibition may be promising to the advancement of cardiovascular medicine. The use of calpain inhibitors improve cardiomyocyte electrical activity (Undrovinas, Maltsev, and Sabbah 2013). Current therapeutics such as trandolapril and candesartan show that inhibition of calpain proteases reduce the rate of cardiomyocyte degradation and ventricular hypertrophy in heart failure (Takahashi et al. 2006). Improvement in perfusion and hemodynamics is evident post-treatment (Perrin, Vergely, and Rochette 2004). Inhibition of the calpain protease family is an important factor mitigating molecular dysfunction within the progressively failing myocardium. Therapeutics directed towards heart failure through calpain activity/expression inhibition may elongate life of heart failure patients (Kunkel, Chaturvedi, and Tyagi 2015b).

SERCA2a

Mitigation of cardiomyocyte deterioration depends upon the regulation of Ca^{2+}, also known as Ca^{2+} handling. A major factor in Ca^{2+} handling within the cardiomyocyte is the sarco(endo)plasmic reticulum Ca^{2+} ATPase 2a (SERCA2a). This is an ATP-dependent Ca^{2+} transporter, responsible for transporting Ca^{2+} into the sarcoplasmic reticulum (SR), while decreasing free Ca^{2+} in the cytoplasm. When down-regulated, excess Ca^{2+} remains in the cytoplasm, initiating calpain activity.

SERCA2a is a member of the P type ATPases and serves as an ion-motive force in Ca^{2+} regulation. The SERCA pumps are encoded by a family of three genes: SERCA 1, 2 & 3. Alternative splicing of the transcripts derives variations of the gene family, and ten known isoforms exist in various tissue groups (Hovnanian 2007). Of the cardiomyocyte-specific SERCA family, SERCA2a is the primary isoform expressed in cardiac muscle, and it exhibits a cardioprotective function when overexpressed. It is observed that SERCA2a over-expression rescues, or inhibits, cardiac hypertrophy in rodent HF models (Nakayama et al. 2003; Sakata et al. 2007). Additional rudimentary studies in animal models describe the necessary function SERCA2a plays in cardiomyopathies.

SERCA2a knockout (KO) models die of HF after 10 weeks, providing insight into its significance (Heinis et al. 2013). Li analyzed the Ca^{2+} dynamics in these KO mice; Ca^{2+} maintenance was best regulated by increased activity of the Na^{+}-Ca^{2+} exchanger and L-type Ca^{2+} currents (Li, Louch, et al. 2011). SERCA2a KO mice show significant changes in Ca^{2+} dynamics. It was observed that Na^{+}/Ca^{2+} exchanger

and L-type Ca^{2+} channels had increased activity in these mice. Loss of SERCA2a drives alternative measures to sustain Ca^{2+} maintenance. Death due to HF occurs after 10 weeks of SERCA2a KO, showing that the compensatory activity of other transporters does not meet the requirements of the cardiomyocyte. Further Ca^{2+} analysis via patch clamp in SERCA2a KO mice reveals a decrease in Ca^{2+} transient amplitudes (Stokke et al. 2010). This finding shows a variation of electrical activity found within SERCA2a KO mice. Additionally, SERCA2a activity has been noted to suppress cellular alternans found in ventricular arrhythmias (Cutler et al. 2009).

In HF, the dependency of Ca^{2+} regulation switches to the Na^+/Ca^{2+} exchanger, which is significantly increased in SERCA2a's absence (Swift et al. 2012). CaMKIIδB regulates NCX; it is stated that pharmacological inhibition of CaMKIIδB improved cardiac function (Lu et al. 2011; Quijada et al. 2015). Electrical activation of the Ca^{2+} wave is SERCA2a-dependent. It was observed that CAMKII inhibition decreased the Ca^{2+} spark, and CAMKII shift of SR Ca^{2+} potentiates the Ca^{2+} wave (Stokke et al. 2011; Sikkel et al. 2014). SERCA2a's absence in heart failure drives alternative measures towards naturally ameliorating the Ca^{2+} issue. This results in electrophysiological changes.

SERCA2a regulation of Ca^{2+} is crucial to cardiomyocyte stability. Multiple laboratories have explored the therapeutic potential of up-regulating SERCA2a in cardiomyopathies. SERCA2a is a key protein involved in the sequestration of Ca^{2+} into the SR; importantly, it is reduced in the heart failure model (Sikkel et al.). Regulation of SERCA2a is essential to a functional myocardium. SERCA2a is a

novel therapeutic approach towards reverse-remodeling the injured myocardium (Stammers et al. 2015).

Gene therapy involving SERCA2a up-regulation is a major topic of discussion in translational research/clinical medicine (Sikkel et al. 2014; Lipskaia et al. 2010; Park and Oh 2013). SERCA2a gene therapy for HF models including acute ischemia/reperfusion, chronic pressure overload, and chronic myocardial infarction models resulted in a reduction in ventricular arrhythmias (Eltzschig and Eckle 2011). Studies show that SERCA2a gene delivery enhanced contractile function and restored electrical stability in the heart failure model caused by SR Ca^{2+} leak (Cutler et al. 2012). SERCA2a gene transfer reduced Ca^{2+} leak and ameliorated ventricular arrhythmias in HF models (Lyon et al. 2011). Use of adenoviral SERCA2a vectors overexpress the SERCA2a protein, causing ameliorating effects in the HF model (Lyon et al. 2011; Xin et al. 2011).

Phase 1 human clinical gene therapy trials support the *in vitro* and *in vivo* findings of other investigators, resulting in positive cardiovascular events post-intracoronary injection of SERCA2a adenovirus vector (Zsebo et al. 2014; Hansen et al. 2014). The clinical study of adeno-associated viral vectors (AAV) of SERCA2a administration is noted as Ca^{2+} up-regulation by Percutaneous of Gene Therapy in Cardiac Disease (CUPID), focusing on gene therapy treatments for patients with advanced heart failure and systolic dysfunction. Viral vectors of SERCA2a show constitutive and persistent expression of SERCA2a transgene in HF patients as well

11

as a significant improvement in biochemical alterations, including reduction of calpain 1 (Gwathmey, Yerevanian, and Hajjar 2013).

Phase 1, or the first 36 months of the trial, exhibited that the SERCA2a AAV had significant beneficial clinical effects on the ventricular myocardium (Greenberg 2015). Evidence of long term transgene presence, cardiac improvement, and reduced worsening of heart failure is found in the clinical trials. Suggesting that a single intracoronary treatment of the SERCA2a AAV vector, maintains positive signals in patients with advanced heart failure for years (Zsebo et al. 2014). Of four randomized clinical trials utilizing SERCA2a gene transfer in heart failure patients, it was observed that patients in the high dose group sustained progressive improvements in left ventricular function and ejection fraction. Concluding that initial experimental analysis of SERCA2a gene transfer in patients is a safe and acceptable approach to treating HF (Penny and Hammond 2017).

In general, scientific literature supports the beneficial aspects of SERCA2a gene therapy, as is readily reported (Hayward et al. 2015). Clinical HF trials utilize SERCA2a gene therapy as a method of therapeutic repair. In addition to reduction of SERCA2a, HF models have reduced mitochondrial function, the Tyagi group and others are focused on mitochondrial therapeutics in HF. Mitochondrial transcription factor A (TFAM) an essential component of MtDNA is a main regulator of SERCA2a gene transcription in cardiomyocytes (Watanabe et al. 2011; Angelini et al. 2015). In HF, TFAM and SERCA2a are significantly reduced. TFAM reduction remains at the

core of mitochondrial dysfunction. In the failing cardiomyocyte, a lack of mitochondrial efficiency drives Ca^{2+} mishandling and ROS production.

Organelles such as the mitochondria and sarcoplasmic reticulum function to reduce and store secondary factors like $Ca^{2+,}$ through active transport systems, and inhibition of ROS producing enzymes. Mitochondria are the molecular powerhouse of cells, shifting the sphere of cardiomyocyte stability and performance. Transcription factors like mitochondrial transcription factor A (TFAM) facilitate an essential role in cellular regulation through mitochondrial interventions, leading to cardiomyocyte protection (Larsson et al. 1998).

Mitochondrial Regulation: Ca^{2+} & ROS Production

An individual's cardiac health is directly related to the state of their mitochondria. The mitochondria plays a significant role in Ca^{2+} and ROS regulation. Ca^{2+} increases ROS production, which activates degratory proteases and hypertrophic factors. Ca^{2+} and ROS proceed to interact, multiplying one another and worsening the condition. Heart failure is a functional lack of myocardial performance that begets proteolytic degradation and cardiac remodeling (Quiros, Langer, and Lopez-Otin 2015). Molecular processes and pathways within cardiomyocytes inhibit the underlying components of maladaptive regulation in the physiological cellular environment (Val-Blasco et al. 2017). Causes of cardiomyocyte degradation include high cystolic concentrations of ROS and Ca^{2+} (Urmaliya and Franchelli 2017). These

secondary factors activate proteolytic enzymes, resulting in the cardiomyocyte's functional decline.

Cytoplasmic Ca^{2+} regulation is imperative to degradative activity within the myocardium. Recent reviews depicting the importance of Ca^{2+} regulation and apoptosis unveil the increased Ca^{2+}-driven proteolytic drive found within cell death (Orrenius, Gogvadze, and Zhivotovsky 2015; Bhosale et al. 2015; Griffiths, Balaska, and Cheng 2010). Excessive Ca^{2+} mishandling causes intra-mitochondrial translocation of calpain 1, affecting mitochondrial bioenergetics.

Calpains within the mitochondrial matrix contribute immeasurably to cardiomyocyte decline. Calpains I, II, & X exist within the mitochondria. Post-(I/R) injury, Calpain 1 is up-regulated, which assists in opening the mitochondrial permeability transition pore (mPTP) (Shintani-Ishida and Yoshida 2015; Elrod and Molkentin 2013). In mitochondrial decline, calpain 1 increases; it cleaves apoptosis inducibility factor (AIF), which is then translocated to the nucleus, inducing cell death (Cao et al. 2007; Nath et al. 2000; Smith and Schnellmann 2012a). Calpain X is a Ca^{2+}-induced mitochondrial protease and a necessity for functional mitochondrial activity. Smith observed that both over-expression and deletion of calpain X provoked mitochondrial decline. Degradation of mitochondrial calpain X is regulated by Lon protease, which is responsible for degrading oxidized proteins within the mitochondria in physiological and pathological states.

The literature has noted that the deficiencies producing ROS lie within the super-complexes of the electron transport chain. The addition of Ca^{2+} to the isolated

mitochondria blocks the electron transport chain at Complex I, inducing ROS production. Disrupting the association of Complexes I-III causes a substantial increase in ROS from Complex I (Maranzana et al. 2013). The leakage of electrons in the electron transport chain produces superoxides. ROS is mainly born of the electrons leaking from the mitochondrial complexes of the electron transport chain. ROS can further oxidize proteins, resulting in aggregation (Borutaite et al. 2001). In cardiomyocytes, cleavage of mitochondrial complexes induces mitochondrial and Ca^{2+}-driven autophagy, increasing ROS concentrations to a pathological level.

The Ca^{2+}/calmodulin/calcineurin-activated pathway and toll-like receptors are critical to the activation of T-cells, increase of NFAT, and regulation of ROS (Vandewalle et al. 2014). Nuclear factor of activated T-cells (NFAT) is a nuclear transcription factor and activator of innate immunity. Our immune systems recognize pattern receptors on immune cells like T-cells, macrophages, and neutrophils. This initiates NF-kB and mitogen-associated protein kinases (MAPK), which span the membrane of immune cells and play a major role in inflammatory activation. A necessary component of toll-like receptors' (TLR) functional activity is its regulation by NFAT (Minematsu et al. 2011). Interestingly, prolonged stimulation of TLR-4 leads to translocation of NFAT into the mitochondria, which reduces ATP production (Ma et al. 2015). Calcineurin, a calmodulin-dependent serine/threonine phosphatase, is a mechanistic component of NFAT up-regulation. Calmodulin dephosphorylates NFAT at the N terminus, causing the translocation of NFAT to the nucleus (Vandewalle et al. 2014). De-phosphorylation of NFAT transcription factors by

15

calcineurin allows for NFAT's transcriptional activation of nuclear encoded genes, influencing gene expression (Hogan et al. 2003). The literature states that activation of the NFAT pathway directly stimulates pathological hypertrophic genes (Li et al. 2017). Therefore, NFAT's inhibition may reduce pathological cardiac hypertrophy. Additionally, NFAT regulates the expression of the cardiac-specific ROS-generating enzymes NOX 2 & 4 (Williams and Gooch 2014).

Mitochondria and NADPH (NOX) enzymes are the leading source of ROS involved in cardiac pathology (Sorescu and Griendling 2002). Interestingly, NOX 5 is a Ca^{2+}-activated ROS generator and acts in pulsatile fashion. Banfi et al. found that Ca^{2+} activation increases NOX 5 activity, which induces large amounts of ROS production. It also acts as a proton channel (Banfi et al. 2001). NOX 5 activity is entirely dependent upon intracellular Ca^{2+} levels and increased phosphorylation of NOX 5 sites, resulting in increased Ca^{2+} sensitivity (Jagnandan et al. 2007). Ca^{2+} activates NFAT, increasing the concentration of superoxides within the cytoplasm of cardiomyocytes.

Free Ca^{2+} and excess ROS drive a cardiomyocyte towards eventual failure. Regulation of Ca^{2+} and ROS prevents the progression of HF. Increasing mitochondrial efficiency reduces Ca^{2+} mishandling and oxidative damage in cardiomyocytes.

Mitochondrial Transcription Factor A (TFAM)

TFAM Roles and Function

Mitochondrial dysfunction is correlated with disease states at the core of oxidative phosphorylation and energy efficiency, focused on mitochondrial DNA (mtDNA). MtDNA is a 16.5 Kd double stranded circular molecule encoding thirteen essential components of oxidative phosphorylation. Therefore, since efficient energy production is necessary for all basic human processes, mtDNA is vital to the restoration of physiological conditions. As noted unanimously in the literature, the major regulator of mtDNA copy number in mammalian models is TFAM (Ekstrand et al. 2004; Hoppel et al. 2017). The mtDNA copy number is reflective of mtDNA transcription and ATP production. TFAM is a promoter-specific enhancer of mtDNA and a member of the high-mobility protein group (Larsson et al. 1998; Lyonnais et al. 2017). This transcription factor is essential for mitochondrial DNA maintenance, seeing as it coats mitochondrial DNA, playing a factor in mtDNA stability (Alam et al. 2003). TFAM is produced in the nucleus and then transported to the mitochondria. TFAM is a major mitochondrial gene-regulator, and, as a transcription factor, it modifies gene expression.

Nuclear regulatory factors including nuclear respiratory factors 1 and 2 (NRF 1, 2) are upstream regulators of TFAM; this is a link between nuclear activity and energy production (Virbasius and Scarpulla 1994; Chouinard et al. 1998). A finding through super-resolution microscopy reveals that mitochondrial nucleoids (mtDNA-protein complexes) are a uniform size, and TFAM is a main component (Kukat et al.

2011). TFAM acts as a packaging molecule by storing a single copy of mtDNA in a functional mitochondrial nucleoid (Kukat et al. 2015). Mitochondrial nucleoids contain essential enzymes of an integral antioxidant system, including manganese superoxide dismutase (SOD2) and mitochondrial glutathione peroxidase (GPx1) (Kienhofer et al. 2009; Ishihara et al. 2015; Pohjoismaki and Goffart 2017). These antioxidant enzymes mitigate oxidative damage and protect mtDNA. Components of the nucleoid create a safe environment for functional mtDNA processes such as transcription, transduction, and repair (Hensen et al. 2014). The molecular components of TFAM are a benefactor to cardiomyocyte cellular functions.

TFAM transcriptional machinery consists of two high-mobility groups: HSP (heavy strand promoter) and LSP (light strand promoter). TFAM allows mitochondrial-directed RNA-polymerase (POLRMT) to interact with the DNA promoter to initiate transcription and produce the primary transcripts of mRNA, rRNA, and tRNA (Falkenberg, Larsson, and Gustafsson 2007). As a major regulator of mtDNA transcriptional machinery, TFAM has direct regulation over the minor transcription factors TFB1M and TFB2M. These transcription factors directly promote transcription, using POLRMT (Falkenberg et al. 2002; Song et al. 2012). TFBM1 is a dual-function protein acting as a transcription factor and an RNA methyl-transferase enzyme (Seidel-Rogol, McCulloch, and Shadel 2003).

Aside from indirect gene regulation through TFBM 1&2, TFAM also directly regulates promoter regions of DNA by binding to the promoter-specific region, which causes an unwinding reaction that initiates transcription (Fisher et al. 1992). An

18

additional function of the TFBM 1&2 is binding single-stranded DNA to stabilize unwound promoter regions. There is a strong correlation between TFAM/TFBM 1&2 expression and initiation of mtDNA replication. Additionally, increased TFAM expression reduced neuronal pathologies and increased patient survival rate, deeming it clinically beneficial (Correia et al. 2011). A significant component of mitochondrial transcription, the mitochondrial RNA polymerase, requires TFAM and TFBM2 for efficient initiation (Morozov et al. 2014; St John et al. 2006).

Mapping the binding sites of TFAM and TFBM2 resulted in novel functional aspects of TFBM2 binding. TFAM binding to an upstream promoter region activates the pre-initiation complex, which requires the binding of TFB2M for specific contact with promoter DNA. Loss of TFBM2 leads to nonspecific contact with DNA. Functionally, TFB2M separates the DNA strands and plays a role in initiating transcription. TFBM2 can reposition the specificity loop of mtRNAP to recognize specific promoters (Morozov et al. 2014; Morozov et al. 2015). Mitochondrial protein formation is regulated by mitochondrial ribosomes, consisting of two subunits: the small (28S) mitochondrial ribosome subunit and the larger (55S) subunit. Post- the regulatory functions of forming the initiation complex, TFB1M regulates the assembly of the 28S subunit by acting as a 12S ribosomal RNA methyltransferase. Observations have concluded that POLRMT's activities catalyze TFB1M's methyltransferase function, resulting in protein formation (Surovtseva and Shadel 2013). POLRMT is essential for mitochondrial protein formation and gene regulation.

It is noted that both of these factors [TFB1M & TFB2M] are cooperative downstream effectors for mitochondrial biogenesis. More specifically, TFB2M functions to maintain mtDNA transcription. TFB1M's 12S rRNA methyltransferase activity is essential for mitochondrial translation and metabolism. Hypermethylation caused by over-expression of TFB1M methyltransferase activity results in cell death and abnormal biogenesis (Cotney, McKay, and Shadel 2009; Chen, Yi, and Sun 2014). To emphasize the importance of the methylation activity of TFB1M, studies show the effects of disrupting cardiac TFB1M. Complete loss of adenine di-methylation of rRNA decreased mitochondrial translation and reduced ribosomal function (Metodiev et al. 2009). As noted above, TFAM has direct regulation over TFB1M & TFB2M. Ablation of TFAM in neonatal mice led to sufficient decreases in the cardiac respiratory chain, affecting mitochondrial biogenesis (Wang et al. 1999; Larsson et al. 1998; Schwarz et al. 2014).

TFAM's major regulatory activities of mtDNA led to direct regulation over mitochondrial gene expression, affecting not only the 13 essential genes required for oxidative phosphorylation, but also mitochondrial biogenesis and ATP production. Understanding the essence of mitochondrial biogenesis and oxidative phosphorylation is the key to cardiovascular pathologies (Vega, Horton, and Kelly 2015). Mitochondrial dysfunction within cardiomyocytes can lead to HF, but the core of mitochondrial defects is found within the stability of mtDNA. As stated previously, TFAM is a DNA-binding protein directly related to mitochondrial stability. Mutant uracil-DNA glycosylase 1 (mutUNG1) was up-regulated in transgenic mouse (Tet-

on) models, which hampered mtDNA function and stability. Impairment of mtDNA via mutUNG1 up-regulation resulted in rapid hypertrophic cardiomyopathy, leading to HF and death. This culminated into pathological effects such as reduced mtDNA replication & transcription, diminished mt respiration, impaired fission/fusion dynamics, and significantly decreased cardiomyocyte contractility (Lauritzen et al. 2015). It would be interesting to observe the effects of exogenous TFAM administration into this mutant model.

TFAM, one of the many mitochondrial stability factors, manages mechanistic components involved in mitochondrial biogenesis. It plays a significant role in genetic and epigenetic control over downstream factors. Although it is known that TFAM's primary purpose is to sustain mitochondrial DNA and mitigate mutagenic activity by creating an antioxidant environment, many secondary functions are in need of further exploration.

TFAM Transport

TFAM is synthesized in the nucleus and transported to the mitochondria. TFAM translocation to the mitochondria for initiation of transcription and translation requires the binding of chaperones, which creates a heat shock protein (HSP) complex. Deocaris and colleagues describe the intimate interaction between HSP60 and HSP70 (Deocaris, Kaul, and Wadhwa 2006). Lon protease is an ATP-dependent protease with chaperone properties; it promotes the association of heat shock protein complex HSP60-HSP70. Kao and colleagues observed an increase in the stability of

the HSP60-70 complex upon Lon's binding to the HSP60 subunit. Loss of Lon leads to HSP60 dislocation, protein degradation, and apoptotic signaling activation upon HSP60's binding to the regulator, P53 (Kao et al. 2015).

Coincidentally, in apoptotic signaling, free HSP-60 binds to the TLR-4 binding domain of T-cells, increasing NFAT activity. Exogenous HSP-60 binds to TLR-4 and induces apoptotic signaling (Kim et al. 2009). Kim et al. assert that this may be a mechanism of myocyte loss in HF. Li states that myocardial ischemia induces an apoptotic signaling cascade, affirming that HSP-60 increases the expression of caspases 3 & 8. In TLR-4 deficient mice (I/R) injury had reduced myocardial apoptosis and cytokine expression (Li, Si, et al. 2011). The interplay between HSP-60 and TLR-4 is essential to mediating apoptotic signaling within cardiovascular diseases. However, the HSP60-70 complex has a positive regulatory function within cardiomyocytes. Interestingly, this is NF-kB dependent, due to NF-kB regulation over NFAT up-regulation (Wei et al. 2015).

Lon protease's coupling with TFAM was observed in drosophila Schneider cells (Matsushima, Garesse, and Kaguni 2004). The HSP60-70 complex is Lon-dependent, and, importantly, TFAM binds to the HSP70 component. The interaction of TFAM bound to HSP-70 at the nucleus allows for transportation of TFAM into the mitochondria (Santos, Mishra, and Kowluru 2014). Lon can be personified as TFAM's personal trainer, keeping TFAM fit for mitochondrial biogenesis. An article by Naka and colleagues suggests that HSP70 transgenic mice are cardioprotective in a doxorubicin heart failure model, validating that the transgenic model inhibited

apoptotic signaling by mediating P53, Bax, caspase-3&9, and PARP-1 (Naka et al. 2014). Up-regulation of HSP-70 will increase mitochondrial biogenesis by increasing TFAM transport. This regulates Ca^{2+}, leading to decreased protease activity and apoptotic signaling. Santos describes TFAM's binding to HSP60, but at a lower affinity when compared to HSP70 (Santos, Mishra, and Kowluru 2014). TFAM transport may be inhibited in high ROS conditions such as cardiomyopathies. TFAM's nuclear and mitochondrial role in sustaining cardiomyocyte function is dependent upon inter-organelle transport

TFAM: A Therapeutic Potential

Mitochondrial transcription factor A (TFAM) creates a mitochondrial nucleoid structure around mtDNA, protecting it from mutation, inhibiting NFAT, and transcriptionally activating SERCA2a to decrease Ca^{2+} mishandling. TFAM's regulatory functions over SERCA2a and NFAT contribute to physiological cardiomyocyte stability (Kunkel, Chaturvedi, and Tyagi 2016). Current literature depicts significant decreases in TFAM as HF progresses. Several clinical studies have used gene therapy to up-regulate SERCA2a in heart failure, thereby reducing cytosolic Ca^{2+} and its maladaptive molecular associates (Sikkel et al. 2014; Lyon et al. 2011). Therefore, TFAM's transcriptional activation of SERCA2a should reduce Ca^{2+}-activated calpain proteases, while inhibiting ROS production from the Ca^{2+} activated NFAT cascade, which may reduce ROS-driven MMPs.

TFAM's regulation of the SERCA2a promoter in cardiomyocytes leads to

23

therapeutic function. Therefore, with support of past studies, TFAM over-expression may increase SERCA2a protein expression, increasing Ca^{2+} handling into the SR and reducing protease activity. Due to Ca^{2+} up-regulation in the HF model, calpain activation is persistent. The literature suggests that continuous calpain up-regulation is a major factor in the development of HF (Takahashi et al. 2006; Sonobe et al. 2014). TFAM up-regulation of SERCA2a will decrease Ca^{2+} and calpain activity in the cytoplasm, reducing structural and contractile degradation.

TFAM up-regulation and inhibition of NFAT activation would decrease ROS production by inhibiting NOX 2&4 activity, thereby reducing MMP 2 & 9 proteolytic activities. NOX 4 is significantly increased in HF, and it is an activator of cardiomyocyte autophagy. (Sciarretta et al. 2015). Up-regulation of ROS in cardiomyocyte autophagy induced the nuclear translocation of calpain 2. Inhibition of NOX 4 resisted the translocation of calpain 2 (Chang et al. 2015). Mice with a triple KO of NOX 1, 2, and 4 had no effect on NADPH chemo-luminescent signaling in cardiac, renal, and aortic tissue samples. Over-expression of NOX 4 greatly increased ROS production, inducing MMPs. Oxidative damage decreases TFAM mRNA and protein expression, resulting in cardiomyocyte mitochondrial dysfunction *(*Rezende et al. 2015*)*. Anti-oxidant therapeutic lycopene ameliorated ROS production and TFAM protein decline, resulting in reduced ventricular remodeling (Yue et al. 2015).

The lack of TFAM protein expression causes dilated cardiomyopathy with reduced mtDNA copy number (Wang et al. 1999). In addition, the reduction of TFAM has been reported in many forms of heart failure (Lebrecht et al. 2003; Ide et

24

al. 2001; Kanazawa et al. 2002; Garnier et al. 2003). The mice in which TFAM is overexpressed experience protection from LV remodeling, decreased oxidative stress, preserved mtDNA copy number, and mitochondrial function (Ikeuchi et al. 2005). Moreover, TFAM over-expression attenuated histopathological changes such as interstitial fibrosis, apoptosis, myocyte hypertrophy, and cardiac chamber dilation. In TFAM transgenic mice, TFAM over-expression in HF has been reported to increase (in a timely manner) the mitochondrial DNA copy number and reverse cardiac tissue damage (Russell et al. 2004). Hence, TFAM plays an important role in myocardial protection against adverse cardiac remodeling and heart failure. Molecular regulation over cardiac remodeling and maladaptive factors is key to preventing myocardial decline.

TFAM regulation over SERCA2a may decrease cytoplasmic Ca^{2+} levels and alleviate calpain activity. Post intramitochondrial translocation of calpain 1, an intramitochondrial oxidative burst drives MMP9 activity (Moshal et al. 2006; Casas et al. 2003). Calpains are involved in cardiomyocyte necrosis and apoptosis. (Perrin, Vergely, and Rochette 2004; Marshall et al. 2014). Both intracellular and extracellular proteases perform apoptosis and remodeling in HF. A multitude of proteases are found within the cardiovascular system, including calpains, caspases, cathepsins, and MMPs. While calpains and caspases remodel the intracellular matrix of subcellular organelles, MMPs and cathepsins remodel the extracellular matrix. Aligning specific proteases to diseases may lead to future therapeutic advances (Muller and Dhalla 2012; Bonnans, Chou, and Werb 2014).

Concluding Statement

In conclusion, this review seeks to provide a molecular background and insight into the holistic abnormal conjuncture of degratory processes involved in heart failure and associated cardiomyopathies. As discussed, chaperones transport TFAM to the mitochondria. The absence of TFAM in the failing cardiomyocyte contributes to cardiomyocyte dysfunction. TFAM over-expression reduces ROS production, inhibits NFAT and activates SERCA2a. The extent to which TFAM over-expression changes the proteolytic degratory factors in HF is in need of further exploration.

It is unknown whether TFAM over-expression will mitigate calpain proteolytic and NFAT pathological hypertrophic expression post-TAC-induced HF. Furthermore, we analyze the effects of TFAM knockdown and over-expression on these cardiac remodeling factors. We are the first to examine the effects of aortic banding-induced heart failure on TFAM transgenic animals and whether TFAM reduces NFAT in stress conditions. Our findings suggest that TFAM has molecular potential to reduce cardiac remodeling.
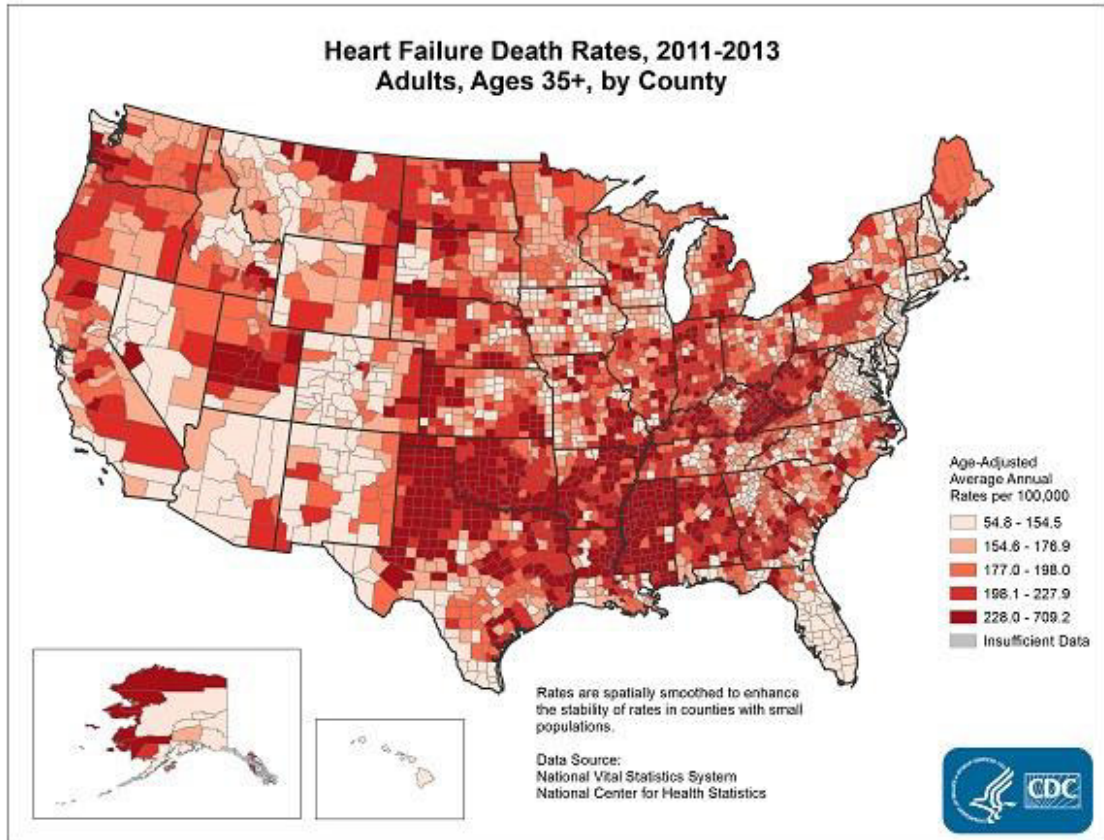
Figure 1. Rate of Heart Failure Attributed Deaths (United States: 2011-2013)

Fig. 1. The thematic map provided by the Center for Disease Control (CDC) shows the HF death rates from 2011-2013 for Americans ages 35+. With regards to the state of Kentucky (KY), the highest rates of HF death are concentrated in eastern and central Kentucky.
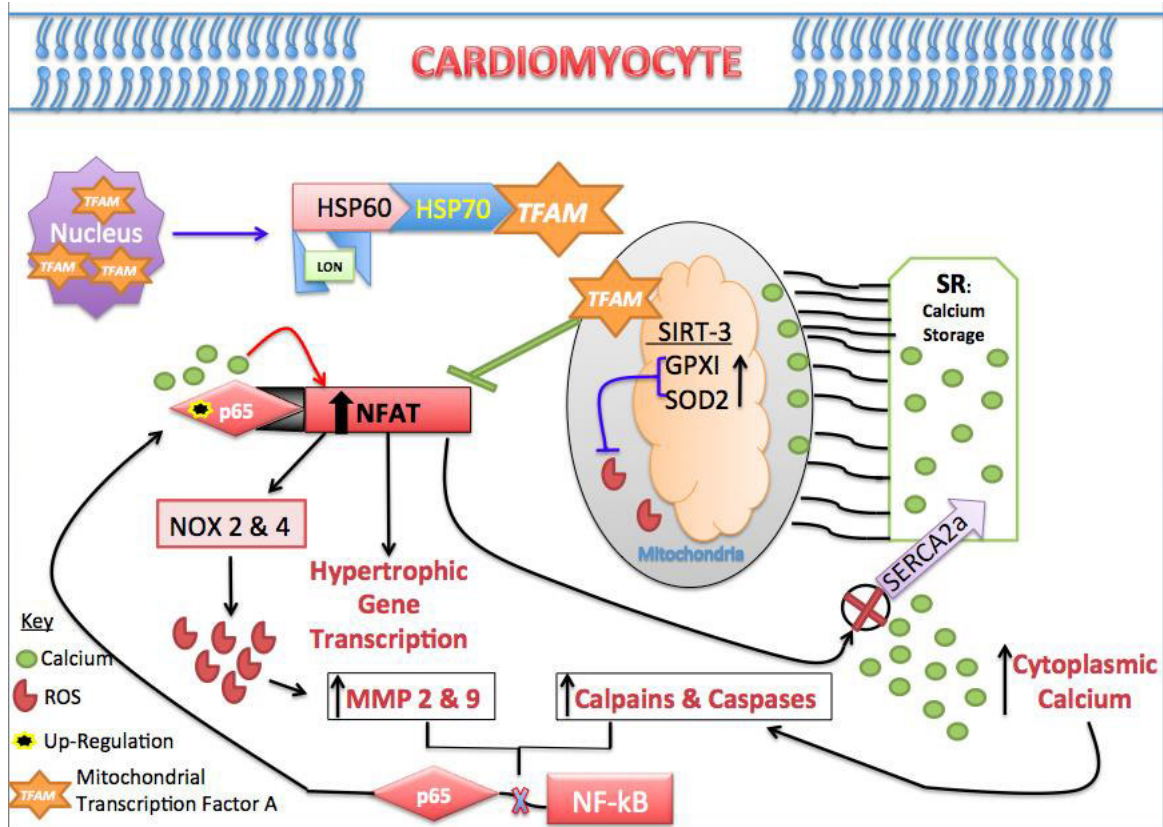
Figure 2. Molecular Abnormalities Associated with Cardiomyocyte Decline

Fig. 2. This diagram depicts the known mechanisms for molecular abnormalities involved with cardiomyocyte decline. The failing cardiomyocyte contains a multitude of dysregulated factors which induce molecular activity leading towards degradation. TFAM's major function of regulatory activity to inhibit NFAT, reduces pathological hypertrophic gene expression and ROS production. Loss of TFAM would result in up-regulation of NFAT and blockage of the SERCA2a ATPase pump. This increases cytoplasmic Ca^{2+} levels inducing protease activity and Ca^{2+} binding calcineurin drives NFAT activation. As an apoptotic trigger, Ca^{2+} induces the translocation of NF-kB resulting in release of the p65 subunit. The p65 subunit binds NFAT greatly stimulating NFAT activity. This mechanistic overview represents the interplay of protease activity, hypertrophic stimulation and the potential TFAM has to block molecular dysfunction.

CHAPTER II

HYPOTHESIS & SPECIFIC AIMS

Key Objective

To investigate the role of Mitochondrial Transcription Factor A in cardiac remodeling.

Hypothesis

TFAM over-expression reduces pathological cardiac remodeling and associated dysregulated mechanistic factors in heart failure.

Specific Aims

- **Specific Aim #1:** To analyze the effect of oxidative stress, TFAM CRISPR knockdown and, TFAM over-expression on HL-1 cardiomyocytes.

- **Specific Aim #2:** To determine if TFAM over-expression reduces cardiac hypertrophy post pressure overload heart failure.

- **Specific Aim #3:** To determine if TFAM over-expression reduces proteases MMP9, Calpain 1 and cardiac hypertrophic stimulator NFAT4 in pathological cardiac remodeling.
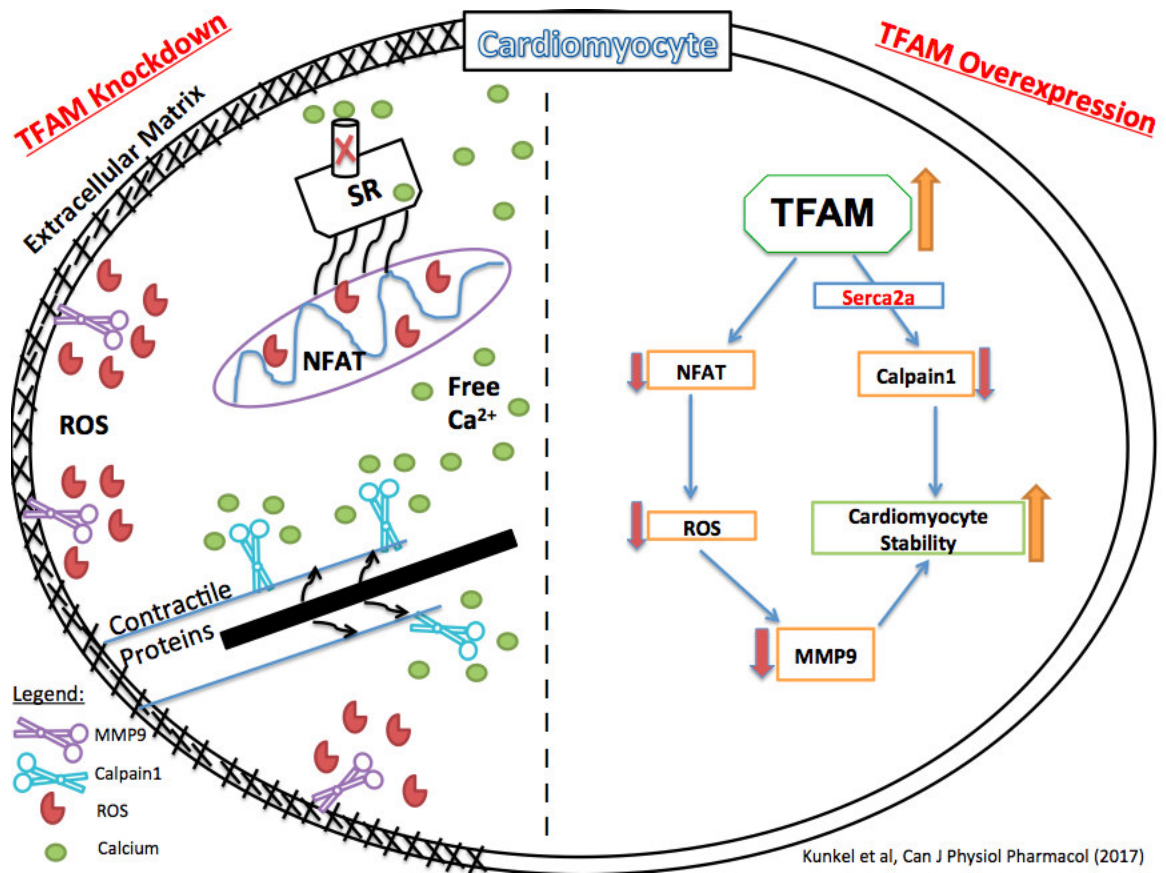
Figure 3. Proposed Mechanism of TFAM- Mediated Cardiomyocyte Protection

Fig. 3. This diagram describes the hypothesized mechanism for TFAM's role in cardiomyocyte protection. TFAM knockdown is hypothesized to lead to mitochondrial dysfunction and an increase in Ca^{2+} and ROS-induced proteases. TFAM Over-expression is hypothesized to reduce Ca^{2+}-driven Calpain proteases and reduce NFATs, ROS production/hypertrophic expression and, thereby reducing MMPs. The former leads to cardiomyocyte dysfunction and the lead to cardiomyocyte stability.

CHAPTER III

TFAM'S MECHANISTIC ROLE IN REMODELING

Introduction:

TFAM is a promoter-specific enhancer of mtDNA, regulator of mitochondrial genes and mtDNA copy number, and a physical protector of mtDNA (Ekstrand et al. 2004; Kunkel, Chaturvedi, and Tyagi 2016). TFAM packages single copies of mtDNA, creating a mitochondrial nucleoid (Kukat et al. 2015; Wang et al. 1999). TFAM is transported from the nucleus into the mitochondria by chaperone HSP70 (Santos, Mishra, and Kowluru 2014). Peroxidase enzymes reside within the nucleoid structure, mitigating oxidative damage to mitochondrial DNA (Larsson et al. 1998; Wang et al. 1999; Mandal et al. 2015). TFAM's physical protective function contributes to the mitigation of molecular abnormalities within the physiological myocardium, and in pathologies such as heart failure, TFAM is decreased. We seek to describe TFAM's effects on protease/hypertrophic molecular expression when influenced by hydrogen peroxide, TFAM over-expression, and CRISPR/Cas9 vector for TFAM knockdown.

TFAM's regulatory function to increase SERCA2a transcriptional activity poses insight into its therapeutic potential (Watanabe et al. 2011). SERCA2a, an ATP-dependent Ca^{2+} transporter, reduces free cytoplasmic Ca^{2+} by storing it in the sarcoplasmic reticulum

(Kunkel, Chaturvedi, and Tyagi 2015b). SERCA2a knockout models result in Heart Failure; SERCA2a activity is significant for cardiomyocyte performance and contains translational components (Heinis et al. 2013; Sikkel et al. 2014; Lipskaia et al. 2010; Park and Oh 2013; Zsebo et al. 2014). TFAM's regulation of SERCA2a decreases cytoplasmic Ca^{2+} levels, effectively decreasing protease Calpain 1 expression. Ca^{2+}-driven calpain proteases are responsible for the proteolytic degradation of both contractile and cytosolic proteins (Kunkel, Chaturvedi, and Tyagi 2015a). Studies show that calpain up-regulation is a major factor in cardiomyocyte functional decline (Takahashi et al. 2006). Physical tethering interactions between the mitochondria and the sarcoplasmic reticulum play a role in Ca^{2+} regulation (Li et al. 2015; Chen et al. 2012).

TFAM's protective function to inhibit NFAT expression reduces cardiomyocyte hypertrophy (Fujino et al. 2012). NFAT transcriptionally activates hypertrophic genes. The Ca^{2+}-calmodulin-calcineurin cascade plays a role in the activation of T cells and related cytokines (Vandewalle et al. 2014). Cytosolic Ca^{2+} activates the calcineurin/NFAT pathway, leading to pathological hypertrophy (Prasad and Inesi 2012). NFAT regulates the expression of mitochondrial ROS-generating NADPH Oxidases (NOX), specifically NOX 2&4 (Williams and Gooch 2014). Mitochondrial NOX enzymes are a leading source of the ROS involved in cardiac pathology (Sorescu and Griendling 2002). TFAM inhibits ROS activator NFAT, decreasing MMP9 expression in cardiomyocytes. ROS-driven Matrix-metalloproteinases (MMPs) are zinc-dependent endopeptidases capable of degrading the extracellular matrix (ECM) of cardiomyocytes. We have assessed the expression of MMP-9

in cardiac hypertrophy (Givvimani et al. 2012) and described MMP up-regulation in heart failure as it pertains to ROS generation (Kunkel, Chaturvedi, and Tyagi 2015b).

Although MMP 2 & 9 have increased activity in all cardiomyopic states (dilated, ischemic and inflammatory), MMP9 has the highest up-regulation in heart failure related cardiomyopathies (Romanic et al. 2001). Oxidative stress is evidently activating catabolic/proteolytic pathways, such as MMPs, in heart failure models. MMP9 is notably up-regulated in pathological conditions of cardiovascular diseases (Iyer, Jung, and Lindsey 2016). In an earlier study, Siwik et al found that hydrogen peroxide oxidative stress induced MMP9 activity (Siwik, Pagano, and Colucci 2001). We have found that MMP9 triggers the signaling cascade leading to pathological cardiac remodeling in human heart end-stage heart failure (Moshal et al. 2005). Additionally, we have described the results of MMP9 knockout models and the ameliorating effects post AVF induced Heart Failure (Moshal, Rodriguez, et al. 2008). ROS-induced MMP9 is highly expressed in pathological human hearts (Moshal et al. 2005).

Using CRISPR technology, we analyzed the effects of knocking down TFAM in HL-1 cardiomyocytes. This study was performed to observe the effects of TFAM vector treatments on protease/hypertrophic expression. Studies have shown that neonatal ablation of TFAM results in decreased mitochondrial biogenesis and death (Larsson et al. 1998). Down regulation of TFAM causes mitochondrial oxidative phosphorylation dysfunction, resulting in increased ROS production and MMP activity (Mendelsohn and Larrick 2014). We have

33

shown the intimate interaction between intramitochondrial translocation of calpain 1, resulting in increased oxidative stress and MMP9 expression (Moshal et al. 2006).

In vivo studies have analyzed the effects of TFAM over-expression, showing decreased myocyte hypertrophy, oxidative stress, protease expression, apoptosis, interstitial fibrosis, increased mtDNA copy number, and cardiomyocyte stability in myocardial infarction/heart failure models (Ikeuchi et al. 2005; Ikeda et al. 2015; Kang, Kim, and Hamasaki 2007; Hayashi et al. 2008). Additionally, TFAM protected cells from oxidative stress in many *in vitro* models (Thomas et al. 2012; Xu et al. 2009; Aguirre-Rueda et al. 2015). Therefore, the purpose of this study is to elucidate TFAM's role in cardiomyocyte stability through protease and hypertrophic regulation.

Materials & Methods

Chemicals and Antibodies

TFAM over-expression and CRISPR vectors were purchased from Genecopia (Rockville, Maryland). All primary antibodies were purchased from Abcam (Cambridge, United Kingdom). Horseradish peroxidase (HRP)-conjugated secondary antibodies were purchased from Santa Cruz Biotechnology (Dallas, Texas, USA). Fluorescent secondary antibodies and lipofectamine 2000 reagent was purchased from Life Technologies (Carlsbad, California, USA).

Cell Culture

The HL-1 Cardiac Muscle Cell line was purchased from EMD Millipore (Darmstadt, Germany). Cells were grown in 25 and 75 cm^2 flasks using Claycomb Media supplemented with 10% FBS, 2 mM L-glutamine, 0.1 mM norepinephrine, and penicillin/streptomycin. The medium was changed every 24 hours. Cells were maintained in a 37°C incubator in an atmosphere of 95% O_2 and 5% CO_2 and passaged with Trypsin, as per EMD-Millipore protocol.

Cell Treatment

Cells were plated in 6-well plates at a count of 600×10^3 cells per well for protein isolation. For immunocytochemistry analysis, cells were plated in 8 well chamber slides at 100×10^3 cells per well. After 24 hours, fresh media was provided prior to treatments.

Abcam primary antibodies used are as follows: Calpain 1 (ab28258), SERCA2 (ab2861), NFAT4 (ab83832), TFAM (ab131607) & MMP9 (ab38898)

Vectors: TFAM Crispr-Cas9 Vector: Genecopia (MCP228370-SG01-1)

TFAM Over-expression Vector: Genecopia (NM_009360.4)

Transfection of HL-1 Cells with TFAM Vector/ TFAM CRISPR-Cas9 Vector

CRISPR/Cas9 knockdown plasmid for TFAM and TFAM over-expression vector were transfected into HL-1 cardiomyocytes using the life technologies lipofectamine 2000 reagent. As per lipofectamine 2000 protocol 1.0 micrograms of TFAM vectors were incubated with

35

Lipofectamine and Opti-MEM and then administered to 6-well plates/chamber slides with media lacking pen/strep for 48 hours. Cells were then washed with PBS and harvested for western blot analysis.

H_2O_2 Treatment

Hydrogen peroxide was administered to HL-1 cardiomyocytes divided into four treatment groups: Control, H_2O_2, TFAM + H_2O_2, TFAM. 127 micromolar H_2O_2 was administered to the cells for the last six hours of the 48 hour TFAM vector treatment.

Western Blot Analysis

Post- a 48 hour treatment period, HL-1 cell protein was isolated using protein extraction buffer (RIPA lysis buffer, protease inhibitor cocktail and PMSF). Wells were scraped and the contents transferred to ependorf tubes. Lysates were spun in extraction buffer for 12 hours and then centrifuged at 12,000g for 15 min. Supernatant was transferred to new tubes and protein concentrations were analyzed via Bradford protein estimation assay. Samples were run on a 10/12% sodium dodecylsulfate (SDS)-polyacrylamide gel with Tris-glycine SDS buffer. The gel was transferred electrophoretically overnight onto a PVDF membrane at 4°C. The membrane was blocked with a 5% milk solution for 1 hour. Primary antibodies were diluted at a concentration 1:1000 in TBST and incubated on the membrane overnight. All membranes were washed in TBST solution 4 times and then incubated with secondary HRP conjugated antibody solution for 1 hour at room temperature. Four TBST washing steps followed before membranes were developed using a chemiluminescent

substrate in a BioRad Chemidoc (Hercules, Calif.). Band intensity was determined using densitometry analysis. Beta-actin was used to normalize protein loading.

Immunocytochemistry

Post-cell treatment, media was aspirated from each well of the eight well chamber slide and cells were rinsed with PBS. Cells were fixed at room temperature in 4% paraformaldehyde solution for 20 min and washed 3 times with PBS. Blocking was performed with a mixed solution of 2% bovine-serum-albumin (BSA) and 0.025% Triton X-100. Cells were permeabilized for 1 hour. All primary antibodies were incubated in the chamber slide at a concentration of 1:100 overnight at 4°C. The wells were aspirated, washed 3 times and incubated for 90 min with the secondary antibody (1:200) at room temp. The chamber slides were washed 3 times more, and DAPI was added at 1:10,000 for 10 min. This analysis was observed via Confocal microscopy.

Statistical Analysis

Data are expressed as means ± SE. Statistical analysis was performed by Graphpad Prism software using a one-way ANOVA followed by a Bonferoni comparison test. *P*<0.05 was considered statistically significant.

Results

CRISPR Vector Significantly Increases SERCA2a and Calpain 1 Protein Expression

To observe the efficacy of the TFAM over-expression vector and the CRISPR-Cas9 knockdown vector for TFAM, we analyzed TFAM expression with both treatments. Through western blotting and confocal analysis, we saw significant decreases in TFAM protein expression with the CRISPR vector compared to both the control ($p < 0.001$) and the TFAM over-expression vector ($p < 0.001$). Additionally, the TFAM over-expression vector showed considerable increases in TFAM expression compared to control ($p < 0.05$) (Fig. 4).

Western blotting and confocal analysis were used to determine changes in SERCA2a expression with both treatments. CRISPR vector significantly increased SERCA2a expression in HL-1 cardiomyocytes as compared with the control groups ($p < 0.001$) (Fig. 5). Confocal analysis and western blotting show the CRISPR vector greatly increased Calpain 1 expression as compared to control groups ($p < 0.001$) (Fig 7).

CRISPR Vector Significantly Increases NFAT4 and MMP9 Protein Expression

Western blotting and confocal analysis show that the CRISPR vector significantly increased NFAT as compared to control groups. ($p < 0.05$) (Fig. 6). Comparisons between the TFAM vector and CRISPR vector were also notable, showing reduction of NFAT with TFAM vector treatment ($p < 0.025$) (Fig 6). Oxidative Stress observed via DHE staining and MMP9 protein expression were significantly increased in HL-1 cardiomyocytes treated with

the CRISPR vector as compared to the control and TFAM vector treatment ($p < 0.001$, $p < 0.05$) (Fig 8)

Hydrogen Peroxide Induced Protease Activity is Attenuated by TFAM Treatment

H_2O_2 treatment to HL-1 cardiomyocytes reduced TFAM protein expression ($p < 0.001$). Conclusive to our hypothesis, western blotting and confocal analysis show that TFAM treatment with H_2O_2 increased TFAM levels compared to the H_2O_2 group alone, but was still reduced when compared with the control ($p < 0.05$) (Fig 9). Additionally, Calpain 1 protein expression increased with ROS-induced stress ($p < 0.001$). TFAM treatment with H_2O_2 reduced calpain 1 expression when compared to the H_2O_2 group alone ($p < 0.025$) but still maintained significantly higher Calpain 1 levels than the control ($p < 0.05$) (Fig 11). Western blotting and confocal analysis show that NFAT protein expression was greatly increased by H_2O_2 ($p < 0.025$). TFAM treatment with H_2O_2 stress shows a significant reduction of NFAT levels in comparison to the H_2O_2 group alone ($p < 0.05$), normalizing the expression to that of the control. Additionally, there is a significant difference between the TFAM + H_2O_2 group and the TFAM vector ($p < 0.05$) (Fig 10). Western blotting and confocal analysis show that ROS-induced protease MMP9 was significantly increased by H_2O_2 compared to the control ($p < 0.001$). The TFAM treatment group had decreased MMP9 expression under ROS stress conditions when compared with the H_2O_2 group ($p < 0.05$), but MMP9 was still significantly increased as compared to the control group ($p < 0.05$) (Fig 11).
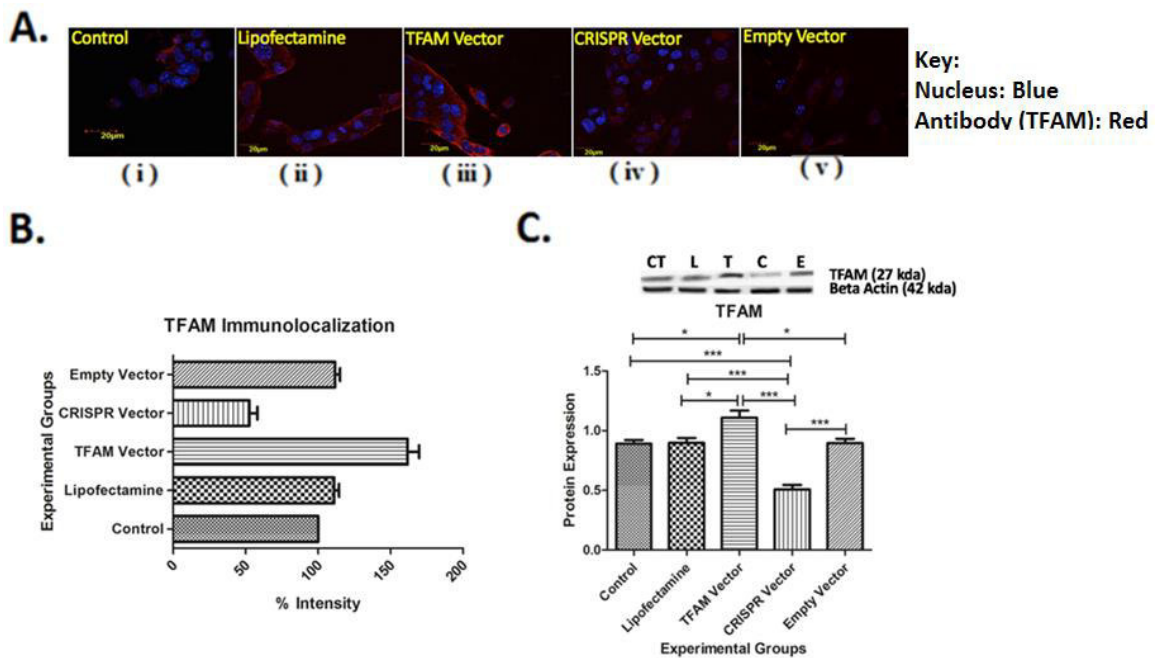
Figure 4. CRISPR-Cas9 (TFAM) vector treatment reduces TFAM expression & TFAM vector treatment increases TFAM expression

Fig. 4A. These images (i-v) captured by confocal microscopy and Immunocytochemistry (ICC) provide intra-cellular visualizations of TFAM within the corresponding experimental groups.

Fig. 4B. This graph exhibits the fluorescent intensity of TFAM that was provided by the data collected from the Image J software. Each fluorescent intensity corresponds to TFAM presence within a specific experimental group. With respect to the experimental controls, the intensity of TFAM was significantly greater under the TFAM Vector and significantly lower when the CRISPR Vector applied.

Fig. 4C. This graph displays TFAM proteins expression in HL-1 cardiomyocytes treated with TFAM over-expression vectors, CRISPR-cas9 vectors and experimental controls. HL-1 cells were treated with 1.0 micrograms of vectors for 48 hours before harvesting. Lysates were analyzed by western blotting for TFAM protein expression. With respect to the experimental controls, the protein expression of TFAM was significantly greater under the TFAM Vector and significantly lower when the CRISPR Vector applied. The bands were quantified using densitometry and the data was graphed for an N of 6 using SEM for significance. Values are expressed as +/- SEM. N=6. * $p < 0.05$, *** $p<0.001$.
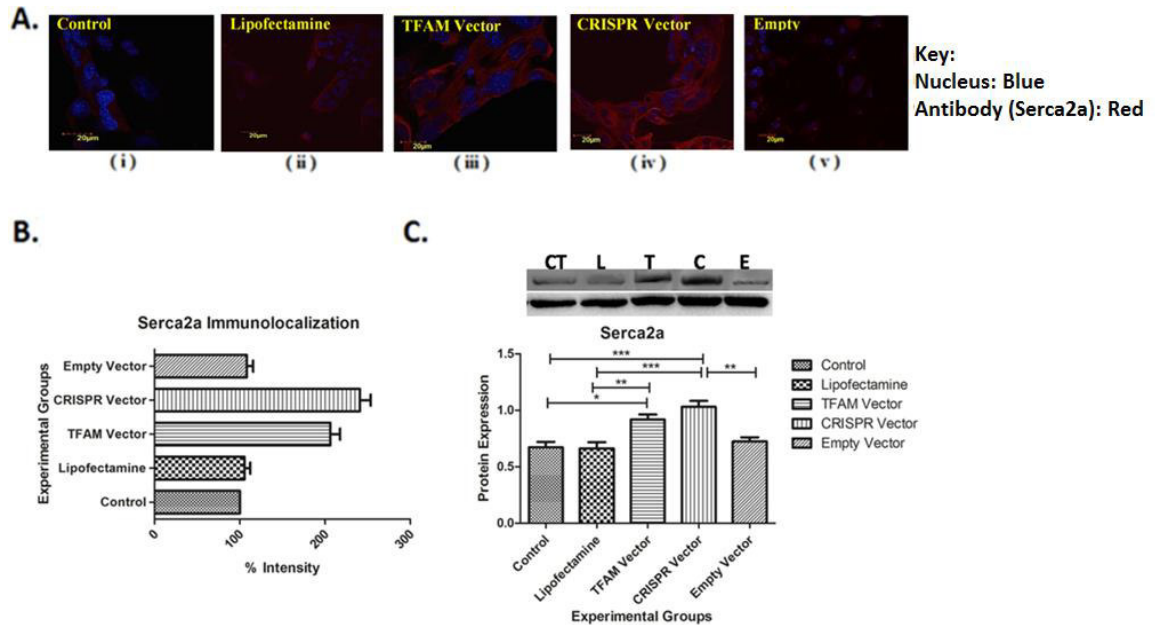
Figure 5. CRISPR-Cas9 (TFAM) vector treatment significantly increases SERCA2a expression & TFAM vector treatment increases SERCA2a expression.

Fig. 5A. These images (i-v) captured by confocal microscopy and ICC provide intra-cellular visualizations of SERCA2a within the corresponding experimental groups.

Fig. 5B. This graph exhibits the fluorescent intensity of SERCA2a that was provided by the data collected from the Image J software. Each fluorescent intensity corresponds to SERCA2a presence within a specific experimental group.

With respect to the experimental controls, the intensity of SERCA2a was the significantly greater under the CRISPR Vector and significantly high when the TFAM Vector applied.

Fig. 5C. This graph displays SERCA2a proteins expression in HL-1 cardiomyocytes treated with TFAM over-expression vectors, CRISPR-cas9 vectors and experimental controls. HL-1 cells were treated with 1.0 micrograms of vectors for 48 hours before harvesting. Lysates were analyzed by western blotting for SERCA2a protein expression. With respect to the experimental controls, the protein expression of SERCA2a was the significantly greater under the CRISPR Vector and significantly high when the TFAM Vector applied. The bands were quantified using densitometry and the data was graphed for an N of 6 using SEM for significance. Values are expressed as +/- SEM. N=6. * $p < 0.05$, ** $p < 0.025$, *** $p < 0.001$.

41

Figure 6. CRISPR-Cas9 (TFAM) vector treatment increases NFAT4 Expression.

Fig. 6A. These images (i-v) captured by confocal microscopy and ICC provide intra-cellular visualizations of NFAT4 within the corresponding experimental groups.

Fig. 6B. This graph exhibits the fluorescent intensity of NFAT4 that was provided by the data collected from the Image J software. Each fluorescent intensity corresponds to NFAT4 presence within a specific experimental group. With respect to the experimental controls, the intensity of NFAT4 was the significantly greater under the CRISPR Vector

Fig. 6C. This graph displays NFAT4 proteins expression in HL-1 cardiomyocytes treated with TFAM over-expression vectors, CRISPR-cas9 vectors and experimental controls. HL-1 cells were treated with 1.0 micrograms of vectors for 48 hours before harvesting. Lysates were analyzed by western blotting for NFAT4 protein expression. With respect to the experimental controls, the protein expression of NFAT4 was the significantly greater under the CRISPR Vector. The Bands were quantified using densitometry and the data was graphed for an N of 6 using SEM for significance. Values are expressed as +/- SEM. N=6. * $p < 0.05$, ** $p<0.025$.
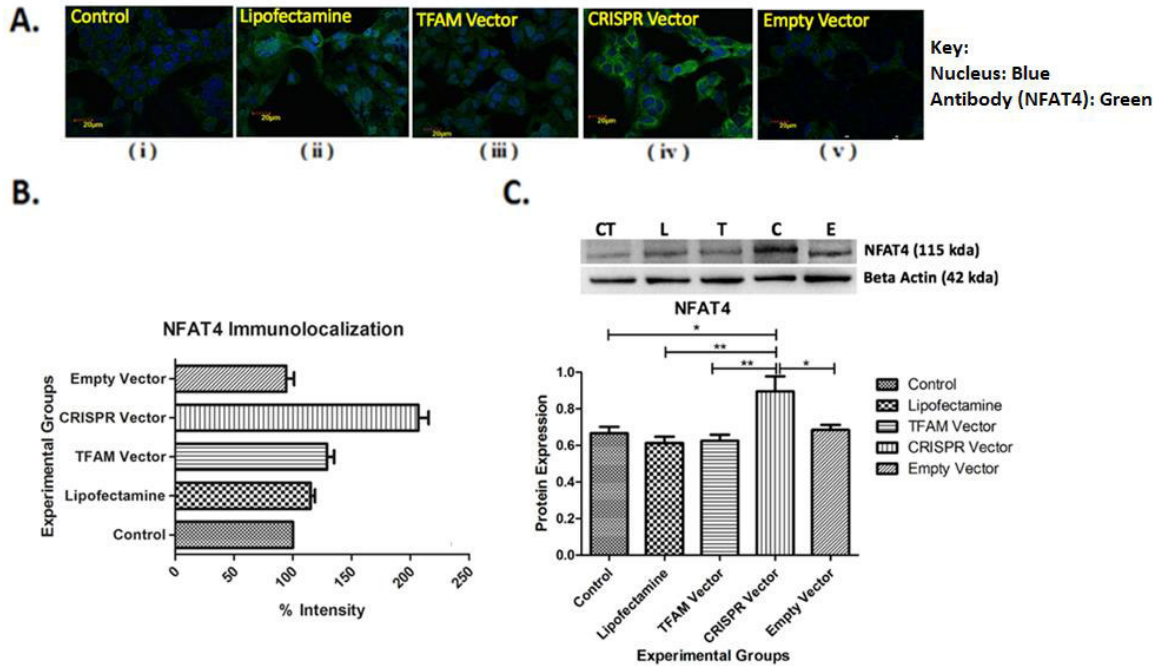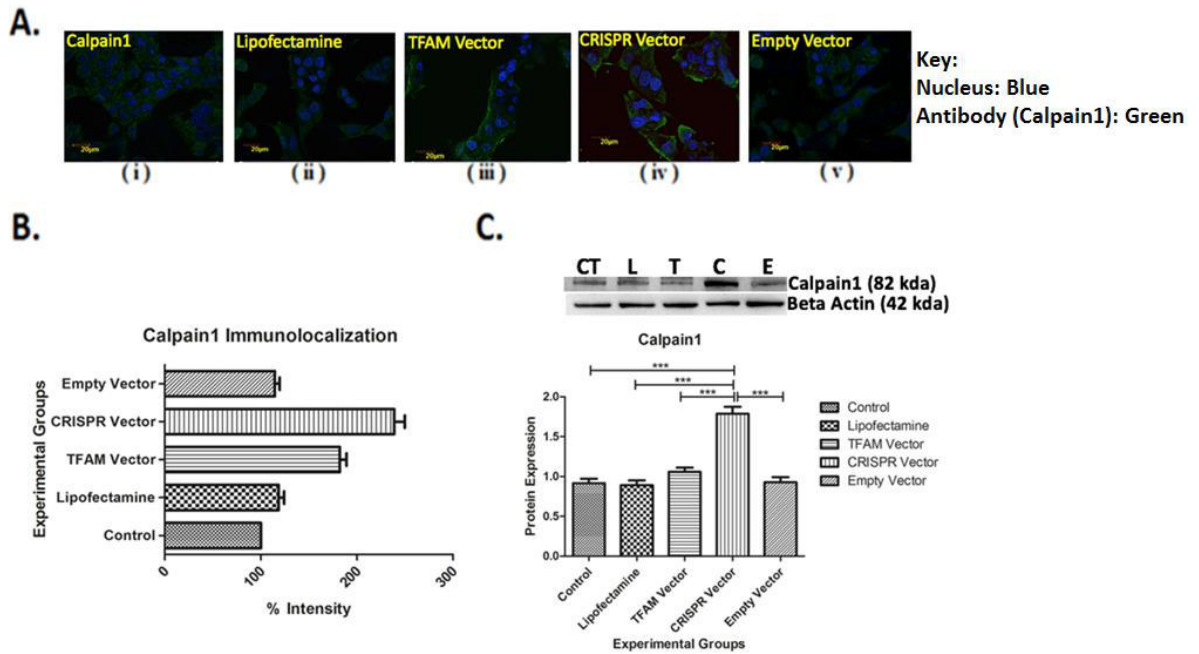
42

Figure 7. CRISPR-Cas9 (TFAM) vector treatment increases Calpain 1 expression.

Fig. 7A. These images (i-v) captured by confocal microscopy and ICC provide intra-cellular visualizations of Calpain 1 within the corresponding experimental groups.

Fig. 7B. This graph exhibits the fluorescent intensity of Calpain 1 that was provided by the data collected from the Image J software. Each fluorescent intensity corresponds to Calpain 1 presence within a specific experimental group. With respect to the experimental controls, the intensity of Calpain 1 was the significantly greater under the CRISPR Vector

Fig. 7C. This graph displays Calpain 1 proteins expression in HL-1 cardiomyocytes treated with TFAM over-expression vectors, CRISPR-cas9 vectors and experimental controls. HL-1 cells were treated with 1.0 micrograms of vectors for 48 hours before harvesting. Lysates were analyzed by western blotting for Calpain 1 protein expression. With respect to the experimental controls, the protein expression of Calpain 1 was the significantly greater under the CRISPR Vector. The bands were quantified using densitometry and the data was graphed for an N of 6 using SEM for significance. Values are expressed as +/- SEM. N=6. *** $p < 0.001$.
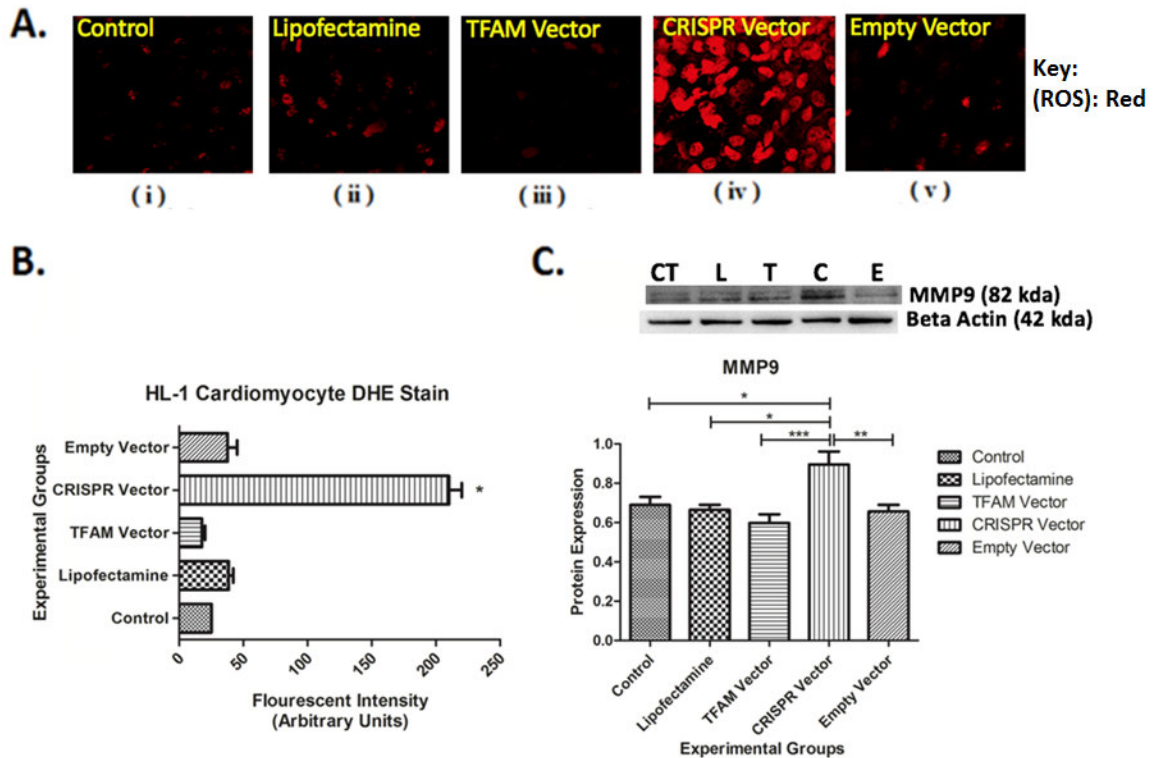
Figure 8. CRISPR-Cas9 (TFAM) vector treatment increases MMP9 Expression.

Fig. 8A. These dihydroethidium staining images (i-v) captured by confocal microscopy provide intra-cellular visualizations of MMP9 within the corresponding experimental groups.

Fig. 8B. This graph exhibits the fluorescent intensity of MMP9 that was provided by the data collected from the Image J software. Each fluorescent intensity corresponds to MMP9 presence within a specific experimental group. With respect to the experimental controls, the intensity of MMP9 was the significantly greater under the CRISPR Vector

Fig. 8C. This graph displays MMP9 proteins expression in HL-1 cardiomyocytes treated with TFAM over-expression vectors, CRISPR-cas9 vectors and experimental controls. HL-1 cells were treated with 1.0 micrograms of vectors for 48 hours before harvesting. Lysates were analyzed by western blotting for MMP9 protein expression. With respect to the experimental controls, the protein expression of MMP9 was the significantly greater under the CRISPR Vector. The bands were quantified using densitometry and the data was graphed for an N of 6 using SEM for significance. Values are expressed as +/- SEM. N=6. * p < 0.05, ** p<0.025, *** p<0.001.

44
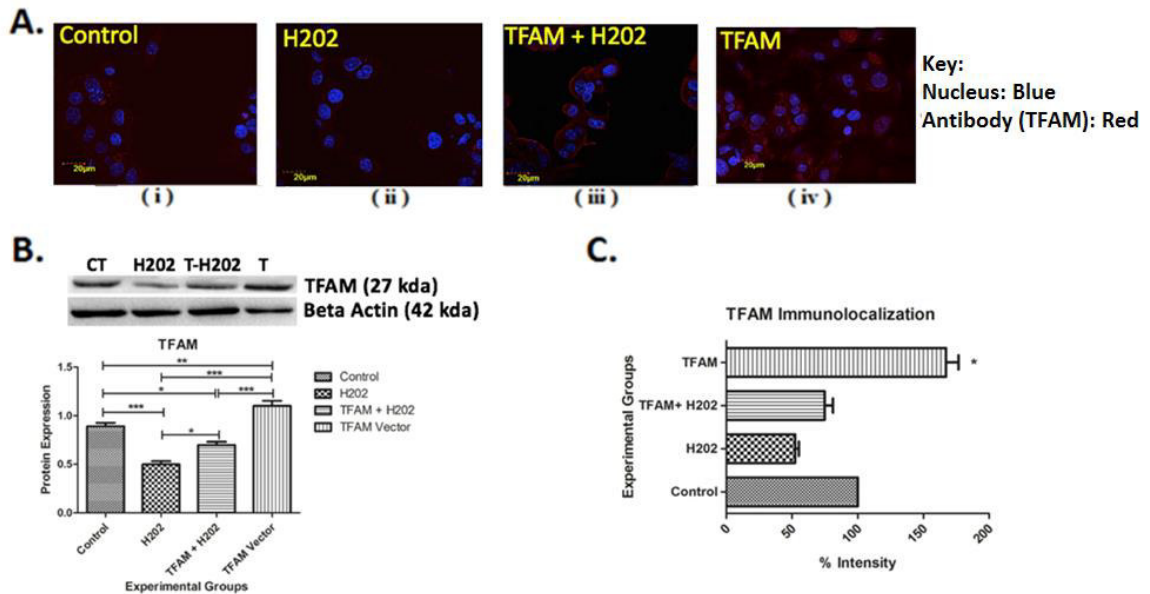
Figure 9. Hydrogen Peroxide treatment reduces TFAM expression & TFAM vector increases TFAM expression.

Fig. 9A. These images (i-iv) captured by confocal microscopy and ICC provide intra-cellular visualizations of TFAM within the corresponding experimental groups.

Fig. 9B. This graph displays TFAM proteins expression in HL-1 cardiomyocytes treated with a TFAM over-expression vector, H_2O_2, a TFAM & H_2O_2 vector combination and a control. HL-1 cells were treated with 1.0 micrograms of vectors for 48 hours before harvesting. Lysates were analyzed by western blotting for TFAM protein expression. With respect to the experimental controls, the protein expression of TFAM was the significantly greater under the H_2O_2 Vector. The bands were quantified using densitometry and the data was graphed for an N of 6 using SEM for significance. Values are expressed as +/- SEM. N=6. * $p < 0.05$, ** $p<0.025$, *** $p<0.001$.

Fig. 9C. This graph exhibits the fluorescent intensity of TFAM that was provided by the data collected from the Image J software. Each fluorescent intensity corresponds to TFAM presence within a specific experimental group. With respect to the experimental controls, the intensity of TFAM was the significantly greater under the significantly greater under the H_2O_2 Vector.
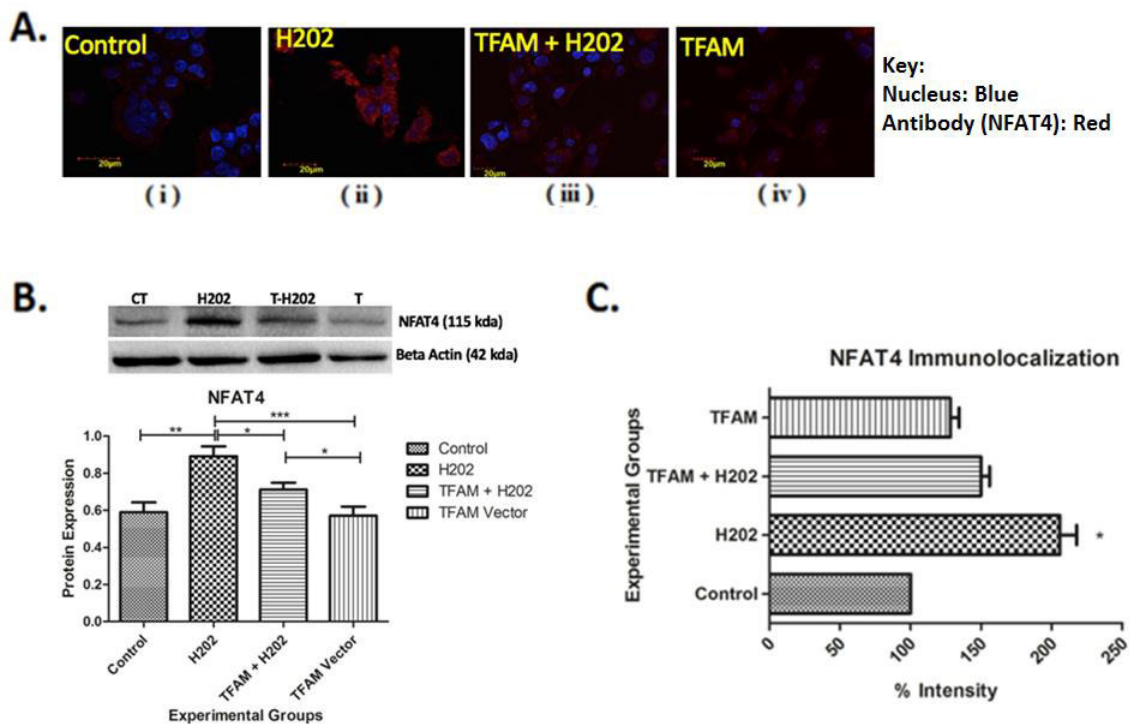
Figure 10. Hydrogen Peroxide treatment increases NFAT4 expression

Fig. 10A. These images (i-iv) captured by confocal microscopy and ICC provide intra-cellular visualizations of NFAT4 within the corresponding experimental groups.

Fig. 10B. This graph displays NFAT4 proteins expression in HL-1 cardiomyocytes treated with a NFAT4 over-expression vector, H_2O_2, a TFAM & H_2O_2 vector combination and a control. HL-1 cells were treated with 1.0 micrograms of vectors for 48 hours before harvesting. Lysates were analyzed by western blotting for NFAT4 protein expression. With respect to the experimental controls, the protein expression of NFAT4 was the significantly greater under the H_2O_2 Vector. The bands were quantified using densitometry and the data was graphed for an N of 6 using SEM for significance. Values are expressed as +/- SEM. N=6. * $p < 0.05$, ** $p<0.025$, *** $p<0.001$.

Fig. 10C. This graph exhibits the fluorescent intensity of NFAT4 that was provided by the data collected from the Image J software. Each fluorescent intensity corresponds to NFAT4 presence within a specific experimental group. With respect to the experimental controls, the intensity of NFAT4 was the significantly greater under the H_2O_2 Vector.
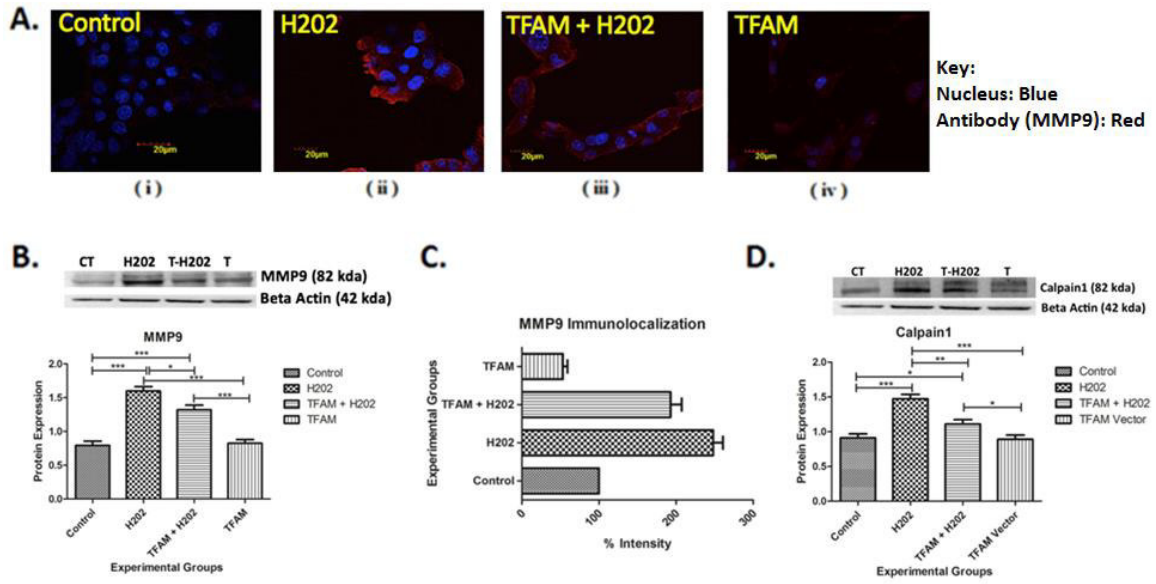
Figure 11. Hydrogen Peroxide treatment increases MMP9 expression and Calpain 1 expression.

Fig. 11A. These images (i-iv) captured by confocal microscopy and ICC provide intra-cellular visualizations of MMP9 within the corresponding experimental groups.

Fig. 11B. This graph displays MMP9 proteins expression in HL-1 cardiomyocytes treated with a MMP9 over-expression vector, H_2O_2, a TFAM & H_2O_2 vector combination and a control. HL-1 cells were treated with 1.0 micrograms of vectors for 48 hours before harvesting. Lysates were analyzed by western blotting for MMP9 protein expression. With respect to the experimental controls, the protein expression of MMP9 was the significantly greater under the H_2O_2 Vector. The bands were quantified using densitometry and the data was graphed for an N of 6 using SEM for significance. Values are expressed as +/- SEM. N=6. * $p < 0.05$, *** $p < 0.001$.

Fig. 11C. This graph exhibits the fluorescent intensity of MMP9 that was provided by the data collected from the Image J software. Each fluorescent intensity corresponds to MMP9 presence within a specific experimental group. With respect to the experimental controls, the intensity of MMP9 was the significantly greater under the H_2O_2 Vector

Fig. 11D. This graph displays Calpain 1 proteins expression in HL-1 cardiomyocytes treated with a Calpain 1 over-expression vector, H_2O_2, a TFAM & H_2O_2 vector combination and a control. With respect to the experimental controls, the protein expression of Calpain 1 was the significantly greater under the H_2O_2 Vector. The bands were quantified using densitometry and the data was graphed for an N of 6 using SEM for significance. Values are expressed as +/- SEM. N=6. * $p < 0.05$, ** $p < 0.025$, *** $p < 0.001$

47

CHAPTER IV

TFAM'S PROTECTIVE ROLE
IN PATHOLOGICAL REMODELING

Introduction

Hypertensive heart disease and HF are the leading causes of death in the United States (Mozaffarian et al. 2016). HF is characterized by activation of cell death pathways and mechanisms of degradation (Givvimani et al. 2014). The culmination of Ca^{2+} mishandling and ROS-driven degradation within cardiomyocytes leads to a functional decline of the myocardium and hypertrophic expansion, as is observed in the HF models discussed later in this chapter. TFAM's inhibitory function to mitigate molecular abnormalities has previously resulted in cardioprotective effects when over-expressed (Kunkel, Chaturvedi, and Tyagi 2016). A mechanistic analysis of TFAM's protective role in pathological cardiac remodeling gives further insight into both TFAM's inhibitory effect on the NFAT-ROS-MMP9 pathway and regulatory effect on the SERCA2a-Calpain 1 pathway.

The usage of animal models to study cardiac hypertrophy and HF is vital to further elucidation of pathophysiological mechanisms. Rickman et al. developed the murine TAC procedure, also known as aortic banding. TAC narrows the transverse aorta, causing both a pressure increase in the left ventricular chamber and the

48

resultant force required for blood ejection. Increased resistance within this model causes a pressure overload, resulting in severe hypertension and heart failure.

Calpain 1 is responsible for the degradation of contractile proteins, initiation of mitochondrial-driven apoptosis, and decrease of Ca^{2+} transporters in HF (Patterson et al. 2011; Chen et al. 2002; Wanichawan et al. 2014). Heart failure patients exhibit marked increases in calpains (Yang et al. 2010). Within the Ca^{2+}-driven catabolic pathway, Ca^{2+} activates and increases the expression of calpain proteases and the Ca^{2+}-calcineurin-NFAT cascade that promotes pathological hypertrophy and activates NADPH oxidases to increase ROS production (Williams and Gooch 2014).

NFAT is a pathological hypertrophic gene regulator and inducer of ROS via activation of NADPH oxidases (Chang et al. 2016; Williams and Gooch 2014). NFAT increases in cardiac remodeling and hypertrophy (Houser and Molkentin 2008). Cytoplasmic Ca^{2+} increases maladaptive factors NFAT4 and calpain 1.

MMP9 is a known pathological indicator of HF, and its expression is highly up-regulated in the pathological myocardium (Mujumdar, Smiley, and Tyagi 2001). In alignment with this logic, the erasure of MMP9 evokes opposite effects: targeted deletion of MMP9 prevents cardiac dysfunction (Prathipati et al. 2016). Inhibitors of MMP9 are reduced in heart failure, allowing for MMP9 propagation (Chaturvedi and Tyagi 2016). Early-stage aortic banding results in inhibition of MMP9, but sustained mechanical overload causes de-compensatory heart failure, leading to increased MMP9 expression and cardiac fibrosis in end-stage heart failure. As aforementioned, activation of MMP9 increases extracellular matrix turnover in the failing heart,

resulting in increased apoptotic signaling in pressure overload heart failure (Mishra et al. 2013). Mitochondrial dysfunction induces ROS production, activating MMPs in cardiomyocytes. Superoxides create stress, potentially mutating and damaging mitochondrial DNA.

TFAM physically wraps around mitochondrial DNA, forming a mitochondrial nucleoid; it is essential to mitochondrial biogenesis. One transcriptional function of TFAM is regulation over factors such as NFAT and SERCA2a, which provides insight into reducing Ca^{2+} mishandling and ROS production (Watanabe et al. 2011; Fujino et al. 2012). Within TFAM over-expression models, it is observed that proteolytic enzyme MMP9 is reduced in MI-induced HF, along with functional morphologies (Ikeuchi et al. 2005). Contrastingly, our previous study shows that CRISPR-CAS9 knockdown of TFAM induces the activation of proteases MMP9 and Calpain 1, as well as pathological hypertrophic stimulator and ROS-producer NFAT4 (Kunkel et al. 2017).

The purpose of this study is to investigate the role of TFAM over-expression in cardiac remodeling within the TAC HF model. We hypothesized that TFAM over-expression would reduce molecular remodeling factors and associated morphologies. We examined whether TFAM over-expression would reduce molecular hypertrophic and proteolytic factors involved in adverse remodeling. Our results affirm that TFAM over-expression in TAC HF models reduces cardiac hypertrophy and molecular hypertrophic factors.

Materials and Methods

Animal Models & Experimental Design

Wild type mice (WT, C57/BL6/J) were purchased from the Jackson Laboratory (Bar Harbor, ME). TFAM transgenic mice were procured from Cyagen Biosciences (Santa Clara, CA,USA) and housed in the animal care facility at the University of Louisville with access to standard chow and water. The aortic banding surgical procedure was performed in mice of 8-10 weeks of age with starting weights of 22-26 grams. The groups were further divided into Control Sham, Control TAC, TFAM Sham and TFAM TAC. Animals were euthanized according to National Institute of Health Guidelines for animal research and were reviewed and approved by the Institute of Animal Care and use committee of the University of Louisville (IACUC #16684 & 14028)

Genotyping

The TFAM transgenic mice background was confirmed according to the Cyagen Bioscience protocol for genotyping. Samples from the tails of the mice were collected for DNA extraction. DNA was amplified with TFAM Primer sets and run on PCR. The PCR product samples were run on a 1.2% agarose gel containing [Acetic Acid, Tris Base, EDTA, pH 8.4] with ethidium bromide. Gel images were recorded on a Bio-Rad gel documentation system (Bio-Rad, Hercules, CA). The

transgenic TFAM gene yields a product size of 363 bp in a 2% agarose gel and is observed in the BioRad ChemiDoc.

Antibodies and Reagents

All primary antibodies were purchased from Abcam (Cambridge, United Kingdom). Horseradish peroxidase (HRP)-conjugated secondary antibodies were purchased from Santa Cruz Biotechnology (Dallas, Texas, USA). Fluorescent secondary antibodies and lipofectamine 2000 reagent was purchased from Life Technologies (Carlsbad, California, USA).

Western Blot Analysis

Post- a 48-hour treatment period, HL-1 cell protein was isolated using protein extraction buffer (RIPA lysis buffer, protease inhibitor cocktail and PMSF). Wells were scraped and the contents transferred to ependorf tubes. Lysates were spun in extraction buffer for 12 hours and then centrifuged at 12,000g for 15 min. Supernatant was transferred to new tubes and protein concentrations were analyzed via Bradford protein estimation assay. Samples were run on a 10/12% sodium dodecylsulfate (SDS)-polyacrylamide gel with Tris-glycine SDS buffer. The gel was transferred electrophoretically overnight onto a PVDF membrane at 4°C. The membrane was blocked with a 5% milk solution for 1 hour. Primary antibodies were diluted at a concentration 1:1000 in TBST and incubated on the membrane overnight. All membranes were washed in TBST solution 4 times and then incubated with

secondary HRP conjugated antibody solution for 1 hour at room temperature. Four TBST washing steps followed before membranes were developed using a chemiluminescent substrate in a BioRad Chemidoc (Hercules, Calif.). Band intensity was determined using densitometry analysis. Beta-actin was used to normalize protein loading.

Immunohistochemistry

Post- cell treatment, media was aspirated from each well of the eight well chamber slide and cells were rinsed with PBS. Cells were fixed at room temperature in 4% paraformaldehyde solution for 20 min and washed 3 times with PBS. Blocking was performed with a mixed solution of 2% bovine-serum-albumin (BSA) and 0.025% Triton X-100. Cells were permeabilized for 1 hour. All primary antibodies were incubated in the chamber slide at a concentration of 1:100 overnight at 4°C. The wells were aspirated, washed 3 times and incubated for 90 min with the secondary antibody (1:200) at room temp. The chamber slides were washed 3 times more, and DAPI was added at 1:10,000 for 10 min. This analysis was observed via Confocal microscopy.

Blood Pressure

Non-invasive tail cuff method was used to measure blood pressure in conscious mice (CODA, Kent Scientific, Torrington CT). Animals were allowed time to acclimate to chambers and warming pad prior to data recordings. BP was recorded under standard conditions.

Ultrasound

Through Vevo 2100 imaging system, cardiac and aortic data was collected in pre-surgical and post-surgical animal models. Post epilation the animal is placed supine on a warm platform (37°C), under isoflourane anesthesia and fixed. Using a MS550D (22-25 mHz) transducer, the thoracic cavity was imaged. Aortic arch velocity and cardiographic function were assessed in pulse wave and color Doppler modes.

Cryosectioning

Cardiac tissue was preserved in plastic tissue embedding molds (polysciences) containing tissue freezing media (Triangle Biosciences, Durham, NC). Tissues were stored at -80°C. Sections of 8μm were created using a cryocut (leica CM 1850). Cryosections were placed on superfrost plus (lysine coated) microscope slides and stored at -80°C for further use.

Histology Staining

To measure the deposition of collagen within the myocardium, tissue sections were stained with a Masson's Trichrome kit following all manufacturer's instructions. Collagen deposition is represented as a blue color. Images were captured with a light microscope (Olympus Fluoview1000). Additionally, sections were stained with Hemotoxylin - Eosin stain to show general morphology.

Statistical Analysis

Data are expressed as means ± SE. Statistical analysis was performed by Graphpad Prism software using a one-way ANOVA followed by a Bonferoni comparison test. $P<0.05$ was considered statistically significant.

Results

Verification of Aortic Banding Procedure

Through genotyping PCR we confirmed Cyagen Biosciences TFAM transgenic mouse protocol to ensure pups are genetically modified with TFAM over-expression. TFAM gene is overexpressed at 363 base pairs (Fig 12). The aortic banding procedure is verified via ultrasound, at which high aortic arch velocity, as well as turbulence, is seen at the transverse aorta, comparing WT & TFAM sham groups to the aortic banded counterpart ($p < 0.001$) (Fig 14). Pictographic representation of resultant outcome post banding (Fig 13)

Effect of Aortic Banding on Cardiac Function

TFAM Over-expression Reduced Cardiac Hypertrophy

Figure 17A shows a pictographic image of C57 and TFAM-TG mice subjected to aortic banding and visually comparing the hearts. This image shows a significant visual difference is found when comparing the TAC and sham groups and the C57 TAC to the TFAM-TG TAC model. Heart weight is significantly increased in the C57 TAC group compared to the C57 sham, TFAM sham and TFAM TAC group (Fig. 17B). The heart weight/body weight (Hw/Bw) ration was also significantly increased in both the C57 TAC and TFAM TAC groups. The C57 TAC group had significantly increased Hw/Bw ratio when compared to the C57 sham, TFAM sham and the TFAM TAC (Fig. 17C). Additionally, a weight gain is observed within the

banded animals. The C57 TAC gained approximately 2 grams more than the sham group and 1 gram more than the TFAM-TAC group (Fig. 17D).

Analysis of Echocardiography and Blood Pressure Results

Echocardiography and blood pressure analysis show significant differences between the aortic banded and sham animals. Ejection fraction (EF) of both TFAM-TG and WT banded groups showed a significant reduction in comparison to respective shams (Fig 15). Changes in LV mass post banding were also observed, significantly increased LV mass was found within the C57 TAC & TFAM TAC groups when compared to the Sham groups. Additionally, a significant increase in LV mass was found in the C57 TAC group when compared to the TFAM TAC group. Cardiac muscle hypertrophy is a compensatory response to pressure overload (Fig. 15). Within the table (Table.1), we observe that many significant functional changes occur during pressure overload heart failure, as is observed when comparing the Sham and TAC groups. Functional differences are also observed between the WT surgical model and the TFAM-TG model, such differences include increased fractional shortening, LV volume in systole, LV Mass, LV volume in systole had a significant increase in volume in the C57 TAC compared to the C57 sham (Table. 1). Variations exist between the TFAM transgenic and its wildtype counterpart suggesting that known and unknown mechanisms of mitochondrial protection are inhibiting functional decline in the failing myocardium.

57

The Physiological functional assessment of hemodynamic blood pressure measurements was observed at three-time points: 0, 4, 8 weeks, via CODA tail cuff blood pressure system. Time point 0 was a pre-surgical assessment and is used as a baseline. At 4 weeks, severe hypertension is observed in both TAC groups and is significantly higher than the sham group (Fig. 16). Between four weeks and eight weeks the C57 group maintains a trending decline in systolic blood pressure, this functional change is associated with cardiac remodeling allowing for the heart to adapt to the pressure overload through hypertrophic expansion (Fig. 16A). The TFAM TAC group maintains a higher systolic blood pressure than the C57 TAC group in the four to eight-week time point, therefore a functional difference remains between the C57 and TFAM TAC animals. Diastolic blood pressure was assessed and revealed a significant difference between the C57 TAC and TFAM TAC groups and their sham counterparts at both 4 and 8-week time points (Fig. 16B). Mean blood pressure assessment showed a significant difference between the C57 TAC and TFAM TAC groups and their sham counterparts (Fig. 16C).

TFAM Over-expression Reduced Histopathologies in HF Mice

Hemotoxylin & Eosin Staining (H&E), pink color represents myofibers, Purple color is Nuclei. In the C57 TAC we observed misplaced/off centered nuclei and a dysregulated arrangement of cardiac myofibers, as well as a deformation in size and shape. Additionally, an inflammatory response is observed within the WT TAC tissue subjected to aortic banding. The nuclei of the C57 TAC group are in a

disarrayed pattern compared to all other groups. The TFAM-TG group subjected to banding shows a deformation of cardiac myofibers but is not as significant as the WT TAC group (Fig. 18A).

Through mason trichrome staining we observed histopathologies involved in HF. Muscle is red and collagen is blue. Comparisons between the C57 TAC group and the C57 Sham show a significant increase in collagen in the TAC model. This major significance was not observed when comparing the TFAM-TG and its Sham counterpart (Fig. 18B).

The Effect of TFAM Over-expression on the NFAT-ROS-MMP9 Pathway

TFAM efficacy in transgenic models was confirmed via western blotting and immunohistochemistry for TFAM. Fluorescent intensity was observed via confocal microscopy (Fig. 19A). Concluding that the TFAM sham had significantly increased TFAM fluorescent intensity (Fig. 19B). Western blotting confirmed a significant increase in TFAM protein expression in both TFAM sham and TFAM TAC models. There was a significant decrease in TFAM protein expression in the C57 TAC model (Fig. 19C).

Determining if TFAM overexpression affected NFAT4, we observe NFAT4 fluorescent intensity and Western blotting. The C57 TAC group had significantly increased NFAT4 expression compared to all groups (Fig. 20A & B). The TFAM TAC group had significantly higher NFAT4 protein expression in comparison to its sham (Fig 20C). These findings were observed in Western blotting and IHC. MMP9

fluorescent intensity is increased in the C57 TAC model in comparison to the C57 sham, TFAM sham and TFAM TAC (Fig. 21A &B). Western blotting analysis revealed a significant increase in MMP9 protein expression (Fig. 21C). TFAM overexpression plays a role in the NFAT-ROS-MMP9 pathway.

The Effect of TFAM Over-expression on The SERCA2a-Calpain1 Pathway.

Analysis of protein expression from cardiac tissue of mice subjected to aortic banding and sham controls show that SERCA2a is significantly decreased in pressure overload HF. Through Western blotting and immunohistochemistry, the SERCA2a-Calpain1 pathway was observed for protein and fluorescent expression. Fluorescent intensity was viewed via confocal microscopy. Both aortic banded groups C57 & TFAM-TG had significantly decreased SERCA2a expression. This was observed in western blotting and IHC (Fig.23 A, B&C).

Analyzing if TFAM overexpression affected calpain1, we observed calpain1 fluorescent intensity and protein expression. The C57 TAC and TFAM-TG group had significantly increased calpain1 protein expression as observed through western blotting. Fluorescent intensity was also as equally increased in IHC. TFAM may play a role in physiological SERCA2a expression but this activity is not observed in our study (Fig.22 A, B&C).
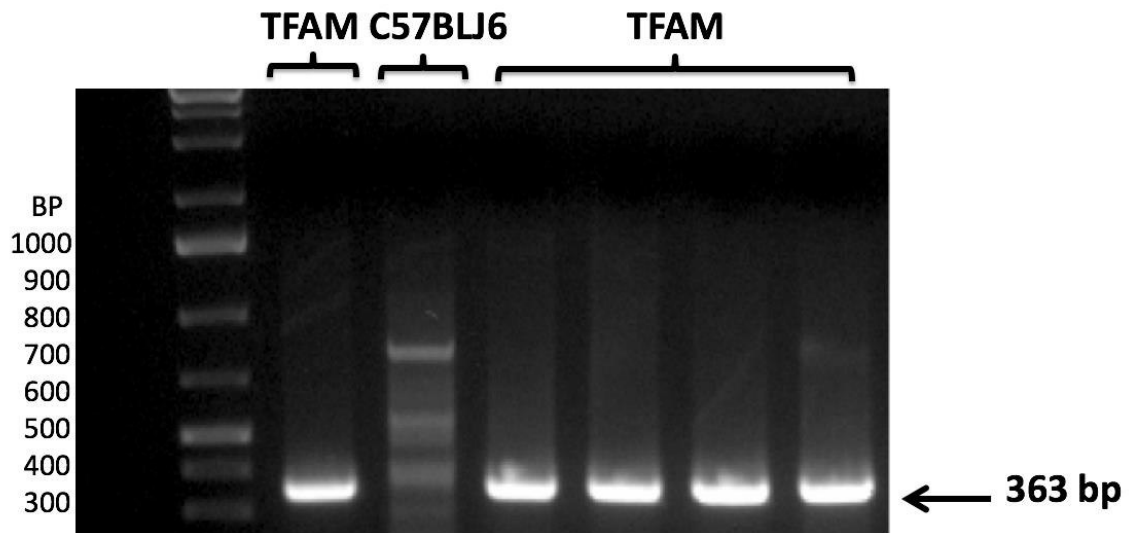
Figure 12. Genotyping PCR for TFAM Gene in TFAM and C57 (WT) Mice

Fig. 12. Genotyping for TFAM gene in TFAM transgenic and C57BLJ6 mice. As per Cyagen Biosciences protocol, primers for TFAM gene expression are identified at 363 bp in a 1% agarose gel and analyzed via BioRad ChemiDoc.
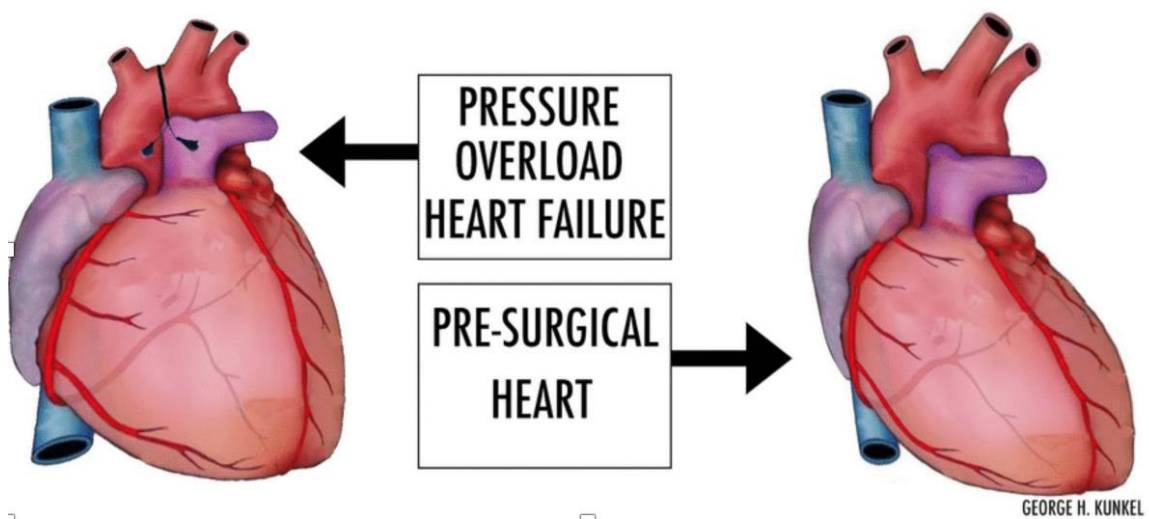
Figure 13. Effect of Pressure Overload on Myocardium

Fig. 13. Pictographic representation of the transformation of the myocardium from a pre-surgical heart to a pressure overload aortic banding model, 8 weeks post-surgery. Cardiac remodeling and hypertrophic factors expand the left ventricular wall.
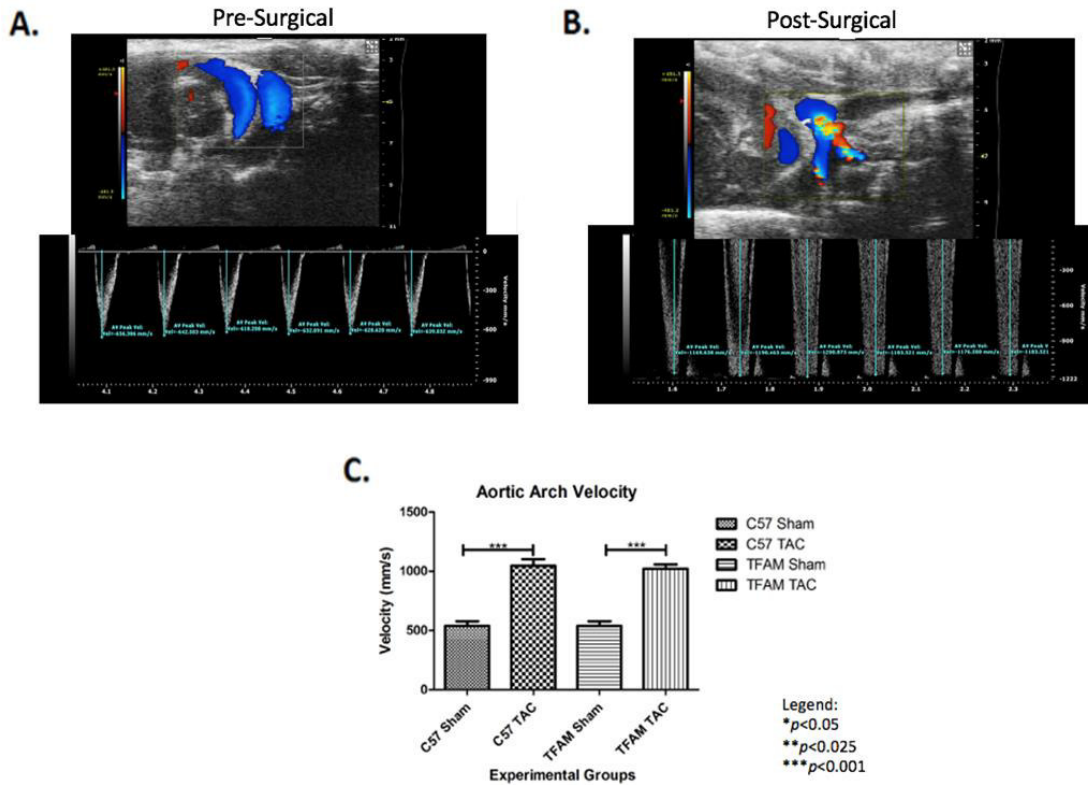
Figure 14. Aortic Banding significantly increased Aortic Arch Velocity (AAV).

Fig. 14A. The top, an ultrasound-echocardiographic snapshot, displays blood flow through the aorta of a particular pre-surgical mouse performed with a Vevo 2100 ultrasound pulse wave and color doppler analysis. As indicated by the blue coloration, the blood flow is rhythmically non-turbulent. Below, the respective real-time graph of AAV versus time displays a consistent AAV average value of 636.14 mm/s.

Fig. 14B. The ultrasound-echocardiographic snapshot shows blood flow through the aorta performed with a Vevo 2100 ultrasound pulse wave and color doppler analysis. As indicated by the blue-red-yellow amalgamation, the blood flow is rhythmically turbulent. The respective real-time graph of AAV versus time displays an increased AAV average value of 1184.10 mm/s from its pre-surgical value seen in 14A.

Fig. 14C. This graph displays the AAV corresponding to the specified experimental groups and the data was graphed for an N of 6 using SEM for significance. The substantial increase in aortic velocity from C57 Sham group to the C57 TAC group and the substantial increase from TFAM Sham group to the TFAM TAC group verify that the surgery worked. Values are expressed as +/- SEM. N=6. *** $p < 0.001$.
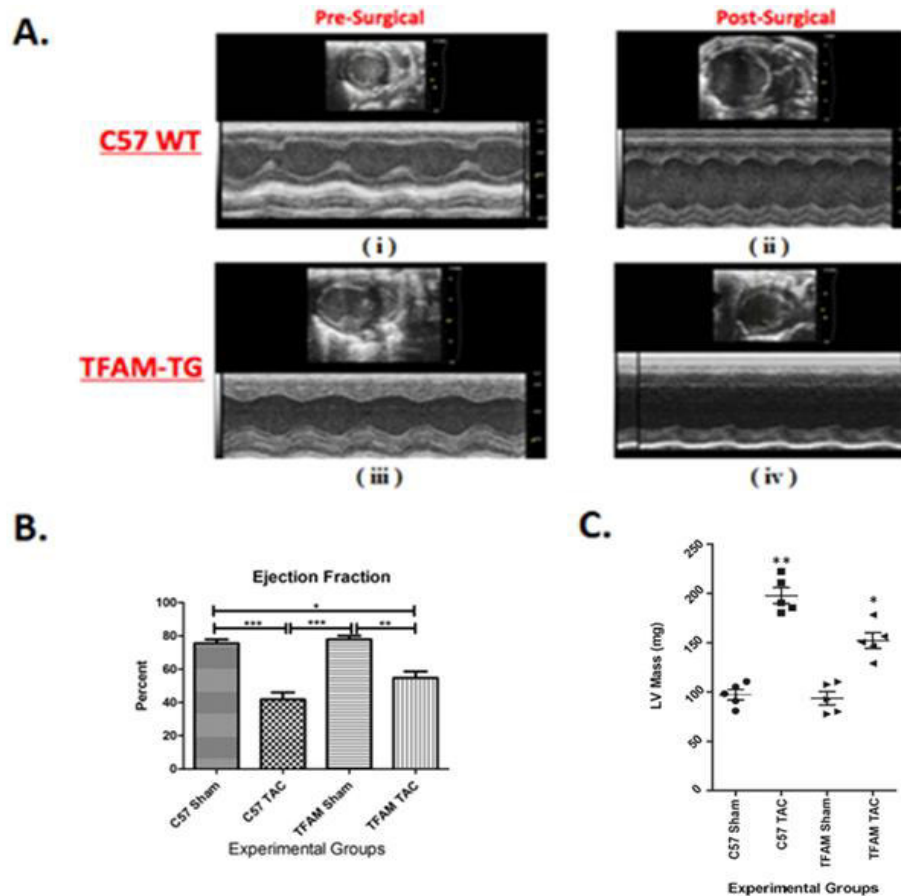
Figure 15. Reduced Ejection Fraction (EF) and increased Left Ventricular LV Mass in HF.

Fig. 15A. These images (i-iv) captured by echocardiographic-ultrasound corresponding to the specified experimental groups and data taken after 8 weeks. The specified values taken from these images correspond to the values discussed in Table 1.

Fig. 15B. This graph displays the EF corresponding to the specified experimental groups and the data was taken after 8 weeks. The significant decrease in EF from C57 Sham group to the C57 TAC group and the significant decrease from TFAM Sham group to the TFAM TAC group verify that the aortic banding induced HF. Values are expressed for an N of 6 using SEM for significance as +/- SEM. N=6. * p < 0.05, ** p < 0.025, *** p<0.001.

Fig. 15C. This graph displays the LV mass corresponding to the specified experimental groups and the data was taken after 8 weeks. The significant increase in LV mass from C57 Sham group to the C57 TAC group and the significant increase from TFAM Sham group to the TFAM TAC group verify that the aortic banding induced HF. Values are expressed for an N of 6 using SEM for significance as +/- SEM. N=6. * p < 0.05, ** p < 0.025.

64

| Groups	Baseline				8 -week			
	N = 6	N = 7	N = 6	N = 6	N = 6	N = 5	N = 6	N = 5
	C57 Sham	C57 TAC	TFAM Sham	TFAM TAC	C57 Sham	C57 TAC	TFAM Sham	TFAM TAC
IVS$_d$ (mm)	0.65 ± 0.03	0.60 ± 0.04	0.62 ± 0.02	0.61 ± 0.03	0.60 ± 0.02	0.88 ± 0.02***###	0.64 ± 0.02	0.79 ± 0.03***###
LVD$_d$ (mm)	3.49 ± 0.15	3.57 ± 0.22	3.6 ± 0.07	3.53 ± 0.14	3.58 ± 0.05	4.13 ± 0.09*#	3.7 ± 0.08	3.97 ± 0.12*#
LVPW$_d$ (mm)	0.63 ± 0.02	0.67 ± 0.03	0.61 ± 0.04	0.65 ± 0.01	0.64 ± 0.07	0.97 ± 0.05***##	0.65 ± 0.01	0.88 ± 0.09***##
LVD$_s$ (mm)	1.74 ± 0.11	1.81 ± 0.08	1.85 ± 0.08	1.80 ± 0.10	1.91 ± 0.15	2.98 ± 0.15***###	1.94 ± 0.09	2.45 ± 0.07***###
LV Vol$_d$ (ml)	58.2 ± 5.32	61.4 ± 3.88	60.9 ± 5.14	65.3 ± 3.21	63.24 ± 4.06	88.6 ± 4.35*#	62.05 ± 3.54	72.4 ± 3.86*#$
LV Vol$_s$ (ml)	9.12 ± 0.88	10.24 ± 1.56	10.12 ± 1.04	11.48 ± 2.56	10.81 ± 2.09	66.54 ± 5.63***###	11.12 ± 2.08	48.39 ± 4.11**###$
EF (%)	81.7 ± 2.01	80.1 ± 1.35	82.4 ± 1.21	82.8 ± 1.19	81.6 ± 1.83	48.4 ± 3.69***###	80.2 ± 1.85	53.1 ± 4.81***###
FS (%)	48.2 ± 1.58	49.4 ± 1.08	48.6 ± 1.32	49.6 ± 1.78	49.5 ± 0.82	24.2 ± 1.84***###	48.4 ± 0.9	28.32 ± 4.64***###
LV Mass (mg)	75.5 ± 4.62	78.4 ± 5.51	82.4 ± 3.8	84.2 ± 4.28	81.6 ± 5.6	191.6 ± 16.9***###	83 ± 4.84	164 ± 13.67***###$
HR (beats/min)	640 ± 27	690 ± 11.4	670 ± 33	648 ± 23	694 ± 15	701 ± 11	686 ± 10	691 ± 18

Table 1. Echocardiographic measurements of TFAM-TG mice at baseline and 8 weeks after sham/TAC surgery.

Table. 1. The table above depicts the echocardiographic measurements after 8 weeks of aortic banding surgery. The groups above signify the following:

(1) IVS$_d$, intra-ventricular septal diameter, (2) LVD$_d$, Left ventricular dimension in diastole, (3) LVPW$_d$, left ventricular posterior wall diameter, (4) LVD$_s$, left ventricular dimension in systole, (5) LV Vol$_d$, left ventricular volume in diastole, (6) LV Vol$_s$, left ventricular volume in systole, (7) EF, ejection fraction, (8) FS, fractional shortening, (9) LV, left ventricular, (10) HR, heart rate. ***$p < 0.001$, **$p < 0.025$, *$p < 0.05$ vs baseline in the same group; ###$p < 0.001$, ##$p < 0.025$, #$p < 0.05$ vs sham in the same group at the same time point; $$$$p < 0.001$, $$$p < 0.025$, $$p < 0.05$ vs TAC-operated WT mice. Values are expressed as +/- SEM.

65
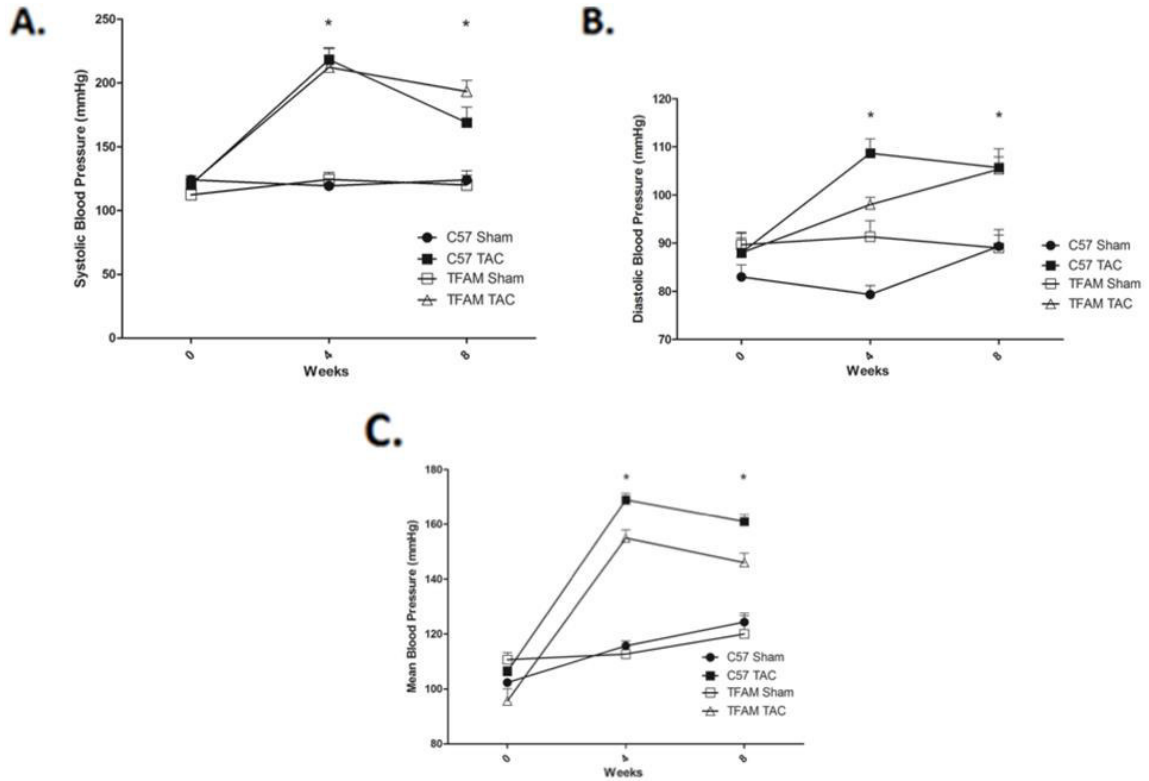
Figure 16. Increased Systolic and Diastolic Blood Pressure Post Banding.

Fig. 16A. This graph displays the Systolic Blood Pressure measured by the CODA (Tail-cuff) blood pressure system. The values correspond to the specified experimental groups throughout the course of 8 weeks. The significant decline occurs after 4 weeks. Values are expressed as +/- SEM. N=5; * $p < 0.05$, ** $p < 0.025$, *** $p<0.001$.

Fig. 16B. This graph displays the Diastolic Blood Pressure measured by the CODA (Tail-cuff) blood pressure system. The values correspond to the specified experimental groups throughout the course of 8 weeks. The significant decline occurs after 4 weeks. Values are expressed as +/- SEM. N=5; * $p < 0.05$, ** $p < 0.025$, *** $p<0.001$.

Fig. 16C. This graph displays the Mean Blood Pressure measured by the CODA (Tail-cuff) blood pressure system. The values correspond to the specified experimental groups throughout the course of 8 weeks. The significant decline occurs after 4 weeks. Values are expressed as +/- SEM. N=5; * $p < 0.05$, ** $p < 0.025$, *** $p<0.001$.
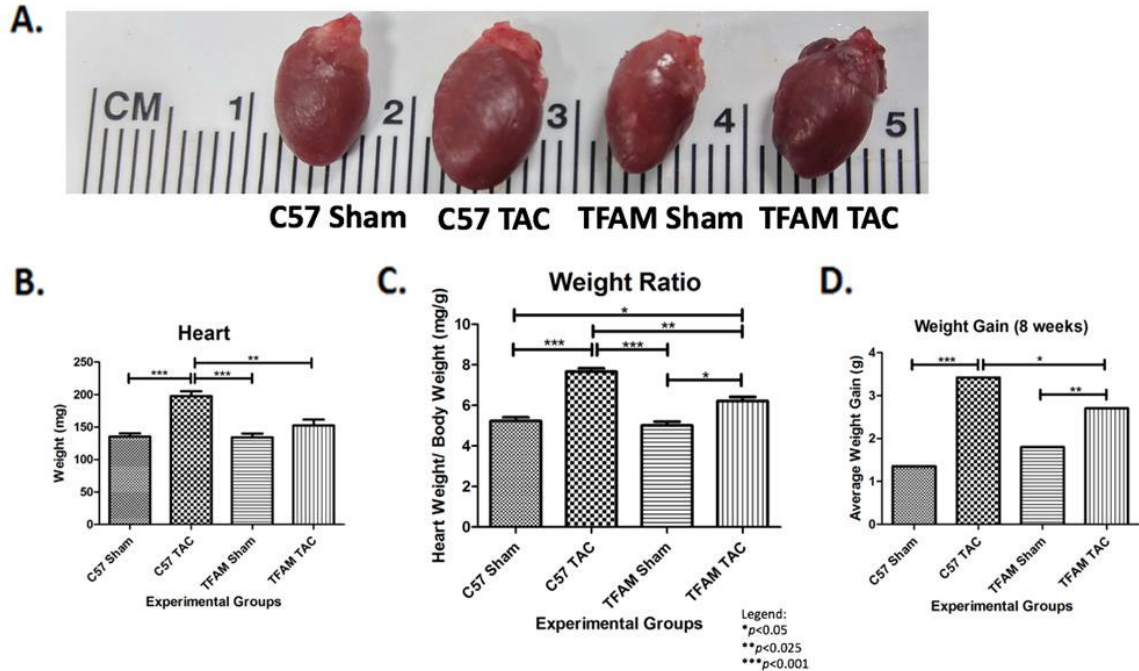
Figure 17. TFAM Over-expression Reduced Cardiac Hypertrophy.

Fig. 17A. The image displays the cardiac hypertrophy state after 8 weeks correlating to the respective experimental groups. Using visual confirmation, significantly enlarged WT heart due to aortic banding surgical procedure was observed when compared to the sham. Additionally, TFAM-TG reduced hypertrophic expansion compared to the TFAM-TG control.

Fig. 17B. This graph displays heart mass as assessed by micro-calibrated weight scale. The values correspond to the specified experimental groups after the course of 8 weeks. The TFAM TAC heart maintained a significantly lower mass when compared to the C57 TAC.

Fig. 17C. This graph depicts the heart weight to body weight ratio that correspond to the specified experimental groups after the course of 8 weeks. The TFAM TAC heart maintained a significantly lower ratio when compared to the C57 TAC.

Fig. 17D. This graph shows overall weight gain of the corresponding to the specified groups after the course of 8 weeks. This was performed by deducting the initial and final mouse weights allowed for an assessment of weight gain and variation among controls and transgenic animals. Furthermore, the TFAM TAC mice maintained a significantly lower mass weight gain compared to the C57 TAC mice.

Values are expressed as +/- SEM. N=5; * p < 0.05, ** p < 0.025, *** p<0.001

67
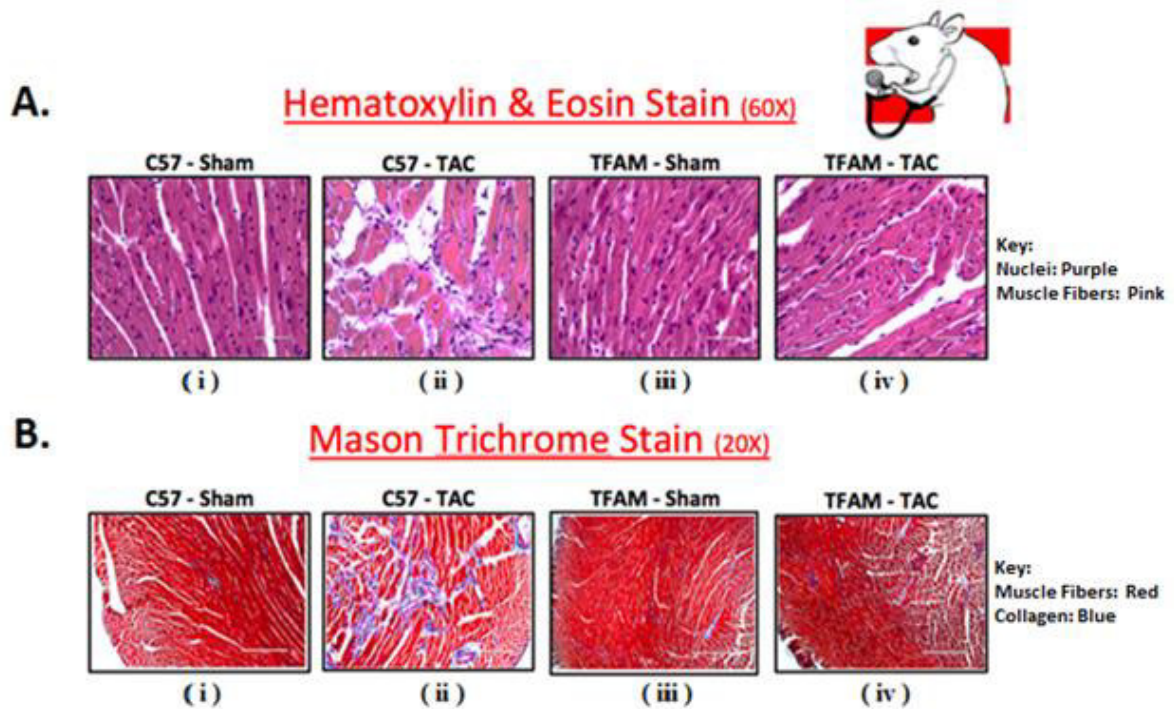
Figure 18. TFAM Reduced Histopathologies in HF.

Fig. 18A. Histology staining using Haematoxylin & Eosin Stain and observed via confocal microscopy (i-iv) provide a histopathology analysis of the effects of aortic banding on the myocardium. TFAM overexpression reduced cardiac remodeling (Fibrosis, Hypertrophy and Inflammation) *in vivo*. Representative cardiac cross sections of Sham and TAC animals sliced at the mid-ventricle level of WT and TFAM-TG mice hearts. Pictomicrograph sections in (i) C57 Sham, (ii) C57 TAC, (iii) TFAM Sham, (iiii) TFAM TAC. Hematoxylin and Eosin staining for histopathology. Dark pink is muscle and purple is nuclei. Magnification of 60x. Significant histopathology in the C57 TAC group.

Fig. 18B. Histology staining for collagen intensity. Mason Trichrome Staining for collagen intensity (i – v). (i) C57 Sham, (ii) C57 TAC, (iii) TFAM Sham, (iv) TFAM TAC; collagen is stained blue and muscle red. Magnification of 20x. Significant collagen intensity in the C57 TAC

Values are expressed as +/- SEM. N=5; * $p < 0.05$, ** $p < 0.025$, *** $p<0.001$.
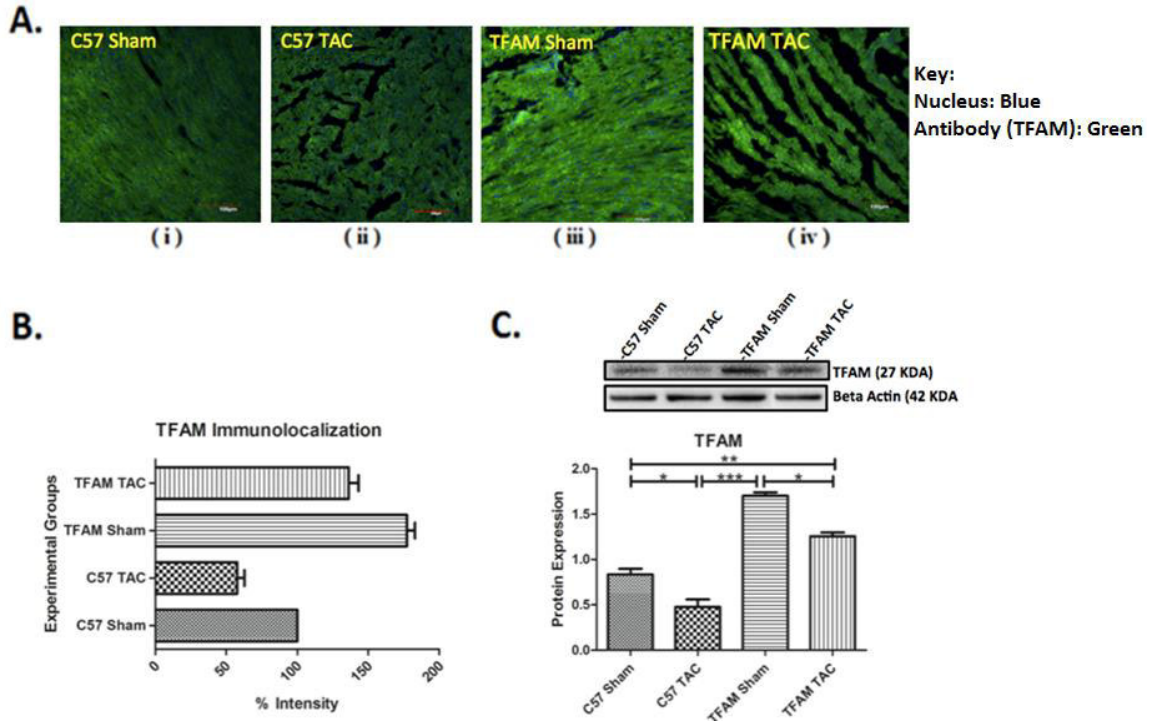
Figure 19. TFAM-TG Mice Maintained TFAM Expression in HF.

Fig. 19A. These confocal microscopy and ICC images (i-iv) provide intra-cellular visualizations of TFAM within the corresponding experimental groups. TFAM is identified in green fluorescence and nuclei are identified by blue fluorescence.

Fig. 19B. This graph exhibits the fluorescent intensity of TFAM 8-weeks after TAC and was provided by the data collected from the Image J software. Each fluorescent intensity corresponds to TFAM's presence within the specific experimental groups. With respect to TFAM fluorescent intensity, the TFAM overexpression Sham group was significantly greater relative to the C57 Sham group. Also, the TFAM TAC group was shown to be significantly greater in intensity of TFAM relative to the C57 TAC group.

Fig. 19C. This graph displays TFAM proteins expression 8 weeks after the aortic banding surgery. Lysates were analyzed by western blotting for TFAM protein expression. The TFAM overexpression Sham group was significantly greater in protein expression of TFAM relative to the C57 Sham group. The TFAM overexpression TAC group was significantly greater in protein expression of TFAM relative to the C57 TAC group. Both TAC groups were significantly decreased in TFAM protein expression when compared to their Sham counterparts. The bands were quantified using densitometry and the data was graphed for an N of 5 using SEM for significance. Values are expressed as +/- SEM. N=5. * $p < 0.05$, ** $p < 0.025$, *** $p < 0.001$.
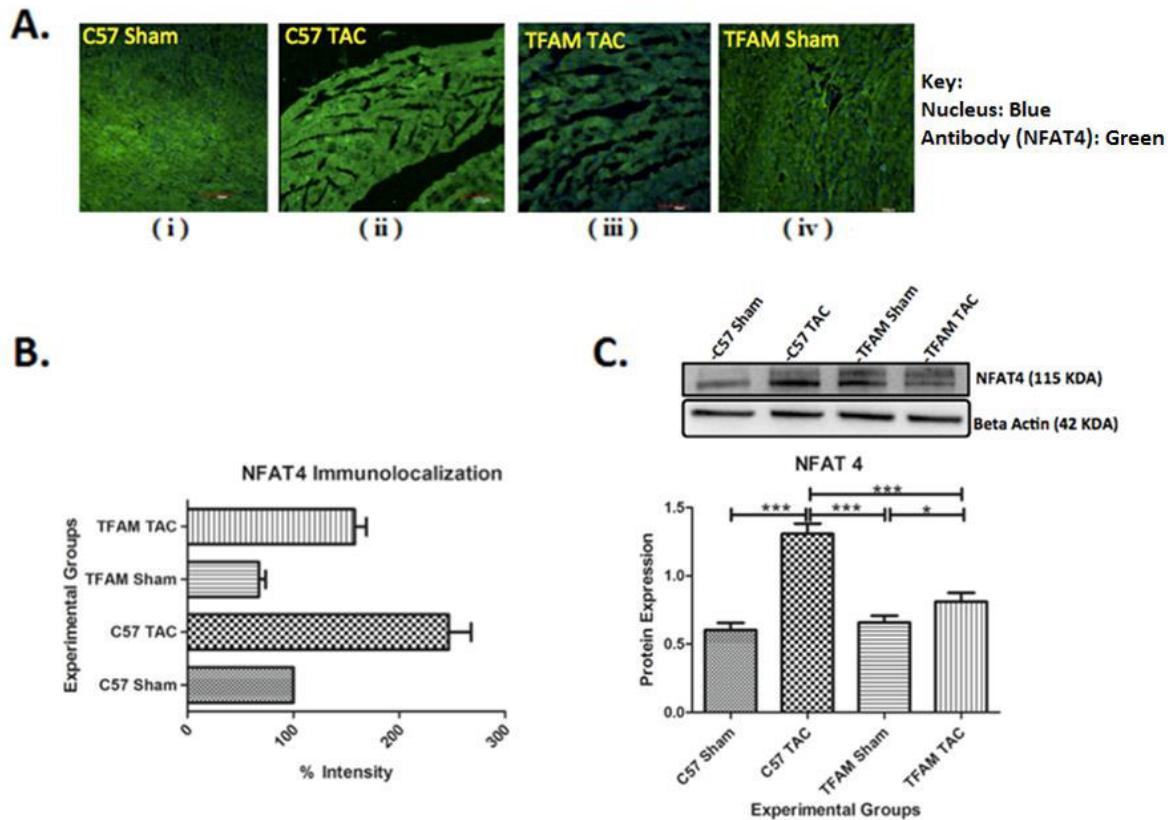
Figure 20. TFAM-TG Mice Decreased NFAT4 Expression in HF.

Fig. 20A. These confocal microscopy and ICC images (i-iv) provide intra-cellular visualizations of NFAT4 within the corresponding experimental groups. TFAM is identified in green fluorescence and nuclei are identified by blue fluorescence.

Fig. 20B. This graph exhibits the fluorescent intensity of NFAT4 8-weeks after TAC and was provided by the data collected from the Image J software. Each fluorescent intensity corresponds to NFAT4's presence within the specific experimental groups. With respect to NFAT4 fluorescent intensity, the TFAM TAC group was shown to be significantly lower in intensity of NFAT4 relative to the C57 TAC group.

Fig. 20C. This graph displays NFAT4 proteins expression 8 weeks after the aortic banding surgery. Lysates were analyzed by western blotting for NFAT4 protein expression. The TFAM overexpression TAC group was significantly lower in protein expression of NFAT4 relative to the C57 TAC group. Both TAC groups were significantly increased in NFAT4 protein expression when compared to their Sham counterparts. The bands were quantified using densitometry and the data was graphed for an N of 5 using SEM for significance. Values are expressed as +/- SEM. N=5. * p < 0.05, *** p<0.001.

A.

Key:
Nucleus: Blue
Antibody (MMP9): Green

(i) C57 Sham   (ii) C57 TAC   (iii) TFAM Sham   (iv) TFAM TAC

B. MMP9 Immunolocalization

C. MMP9 (82 KDA)
Beta Actin (42 KDA)

MMP9

Figure 21. TFAM-TG Mice Decreased MMP9 Expression in HF.

Fig. 21A. These confocal microscopy and ICC images (i-iv) provide intra-cellular visualizations of MMP9 within the corresponding experimental groups. MMP9 is identified in green fluorescence and nuclei are identified by blue fluorescence.

Fig. 21B. This graph exhibits the fluorescent intensity of MMP9 8-weeks after TAC and was provided by the data collected from the Image J software. Each fluorescent intensity corresponds to MMP9's presence within the specific experimental groups. With respect to MMP9 fluorescent intensity, the TFAM TAC group was shown to be significantly lower in intensity of MMP9 relative to the C57 TAC group.

Fig. 21C. This graph displays MMP9 proteins expression 8 weeks after the aortic banding surgery. Lysates were analyzed by western blotting for MMP9 protein expression. The TFAM overexpression TAC group was significantly lower in protein expression of MMP9 relative to the C57 TAC group. Both TAC groups were significantly increased in MMP9 protein expression when compared to their Sham counterparts. The bands were quantified using densitometry and the data was graphed for an N of 5 using SEM for significance. Values are expressed as +/- SEM. N=5. * $p < 0.05$, ** $p < 0.025$.
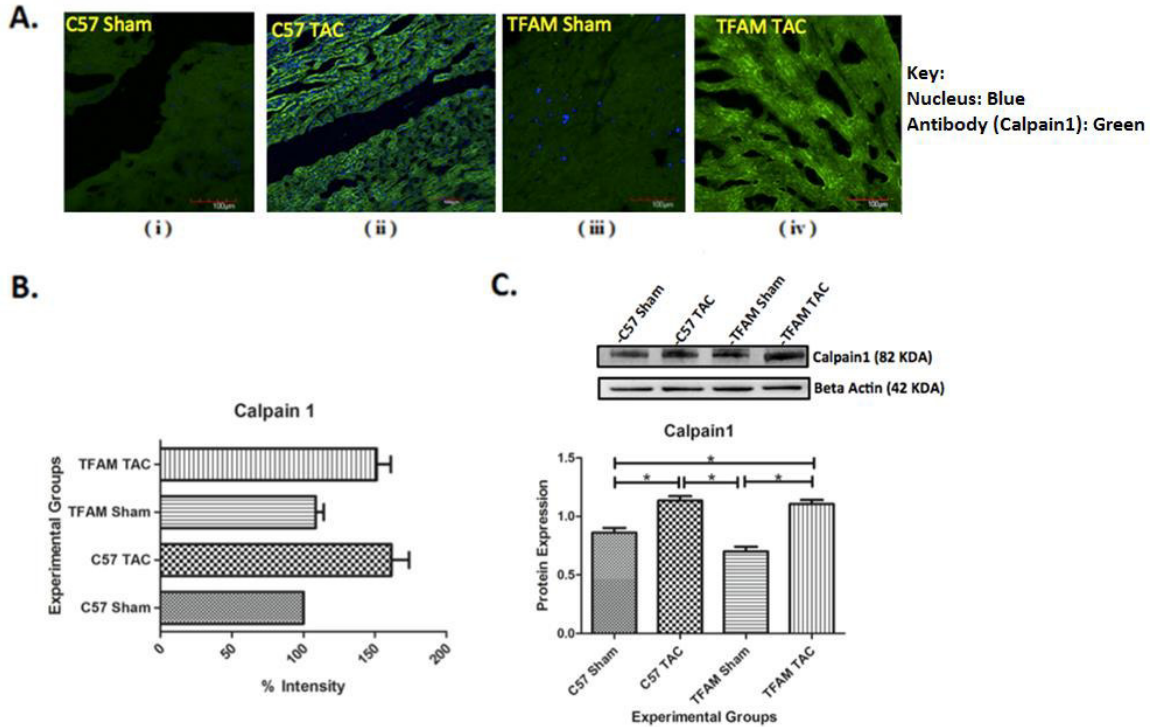
Figure 22. Up-regulated Calpain 1 Expression In HF

Fig. 22A. These confocal microscopy and ICC images (i-iv) provide intra-cellular visualizations of Calpain1 within the corresponding experimental groups. Calpain1 is identified in green fluorescence and nuclei are identified by blue fluorescence.

Fig. 22B. This graph exhibits the fluorescent intensity of Calpain1 8-weeks after TAC and was provided by the data collected from the Image J software. Each fluorescent intensity corresponds to Calpain1's presence within the specific experimental groups. With respect to Calpain1 fluorescent intensity, the TFAM TAC group was shown to be significantly greater in intensity of TFAM relative to the C57 TAC group.

Fig. 22C. This graph displays Calpain1 proteins expression 8 weeks after the aortic banding surgery. Lysates were analyzed by western blotting for Calpain1 protein expression. The TFAM overexpression TAC group was significantly greater in protein expression of Calpain1 relative to the C57 TAC group. The bands were quantified using densitometry and the data was graphed for an N of 5 using SEM for significance. Values are expressed as +/- SEM. N=5. * p < 0.05, ** p<0.025, *** p<0.001.
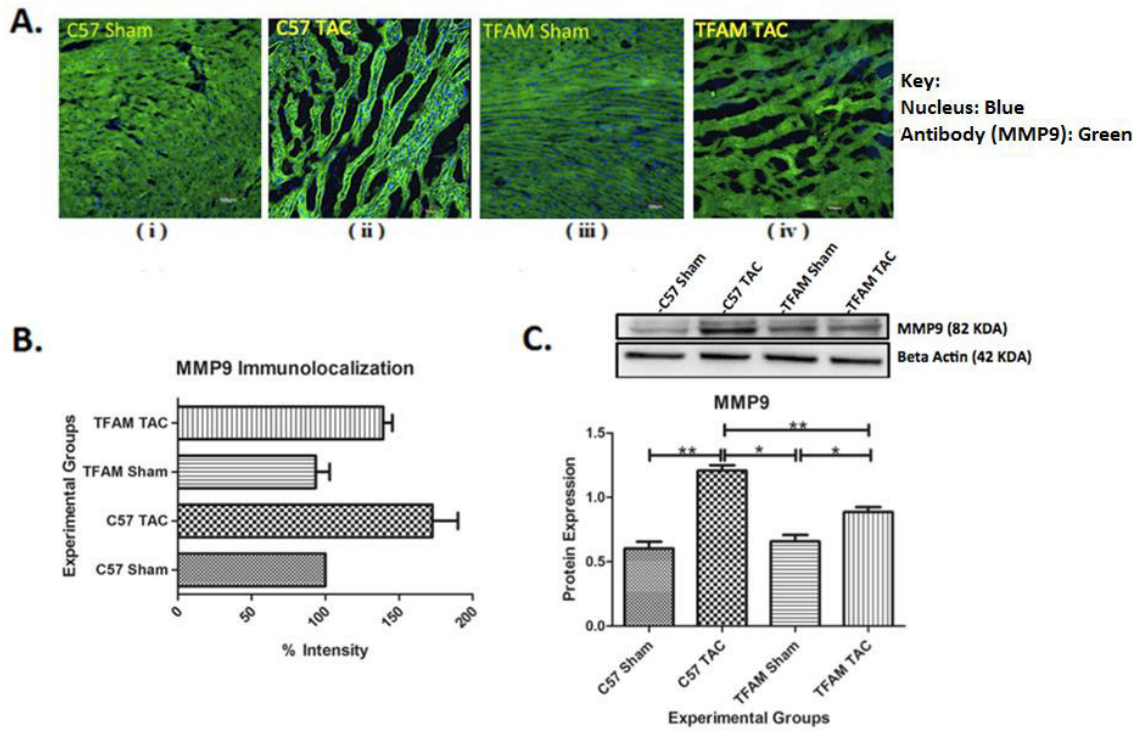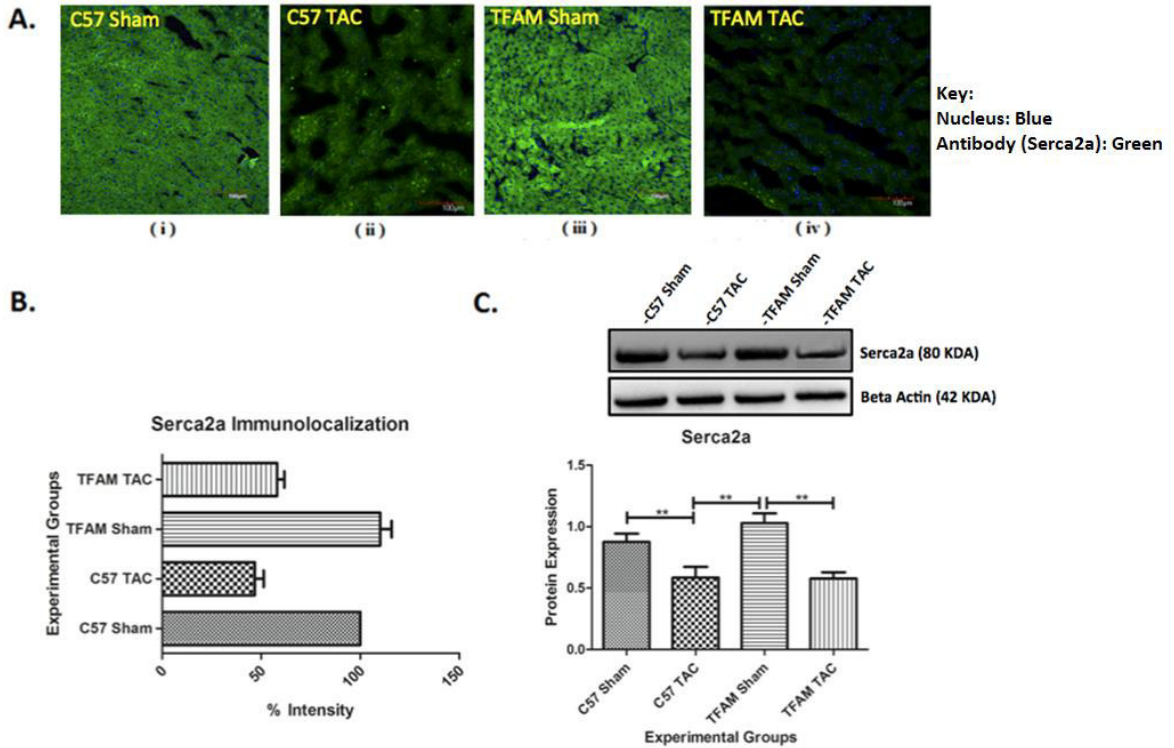
Figure 23. Decreased SERCA2a Expression in HF

Fig. 23A. These confocal microscopy and ICC images (i-iv) provide intra-cellular visualizations of SERCA2a within the corresponding experimental groups. SERCA2a is identified in green fluorescence and nuclei are identified by blue fluorescence.

Fig. 23B. This graph exhibits the fluorescent intensity of SERCA2a 8-weeks after TAC and was provided by the data collected from the Image J software. Each fluorescent intensity corresponds to SERCA2a's presence within the specific experimental groups. With respect to SERCA2a fluorescent intensity, the TFAM overexpression Sham group was significantly greater relative to the C57 Sham group. Also, the TFAM TAC group was shown to be significantly greater in intensity of TFAM relative to the C57 TAC group.

Fig. 23C. This graph displays SERCA2a proteins expression 8 weeks after the aortic banding surgery. Lysates were analyzed by western blotting for SERCA2a protein expression. The TFAM overexpression Sham group was significantly greater in protein expression of SERCA2a relative to the C57 Sham group. The TFAM overexpression TAC group was significantly greater in protein expression of SERCA2a relative to the C57 TAC group. Both TAC groups were significantly decreased in SERCA2a protein expression when compared to their Sham counterparts. The bands were quantified using densitometry and the data was graphed for an N of 5 using SEM for significance. Values are expressed as +/- SEM. N=5. * p < 0.05, ** p<0.025, *** p<0.001.

73
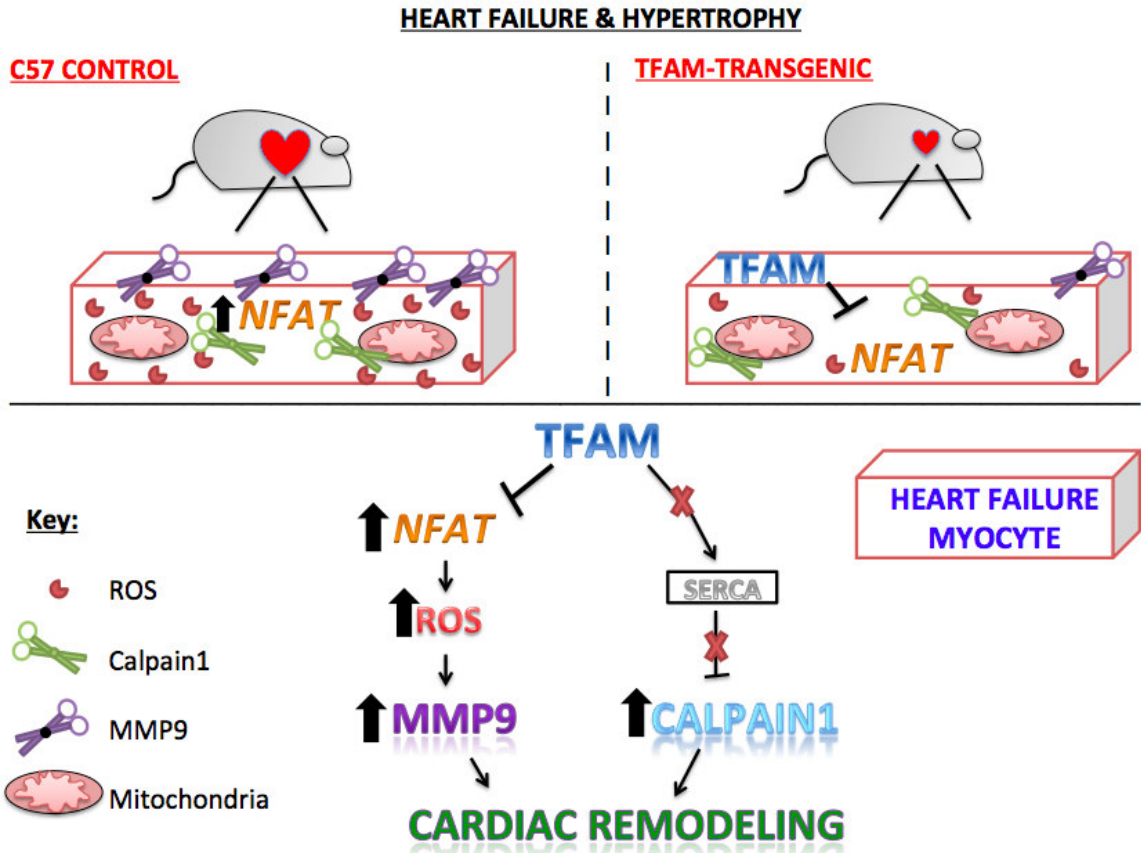
Figure 24. Interplay of TFAM Over-expression & Cardiac Remodeling Factors

Fig. 24. The diagram above depicts the figurative comparison of WT control and TFAM overexpression cardiomyocytes. It shows the positive conclusion of reduced cardiac remodeling by decreasing MMP9 expression and shows TFAM over-expression inhibits NFAT activation. In lack of such inhibition, NFAT would stimulate ROS production via NOX 2 & 4 which activates ROS driven MMP9 expression. MMP9 activation is a noted pathological marker for cardiac remodeling. Our original hypothesis regarding TFAM activation of SERCA2a and reduction of Calpain 1 was not observed.

Kunkel et al, Can J Physiol Pharmacol (2017)
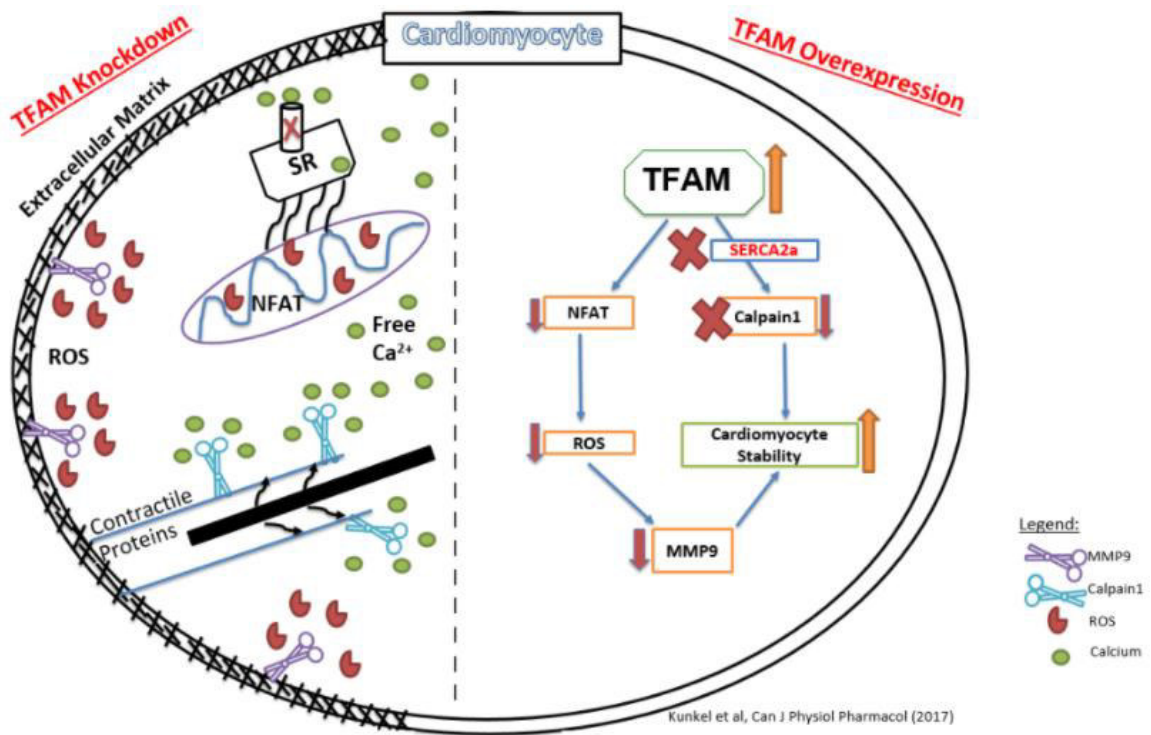
Figure 25. Visual re-evaluation of the Proposed Mechanism of TFAM- Mediated Cardiomyocyte Protection

Fig. 25. This diagram depicts the re-evaluation of the hypothesized mechanism for TFAM's role in cardiomyocyte protection (Fig.3). With respect to the hypothesis, the mechanism for TFAM knockdown was verified but the mechanism for TFAM over-expression exhibits two inconsistencies. In the failing cardiomyocyte with TFAM over-expression, SERCA2a expression was decreased while the expression of Calpain 1 was increased.

75

CHAPTER V

DISCUSSION OF RESULTS

We demonstrate for the first time that TFAM maintains an inhibitory relationship with the NFAT4-ROS-MMP9 proteolytic pathway in TFAM transgenic mice subjected to aortic-banding-induced HF. We also found a mechanistic inconsistency in the SERCA2a-Calpain 1 pathway in banded TFAM transgenic mice. This finding varied in respect to the literature and our initial proposed mechanism. These findings have been expressed in both models of TFAM reduction and over-expression.

We preface this discussion with our findings on TFAM reduction and overexpression experimentation. Through *in vitro* experiments, we observed a significant decrease in TFAM protein expression in the TFAM-specific (CRISPR-cas9) knockdown treatment (Fig.4) and the oxidative stress treatment (Fig.9). Additionally, in the *in vivo* experiments, the aortic-banded WT mouse group exhibited a significant decrease in TFAM protein expression (Fig.19). Within this experimental analysis, we discovered that NFAT4 and ROS-activated MMP9 are significantly increased.

Using TFAM reduction, in the *in vitro* model, we verified the inverse relationship between TFAM and the NFAT4-ROS-MMP9 mechanism. NFAT4 increases NADPH oxidases 2 & 4 to produce ROS in pathological conditions (Williams and Gooch 2014). CRISPR knockdown of TFAM increased NFAT4 expression (Fig.6), increasing cytoplasmic ROS, as found through DHE staining (Fig.8). The interaction between TFAM and NFAT4 was first found in the Fujino groups work, stating that TFAM mechanistically inhibits NFAT4 transcriptional activation (Fujino et al. 2012).

In HF models in which TFAM is decreased, NFAT4 induces ROS production and activates hypertrophic gene expression. NFAT activates pathological cardiac hypertrophy, which we confirmed in the WT-TAC models. In TFAM reduction, there is a significant increase in heart weight/body weight ratio in comparison to the control groups. Furthermore, we observed a significant weight gain, which we deemed a result of edema, in the WT-TAC model compared to the control. Other papers have found similar results in HF models (Veeraveedu et al. 2017; Ikeda et al. 2015).

Through histology staining, we also observed cardiac muscle misalignment in the WT-TAC model. This observation was supported by H&E staining (Fig.18A), which tested for histopathologies. The aortic banding procedure in WT mice resulted in myofiber deformation, nuclei misalignment, and inflammation. Additionally, we confirmed that TFAM reduction within the WT-TAC group has increased collagen intensity, as found through Masson's Trichrome Staining (Fig.18B). These findings were accompanied by molecular changes in MMP9.

In vitro experimentation shows that significantly decreasing TFAM induces ROS activated MMP9 (Fig.8C). Exogenous treatment of 127 micromolar H_2O_2 to HL-1 cardiomyocytes significantly increased MMP9 protein expression (Fig. 11). Though other groups administered 200 micromolar H_2O_2 to HL-1 cardiomyocytes we experienced increased cell death and standardized the treatment. In AV fistula volume-overload (VO) heart failure, TFAM overexpression suppressed MMP up regulation and limited mitochondrial oxidative stress (Ikeda et al. 2015).

In TFAM knockdown such as found in the failing heart of control animals (Fig.19), excess ROS in the cytoplasm induces MMP9, which we and other groups have found increased (Givvimani et al. 2010; Cox et al. 2002). MMPs are collagenases and MMP9 excessively degrades collagen but in cardiac remodeling collagen turnover is faster than elastin, leading to a stiffening myocardium (Mishra et al. 2013). This interplay is a major factor in hypertrophy and heart failure.

Increased NFAT4 stimulates a cardiac remodeling cascade inducing ROS production to increase MMP9, which degrades the extracellular matrix of cardiomyocytes. MMP9 is a distinguishing factor in pathological cardiac remodeling (Mishra et al. 2013). This observation correlates with known studies showing that increased activation of MMPs is observed in TFAM ablation and oxidative stress models (Larsson et al. 1998; Lamparter and Maisch 2000).

As was expected, TFAM overexpression initiated a chain reaction of decreased NFAT and ROS-activated MMP9. In the *in vitro* and *in vivo* experiments, TFAM overexpression vectors significantly increased TFAM protein expression in

78

Hl-1 cardiomyoctes and in the TFAM transgenic mouse model (Fig.4C). In the TFAM over-expression model, NFAT4 is reduced (Fig.6). Administration of TFAM vector with H_2O_2 treatment had significantly reduced NFAT4 & MMP9 with respect to the H_2O_2 group alone (Fig. 10 &11).

Through TFAM's inhibition of NFAT, we conclude that aortic banding in TFAM-TG mice prevented hypertrophy. In TFAM over-expression, we note a significant decrease in NFAT4, which correlates to our visual confirmation of reduced hypertrophy in the TFAM-TG banded group. Through analysis of heart weight/body weight ratio, we observe a reduction in cardiac hypertrophy with TFAM overexpression (Fig.17). Our results are similar to the current literature In AVF induced HF models, TFAM overexpression reduced protease activity and cardiac hypertrophy (Ikeda et al. 2015). Studies show that TFAM overexpression attenuates cardiac dilation and dysfunction in myocardial infarction induced heart failure models (Ikeuchi et al. 2005).

Oxidized proteins are prevalent in heart failure models, TFAM and mitochondrial repair enzymes serve to reduce oxidation when overexpressed. Overexpression of mitochondrial repair factors in TAC induced HF, decreased left ventricular remodeling (Wang et al. 2011).

In banded TFAM transgenic mice, TFAM overexpression reduced cardiac histopathologies. Since NFAT is involved in T-cell modulation, we may be breaching a novel role of TFAM in heart failure inflammation. By reducing NFAT, we prevent

potential inflammatory cell signaling pathways from negatively affecting the failing myocardium.

The inhibitory activity of TFAM to reduce NFAT4 pathological hypertrophy and ROS-driven MMP9, may delay the myocardium remodeling state, before becoming end-stage heart failure. TFAM overexpression protected the aortic banded myocardium from cardiac hypertrophy. The LV mass of the WT-TAC was significantly heavier than the TFAM-TAC, noting that both were still significantly greater than the controls. This suggests that TFAM overexpression reduces the hypertrophic and cardiac remodeling process resulting in reduced LV mass (Fig.15).

This mechanistic pathway NFAT4-ROS-MMP9 induces cardiac hypertrophy and remodeling. Cardiac remodeling includes both intracellular and extracellular remodeling factors that induce significant molecular and morphological changes to cardiomyocyte structure and function. Remodeling encompasses degradation of the extracellular matrix (ECM), pathological hypertrophy, fibrosis, and resultant organ dysfunction. This study provides further insight into TFAM's therapeutic potential in TFAM knockdown/overexpression, oxidative stress, and aortic banding induced HF. Through this work we have shown that TFAM overexpression has the potential to reduce cardiac remodeling factors MMP9 and NFAT4 (Fig. 25). Analysis of functional and molecular data, within this work may give insight into the TFAM-NFAT-ROS-MMP9 pathway.

The TFAM-SERCA2a-Calpain 1 pathway reveals a potential avenue for further exploration. Our work suggests that there is an anomaly regarding TFAM's

interaction with SERCA2a. Following the proposed mechanistic pathway, we found that SERCA2a protein expression was as equally significantly reduced in both TFAM transgenic and control TAC groups (Fig.23). This finding correlates with reduced SERCA2a expression in HF models (Cutler et al. 2009). The downstream effect of reduced SERCA2a is increased Ca2+ activated Calpain 1 protein expression was significantly increased in the banding animals compared to their controls (Fig.22).

SERCA2a has a major functional role in physiological Ca^{2+} regulation and cardiomyocyte physiology. The Watanabe group found that exogenous over-expression of TFAM increased transcriptional activation of SERCA2a (Watanabe et al. 2011). As a result, we hypothesized that TFAM over-expression would heighten SERCA2a protein expression, due to an increase in SERCA2a transcriptional activation. We presumed that this prominent expression of SERCA2a proteins would then drive more cytoplasmic Ca^{2+} into the SR, reducing Ca^{2+}-activated calpain proteases. However, our results, although consistent, did not reflect this mechanism in our *in vivo* or *in vitro* experiments. In retrospect, we can explain these unexpected discoveries as the effect of proteolytic degradation of SERCA2a and inhibition of SERCA2a gene transcription. We further analyze the role of epigenetic and inflammatory interactions with SERCA2a in HF.

In vitro, the TFAM knockdown vector revealed an intensification of SERCA2a protein expression when TFAM protein expression was reduced by 50%. The TFAM over-expression vector also significantly increased SERCA2a protein expression. *In vivo*, however, TFAM over-expression did not increase SERCA2a

81

protein concentration in the failing myocardium. Quantitatively, there were no significant differences in SERCA2a protein concentration in the failing hearts of both WT and TFAM-TG mice. Upon analysis of these results, we must reevaluate the original proposed mechanism behind TFAM's interaction with SERCA2a.

After a thorough review of the literature, we recognized two potential methods of SERCA2a decline that possibly caused our results to waver from our hypothesis: proteolytic degradation of SERCA2a protein and inhibition of SERCA2a gene transcription. Of the many proteases activated by Ca^{2+}, Calpain 1 protease was significantly increased within the TAC heart failure model and is unaffected by TFAM overexpression (Fig.22). Calpain 1 may degrade the subunits of the SERCA2a protein, affect its inhibitors phospholambin and sarcolipin but evidence supporting this conjecture is nil and is in need of further exploration. Knocking down TFAM increased SERCA2a expression within HL-1 cardiomyocytes. We observe this as an immediate compensatory mechanism to reduce free Ca^{2+} in a stress-induced environment. This excess Ca^{2+} invites proteolytic degratory enzyme Calpain 1, to degrade contractile proteins. Interestingly, the excess Ca^{2+} in the cytoplasm activates calpain 1 in the CRISPR Vector group in which SERCA2a expression is significantly higher. Therefore, Ca^{2+}+-driven calpain 1 levels remain higher than the compensatory activity of the SERCA2a pump. Post-translational modifications like degradation would result in decreased protein expression of SERCA2a as found in our results. SERCA2a inhibition may also be a result of up-stream modifications to SERCA2a

82

mRNA and SERCA2a promoter, these regions may be altered leading to reduced SERCA2a protein expression.

MicroRNAs (miRNA) are small non-coding RNA's, that function in RNA silencing and posttranscriptional regulation of gene expression. MiRNA's modify messenger RNA (mRNA), through cleavage and destabilization. In HF, many MiRNAs are dysregulated leading to further cardiomyocyte failure. Of these many regulators, miR-25 is significantly expressed in the heart failure myocardium and has been shown to inhibit SERCA2a. Mir 25 acts like an SiRNA targeting mRNA for degradation instead of transcription. Its inhibitory activity to block SERCA2a, the loss of SERCA2a in HF, and its significant upregulation in the HF myocardium led us to contemplate whether Mir-25 is inhibiting SERCA2a in the TFAM-TG TAC model where our hypothesis does not match our results.

From a different standpoint; In the presence of a chronic inflammatory state, such as found in heart failure, additional mechanistic components are at play. The cytoplasmic environmental changes found in heart failure drive adverse mechanistic pathways, due to inflammatory cytokine up-regulation (Cocco et al. 2017). We recognize that there is a rise in TNF alpha in chronic inflammatory states, as well as in tissue samples of HF patients (Valgimigli et al. 2005). According to Huang et al., SERCA2a transcription is suppressed via the NFkB-ERK 1,2 pathway (Huang et al. 2014). This activity was observed in a cardiac hypertrophic state of chronic inflammation. We observed that a reduced immune response, the *in vitro* TFAM vector model allowed for a significant increase in SERCA2a in Hl-1 cardiomyocytes

(Fig. 5). The inflammatory response of the *in vivo* model may prohibit SERCA2a expression at the transcriptional level. Additionally, TFAM regulates interactions with TNF alpha in chronic stress environments.

TFAM is viewed as an endogenous danger signal in damaged cells, due to chronic inflammation. Mechanistically, TFAM engages the RAGE factor, (an inflammatory response element) initiating the activation of TNF-alpha (Julian et al. 2013). TNF-alpha, or Tumor Necrosis Factor Alpha, is a cell-signaling cytokine involved in inflammation; it is also a mediator of apoptotic cell death (Baxter et al. 1999). TNF alpha is up-regulated in inflammatory diseases and in heart failure (Ogasawara et al. 2017; Valgimigli et al. 2005; Wang, Jia, et al. 2017). Molecular evaluation of TNF alpha's mechanistic regulation over Ca^{2+} presents TNF alpha's role in activating IP3R and RyR Ca^{2+} channels, releasing Ca^{2+} into the cytoplasm (Wang, Guo, et al. 2017).

SERCA2a, a Ca^{2+} transporter, is functionally inhibited in heart failure; it was found that TNF-alpha inhibits the SERCA2a promoter region via methylation (Kao et al. 2010). Epigenetic modifications to SERCA2a promoter region reduce its transcriptional activity. TNF alpha induces NFkB, which physically binds to the SERCA2a gene promoter, blocking its transcription (Tsai et al. 2015). According to Huang et al, ERK 1, 2 suppress SERCA2a transcription via NFkB-related mechanisms (Huang et al. 2014). This activity was observed in a cardiac hypertrophic state. TFAM's activation of TNF-alpha may be a possible mechanistic pathway

responsible for reducing SERCA2a in the TFAM transgenic animals with pressure overload HF.

There is a possibility that the inflammatory response involved in HF and the induction of extrinsic cell death pathways involving TNF-alpha may be inhibiting SERCA2a's therapeutic potential in the TFAM transgenic model. Inhibition of TNF-alpha in TFAM transgenic animals may be necessary to proper assessment of TNF-alpha's role in the SERCA2a inhibition during HF.

CHAPTER VI

SUMMARY, CONCLUSION, & FUTURE DIRECTIONS

Cardiovascular diseases are a leading cause of death worldwide. Heart failure or the inefficiency of the heart to pump blood, has a high fatality rate five years post onset (Mozaffarian et al. 2016). Mitochondrial factors such as TFAM play a vital role in inhibiting cardiac remodeling factors, which lead to cardiac hypertrophy and heart failure. Heart failure has reduced TFAM expression, increased oxidative stress, Ca^{2+} mishandling, and protease expression leading to cardiomyocyte functional decline (Lauritzen et al. 2015). Previous studies involved in TFAM knockdown have resulted in reduced mitochondrial biogenesis, dilated cardiomyopathy and neonatal death (Larsson et al. 1998).

TFAM over-expression in *in vivo* and *in vitro* studies resulted in cellular/functional recovery by reducing oxidative stress and remodeling factors. Furthermore, evidence suggests that TFAM plays a vital role in the physiological and pathological myocardium. Therefore, mitochondrial-TFAM driven therapeutics are under consideration as a promising approach in various diseases. We studied the potential treatment capabilities of TFAM by examining its molecular and functional effects on the myocardium.

We hypothesized that TFAM overexpression reduces pathological cardiac remodeling and associated factors in heart failure. In testing this hypothesis, we aimed to first analyze the effect of oxidative stress, TFAM CRISPR knockdown and, TFAM over-expression on Hl-1 cardiomyocytes. The TFAM knockdown vector induced oxidative stress and caused an accumulation of proteolytic and hypertrophic remodeling factors. TFAM knockdown triggers a catabolic reaction in which MMPs degrade the extracellular matrix of cardiomyocytes. In administering hydrogen peroxide to HL-1 cardiomyocytes, we mimicked the robust oxidative stress environment of heart failure. Within this objective, we found that TFAM expression is significantly reduced in both oxidative stress and TFAM-knockdown vector. TFAM reduction significantly increased cardiac remodeling factors such as Calpain 1, MMP9 and NFAT4. In contrast, TFAM overexpression plays a major role in inhibiting the up-regulation of ROS producing factors and transcription factors that activate hypertrophic gene regulation. Within this study, we gained support for TFAM's necessary role in cardiomyocyte function.

In an *in vivo* model, we hypothesized that TFAM transgenic mice subjected to aortic banding would have reduced cardiac hypertrophy post-HF. In this study, we found that the aortic banding surgical procedure changed cardiac histopathology and function. This change was demonstrated via histology, echocardiography and blood pressure which showed that TFAM overexpression reduced functional morphologies post-banding. We verified, through visual confirmation and measuring heart

87

weight/body weight ratio, that TFAM overexpression reduced aortic banding induced hypertrophy.

The third aim addresses the effect of TFAM overexpression on molecular cardiac remodeling factors. Molecular insight into the remodeling cascade shows reduced protease and hypertrophic expression in TFAM over-expression models. Molecular techniques, including western blotting and IHC, reveal that TFAM over-expression reduces the NFAT4-ROS-MMP9 cardiac remodeling cascade. However, our initial hypothesis, regarding TFAM activation of SERCA2a and reduction of Calpain 1, was not confirmed. Many regulatory elements of this potential anomaly have been reviewed in the discussion section.

This study provides mechanistic support of TFAM's potential to reduce mechanistic factors involved in cardiac pathologies. Therefore, TFAM overexpression treatment is a possible cardio-therapeutic approach to reducing ROS-induced pathological remodeling.

Future Directions

Within this section, we discuss the potential of TFAM as a therapeutic in diabetic HF, exosomal delivery, natural compounds that increase TFAM, and the limitations we face in TFAM-based therapeutic research.

Diabetes & HF

Diabetes is a devastating, chronic condition that affects millions of Americans. As diabetes evolves into a serious public health issue, researchers strain to advance the management of diabetic HF. Diabetes significantly increases the risk of cardiomyopathies. As we have observed in this work on TFAM's role in the inhibition of cardiac remodeling, considerable molecular changes occur within the failing cardiomyocyte of HF control animals. We found evidence of TFAM's ability to mitigate the NFAT-ROS-MMP9 pathway, but TFAM's cardioprotective potential in diabetic HF remains unexplored. Therapeutic mechanistic avenues that reduce left ventricular dysfunction in the WT HF models are not as effective in diabetic cardiomyopathies. Therefore, we should direct future efforts to the mitigation of oxidative stress and hypertrophy in diabetic HF.

Mitochondrial therapeutic targets such as TFAM are crucial to the reduction of oxidative stress. As noted in the literature, hyperglycemia-induced oxidative stress is significantly increased in the diabetic myocardium (Dludla et al. 2017; Mandavia et al. 2013). Metabolic abnormalities found in diabetes are far more likely to result in cardiac hypertrophy and fibrosis (Tarquini et al. 2011). As confirmed in our results,

TFAM over-expression reduces cardiac hypertrophy and fibrosis; therefore, it may also reduce hyperglycemia-induced hypertrophy. The Santos group found that hyperglycemia diminishes mitochondrial biogenesis and TFAM, suggesting that mitochondrial dysregulation in diabetes may be, in part, due to TFAM loss. ROS causes molecular dysfunction, creating oxidative damage throughout the diabetic myocardium. Clinical methods to reduce oxidative stress are limited, and the world is in dire need of exogenous mitochondrial therapy, such as that produced by TFAM over-expression.

Exogenous Delivery Mechanisms

There exists multiple vehicular methods of transporting regulatory elements; such transport mechanisms include viruses, bacterial & viral vectors, and nanoparticles. The literature thoroughly depicts disadvantages of the various delivery methods, particularly the stimulation of immunogenic factors. Exosomes range from 30-100nm in size and have the potential to be therapeutic game changers in future biomedical technology. These nanoparticles are non-immunogenic and transport molecules with efficient delivery. Infused within their membranous vessels are mRNA, miRNA, siRNA, proteins, and nucleic acids that incite alteration in gene expression. Evidence of therapeutic advances using an exosomal delivery system is ubiquitous in the literature. As conferred in the Discussion section, Mir-25 is vital to the inhibition of the SERCA2a pump. Exosomal delivery of a TFAM over-expression/Mir-25 inhibitor cocktail may have significant cardioprotective effects in

WT and diabetic HF models. This method may ameliorate both Ca^{2+}- and ROS-induced dysfunction.

Natural Methods to Increase TFAM

Natural methods that exaggerate TFAM, increase mitochondrial function, and prevent disease exist in ancient medicinal ingredients. Compounds such as grape seed procyanidin B2 (GSPB2), daidzein, humanin, and honokoil increase mitochondrial copy number and biogenic function while reducing oxidative stress. GSPB2 inhibited glucose-induced apoptosis and suppressed ROS production. Additionally, mRNA expressions of NRF-1, TFAM, and mtDNA copy number vastly increased upon treatment (Cai et al. 2016). Yoshino et al. describe effects of the dietary substance soy isoflavone daidzein on muscle mitochondria. This soy extract directly promotes TFAM expression by increasing mitochondrial biogenesis through activation of PGC-1 alpha(Yoshino et al. 2015). Humanin is a natural mitochondrial peptide that significantly increased mtDNA copy number, up-regulated TFAM, activated STAT3, and decreased caspase-3 activation and intrinsic apoptosis (Sreekumar et al. 2016). Natural remedies have been studied in traditional medicine; as we analyze these compounds, we find the mechanistic route to natural therapy.

Honokoil is a lignan isolated from magnolia tree bark and seed cones. In cardiac hypertrophy, honokoil, a known anti-cancer, anti-oxidative, and anti-inflammatory substance, reduces mitochondrial stress through activation of SIRT-3. Sirtuin-3 protects the myocardium from hypertrophy by inhibiting NFAT and

lessening ROS production. The PGC-1alpha –Sirtuin & TFAM axis plays a major role in cardiomyocyte stability (Pillai et al. 2017). FAs observed, honokoil will increase TFAM levels, resulting in greater mitochondrial stability and reduced hypertrophy. Therefore, the cardioprotective nature of TFAM in diabetic cardiomyopathies is a novel possibility and idea. Within the Future Directions of this work, we observe that not only biomedical derivations of TFAM, but also natural compounds shown to induce TFAM expression, exist and should be tested for therapeutic potential.

Limitations of TFAM's Therapeutic Potential

It would be immeasurably beneficial to explore and analyze both naturally and biomedically derived methods of ameliorating cardiomyopathies through the enhancement mitochondrial efficiency. The extent of TFAM's therapeutic potential is also a notable question for any further research in TFAM therapeutics. Limitations of TFAM therapeutic potential exist. As we are aware, cancer cells thrive in high biogenic environments (Xie et al. 2016). TFAM expression intensifies within a variety of cancers, and TFAM is a target of inhibition in cancer research (Mo et al. 2013). The over-expression of TFAM in a cancer model may cause the cancer to metastasize at a faster rate. Additionally, TFAM's role in protecting and physically wrapping around mtDNA would be similar within cancer cells. This may, in fact, protect the cancer cell mitochondria, and block current cancer therapies.

Mechanistic analysis of TFAM's function in TFAM over-expression models and its potential role in diabetic HF through exosomal delivery and natural compounds are in need of further exploration.

REFERENCES

Aguirre-Rueda, D., S. Guerra-Ojeda, M. Aldasoro, A. Iradi, E. Obrador, A. Ortega, M. D. Mauricio, J. M. Vila, and S. L. Valles. 2015. 'Astrocytes protect neurons from Abeta1-42 peptide-induced neurotoxicity increasing TFAM and PGC-1 and decreasing PPAR-gamma and SIRT-1', *Int J Med Sci*, 12: 48-56.

Alam, T. I., T. Kanki, T. Muta, K. Ukaji, Y. Abe, H. Nakayama, K. Takio, N. Hamasaki, and D. Kang. 2003. 'Human mitochondrial DNA is packaged with TFAM', *Nucleic Acids Res*, 31: 1640-5.

Ali, M. A., A. D. Kandasamy, X. Fan, and R. Schulz. 2013. 'Hydrogen peroxide-induced necrotic cell death in cardiomyocytes is independent of matrix metalloproteinase-2', *Toxicol In Vitro*, 27: 1686-92.

Ali, M. A., A. Stepanko, X. Fan, A. Holt, and R. Schulz. 2012. 'Calpain inhibitors exhibit matrix metalloproteinase-2 inhibitory activity', *Biochem Biophys Res Commun*, 423: 1-5.

Angelini, A., C. Castellani, G. M. Virzi, M. Fedrigo, G. Thiene, M. Valente, C. Ronco, and G. Vescovo. 2015. 'The Role of Congestion in Cardiorenal Syndrome Type 2: New Pathophysiological Insights into an Experimental Model of Heart Failure', *Cardiorenal Med*, 6: 61-72.

Banfi, B., G. Molnar, A. Maturana, K. Steger, B. Hegedus, N. Demaurex, and K. H. Krause. 2001. 'A Ca(2+)-activated NADPH oxidase in testis, spleen, and lymph nodes', *J Biol Chem*, 276: 37594-601.

Bhosale, G., J. A. Sharpe, S. Y. Sundier, and M. R. Duchen. 2015. 'Calcium signaling as a mediator of cell energy demand and a trigger to cell death', *Ann N Y Acad Sci*, 1350: 107-16.

Bonnans, C., J. Chou, and Z. Werb. 2014. 'Remodelling the extracellular matrix in development and disease', *Nat Rev Mol Cell Biol*, 15: 786-801.

Borutaite, V., A. Budriunaite, R. Morkuniene, and G. C. Brown. 2001. 'Release of mitochondrial cytochrome c and activation of cytosolic caspases induced by myocardial ischaemia', *Biochim Biophys Acta*, 1537: 101-9.

Cai, X., L. Bao, J. Ren, Y. Li, and Z. Zhang. 2016. 'Grape seed procyanidin B2 protects podocytes from high glucose-induced mitochondrial dysfunction and apoptosis via the AMPK-SIRT1-PGC-1alpha axis in vitro', *Food Funct*, 7: 805-15.

Campos, Catarina, Arvind Y. M. Sundaram, Luisa M. P. Valente, Luis E. C. Conceição, Sofia Engrola, and Jorge M. O. Fernandes. 2014. 'Thermal plasticity of the miRNA transcriptome during Senegalese sole development', *BMC Genomics*, 15: 525.

Cao, G., J. Xing, X. Xiao, A. K. Liou, Y. Gao, X. M. Yin, R. S. Clark, S. H. Graham, and J. Chen. 2007. 'Critical role of calpain I in mitochondrial release of apoptosis-inducing factor in ischemic neuronal injury', *J Neurosci*, 27: 9278-93.

Casas, F., L. Daury, S. Grandemange, M. Busson, P. Seyer, R. Hatier, A. Carazo, G. Cabello, and C. Wrutniak-Cabello. 2003. 'Endocrine regulation of mitochondrial activity: involvement of truncated RXRalpha and c-Erb Aalpha1 proteins', *Faseb j*, 17: 426-36.

Chang, H., J. J. Sheng, L. Zhang, Z. J. Yue, B. Jiao, J. S. Li, and Z. B. Yu. 2015. 'ROS-Induced Nuclear Translocation of Calpain-2 Facilitates Cardiomyocyte Apoptosis in Tail-Suspended Rats', *J Cell Biochem*.

Chang, T. H., M. C. Chen, J. P. Chang, H. D. Huang, W. C. Ho, Y. S. Lin, K. L. Pan, Y. K. Huang, W. H. Liu, and C. C. Wu. 2016. 'Exploring Regulatory Mechanisms of Atrial Myocyte Hypertrophy of Mitral Regurgitation through Gene Expression Profiling Analysis: Role of NFAT in Cardiac Hypertrophy', *PLoS One*, 11: e0166791.

Chaturvedi, P., A. Kalani, I. Medina, A. Familtseva, and S. C. Tyagi. 2015. 'Cardiosome mediated regulation of MMP9 in diabetic heart: role of mir29b and mir455 in exercise', *J Cell Mol Med*, 19: 2153-61.

Chaturvedi, Pankaj, and Suresh C. Tyagi. 2016. 'Epigenetic silencing of TIMP4 in heart failure', *J Cell Mol Med*, 20: 2089-101.

Chen, M., D. J. Won, S. Krajewski, and R. A. Gottlieb. 2002. 'Calpain and mitochondria in ischemia/reperfusion injury', *J Biol Chem*, 277: 29181-6.

Chen, M., B. Yi, and J. Sun. 2014. 'Inhibition of cardiomyocyte hypertrophy by protein arginine methyltransferase 5', *J Biol Chem*, 289: 24325-35.

Chen, Y., G. Csordas, C. Jowdy, T. G. Schneider, N. Csordas, W. Wang, Y. Liu, M. Kohlhaas, M. Meiser, S. Bergem, J. M. Nerbonne, G. W. Dorn, 2nd, and C. Maack. 2012. 'Mitofusin 2-containing mitochondrial-reticular microdomains direct rapid cardiomyocyte bioenergetic responses via interorganelle Ca(2+) crosstalk', *Circ Res*, 111: 863-75.

Chouinard, R. A., Jr., Y. Luo, T. F. Osborne, A. Walsh, and A. R. Tall. 1998. 'Sterol regulatory element binding protein-1 activates the cholesteryl ester transfer protein gene in vivo but is not required for sterol up-regulation of gene expression', *J Biol Chem*, 273: 22409-14.

Correia, R. L., S. M. Oba-Shinjo, M. Uno, N. Huang, and S. K. Marie. 2011. 'Mitochondrial DNA depletion and its correlation with TFAM, TFB1M, TFB2M and POLG in human diffusely infiltrating astrocytomas', *Mitochondrion*, 11: 48-53.

Cotney, J., S. E. McKay, and G. S. Shadel. 2009. 'Elucidation of separate, but collaborative functions of the rRNA methyltransferase-related human mitochondrial transcription factors B1 and B2 in mitochondrial biogenesis reveals new insight into maternally inherited deafness', *Hum Mol Genet*, 18: 2670-82.

Cox, M. J., H. S. Sood, M. J. Hunt, D. Chandler, J. R. Henegar, G. M. Aru, and S. C. Tyagi. 2002. 'Apoptosis in the left ventricle of chronic volume overload causes endocardial endothelial dysfunction in rats', *Am J Physiol Heart Circ Physiol*, 282: H1197-205.

Cutler, M. J., X. Wan, K. R. Laurita, R. J. Hajjar, and D. S. Rosenbaum. 2009. 'Targeted SERCA2a gene expression identifies molecular mechanism and therapeutic target for arrhythmogenic cardiac alternans', *Circ Arrhythm Electrophysiol*, 2: 686-94.

Cutler, M. J., X. Wan, B. N. Plummer, H. Liu, I. Deschenes, K. R. Laurita, R. J. Hajjar, and D. S. Rosenbaum. 2012. 'Targeted sarcoplasmic reticulum Ca2+ ATPase 2a gene delivery to restore electrical stability in the failing heart', *Circulation*, 126: 2095-104.

Deocaris, C. C., S. C. Kaul, and R. Wadhwa. 2006. 'On the brotherhood of the mitochondrial chaperones mortalin and heat shock protein 60', *Cell Stress Chaperones*, 11: 116-28.

Ekstrand, M. I., M. Falkenberg, A. Rantanen, C. B. Park, M. Gaspari, K. Hultenby, P. Rustin, C. M. Gustafsson, and N. G. Larsson. 2004. 'Mitochondrial transcription factor A regulates mtDNA copy number in mammals', *Hum Mol Genet*, 13: 935-44.

Ellis, C. E., D. Naicker, K. M. Basson, C. J. Botha, R. A. Meintjes, and R. A. Schultz. 2010. 'Damage to some contractile and cytoskeleton proteins of the sarcomere in rat neonatal cardiomyocytes after exposure to pavetamine', *Toxicon*, 55: 1071-9.

Elrod, J. W., and J. D. Molkentin. 2013. 'Physiologic functions of cyclophilin D and the mitochondrial permeability transition pore', *Circ J*, 77: 1111-22.

Eltzschig, H. K., and T. Eckle. 2011. 'Ischemia and reperfusion--from mechanism to translation', *Nat Med*, 17: 1391-401.

Falkenberg, M., M. Gaspari, A. Rantanen, A. Trifunovic, N. G. Larsson, and C. M. Gustafsson. 2002. 'Mitochondrial transcription factors B1 and B2 activate transcription of human mtDNA', *Nat Genet*, 31: 289-94.

Falkenberg, M., N. G. Larsson, and C. M. Gustafsson. 2007. 'DNA replication and transcription in mammalian mitochondria', *Annu Rev Biochem*, 76: 679-99.

Fan, Dong, Abhijit Takawale, Jiwon Lee, and Zamaneh Kassiri. 2012. 'Cardiac fibroblasts, fibrosis and extracellular matrix remodeling in heart disease', *Fibrogenesis & Tissue Repair*, 5: 15-15.

Fisher, R. P., T. Lisowsky, M. A. Parisi, and D. A. Clayton. 1992. 'DNA wrapping and bending by a mitochondrial high mobility group-like transcriptional activator protein', *J Biol Chem*, 267: 3358-67.

Frati, A., B. Ricci, F. Pierucci, S. Nistri, D. Bani, and E. Meacci. 2015. 'Role of Sphingosine Kinase/S1P Axis in ECM Remodeling of Cardiac Cells Elicited by Relaxin', *Mol Endocrinol*, 29: 53-67.

Fujino, T., T. Ide, M. Yoshida, K. Onitsuka, A. Tanaka, Y. Hata, M. Nishida, T. Takehara, T. Kanemaru, N. Kitajima, S. Takazaki, H. Kurose, D. Kang, and K. Sunagawa.

2012. 'Recombinant mitochondrial transcription factor A protein inhibits nuclear factor of activated T cells signaling and attenuates pathological hypertrophy of cardiac myocytes', *Mitochondrion*, 12: 449-58.

Galvez, A. S., A. Diwan, A. M. Odley, H. S. Hahn, H. Osinska, J. G. Melendez, J. Robbins, R. A. Lynch, Y. Marreez, and G. W. Dorn, 2nd. 2007. 'Cardiomyocyte degeneration with calpain deficiency reveals a critical role in protein homeostasis', *Circ Res*, 100: 1071-8.

Garnier, A., D. Fortin, C. Delomenie, I. Momken, V. Veksler, and R. Ventura-Clapier. 2003. 'Depressed mitochondrial transcription factors and oxidative capacity in rat failing cardiac and skeletal muscles', *J Physiol*, 551: 491-501.

Giorgio, M., M. Trinei, E. Migliaccio, and P. G. Pelicci. 2007. 'Hydrogen peroxide: a metabolic by-product or a common mediator of ageing signals?', *Nat Rev Mol Cell Biol*, 8: 722-8.

Givvimani, S., C. Munjal, N. Tyagi, U. Sen, N. Metreveli, and S. C. Tyagi. 2012. 'Mitochondrial division/mitophagy inhibitor (Mdivi) ameliorates pressure overload induced heart failure', *PLoS One*, 7: e32388.

Givvimani, Srikanth, Sathnur Pushpakumar, Sudhakar Veeranki, and Suresh C. Tyagi. 2014. 'Dysregulation of Mfn2 and Drp-1 proteins in heart failure()', *Canadian journal of physiology and pharmacology*, 92: 583-91.

Givvimani, S., N. Tyagi, U. Sen, P. K. Mishra, N. Qipshidze, C. Munjal, J. C. Vacek, O. A. Abe, and S. C. Tyagi. 2010. 'MMP-2/TIMP-2/TIMP-4 versus MMP-9/TIMP-3 in transition from compensatory hypertrophy and angiogenesis to decompensatory heart failure', *Arch Physiol Biochem*, 116: 63-72.

Greenberg, B. 2015. 'Gene therapy for heart failure', *J Cardiol*, 66: 195-200.

Griffiths, E. J., D. Balaska, and W. H. Cheng. 2010. 'The ups and downs of mitochondrial calcium signalling in the heart', *Biochim Biophys Acta*, 1797: 856-64.

Gwathmey, J. K., A. Yerevanian, and R. J. Hajjar. 2013. 'Targeting sarcoplasmic reticulum calcium ATPase by gene therapy', *Hum Gene Ther*, 24: 937-47.

Hammerling, B. C., and A. B. Gustafsson. 2014. 'Mitochondrial quality control in the myocardium: cooperation between protein degradation and mitophagy', *J Mol Cell Cardiol*, 75: 122-30.

Hansen, M., S. Nyby, J. Eifer Moller, L. Videbaek, M. Kassem, T. Barington, P. Thayssen, and A. C. Diederichsen. 2014. 'Intracoronary injection of CD34-cells in chronic ischemic heart failure: 7 years follow-up of the DanCell study', *Cardiology*, 129: 69-74.

Hayashi, Y., M. Yoshida, M. Yamato, T. Ide, Z. Wu, M. Ochi-Shindou, T. Kanki, D. Kang, K. Sunagawa, H. Tsutsui, and H. Nakanishi. 2008. 'Reverse of age-dependent memory impairment and mitochondrial DNA damage in microglia by an over-expression of human mitochondrial transcription factor a in mice', *J Neurosci*, 28: 8624-34.

Hayward, C., N. R. Banner, A. Morley-Smith, A. R. Lyon, and S. E. Harding. 2015. 'The Current and Future Landscape of SERCA Gene Therapy for Heart Failure: A Clinical Perspective', *Hum Gene Ther*, 26: 293-304.

Heinis, F. I., K. B. Andersson, G. Christensen, and J. M. Metzger. 2013. 'Prominent heart organ-level performance deficits in a genetic model of targeted severe and progressive SERCA2 deficiency', *PLoS One*, 8: e79609.

Hensen, F., S. Cansiz, J. M. Gerhold, and J. N. Spelbrink. 2014. 'To be or not to be a nucleoid protein: a comparison of mass-spectrometry based approaches in the identification of potential mtDNA-nucleoid associated proteins', *Biochimie*, 100: 219-26.

Hogan, P. G., L. Chen, J. Nardone, and A. Rao. 2003. 'Transcriptional regulation by calcium, calcineurin, and NFAT', *Genes Dev*, 17: 2205-32.

Hoppel, C. L., E. J. Lesnefsky, Q. Chen, and B. Tandler. 2017. 'Mitochondrial Dysfunction in Cardiovascular Aging', *Adv Exp Med Biol*, 982: 451-64.

Hoshino, A., Y. Okawa, M. Ariyoshi, S. Kaimoto, M. Uchihashi, K. Fukai, E. Iwai-Kanai, and S. Matoba. 2014. 'Oxidative post-translational modifications develop LONP1 dysfunction in pressure overload heart failure', *Circ Heart Fail*, 7: 500-9.

Houser, S. R., and J. D. Molkentin. 2008. 'Does contractile Ca2+ control calcineurin-NFAT signaling and pathological hypertrophy in cardiac myocytes?', *Sci Signal*, 1: pe31.

Hovnanian, A. 2007. 'SERCA pumps and human diseases', *Subcell Biochem*, 45: 337-63.

Ide, T., H. Tsutsui, S. Hayashidani, D. Kang, N. Suematsu, K. Nakamura, H. Utsumi, N. Hamasaki, and A. Takeshita. 2001. 'Mitochondrial DNA damage and dysfunction associated with oxidative stress in failing hearts after myocardial infarction', *Circ Res*, 88: 529-35.

Ikeda, M., T. Ide, T. Fujino, S. Arai, K. Saku, T. Kakino, H. Tyynismaa, T. Yamasaki, K. Yamada, D. Kang, A. Suomalainen, and K. Sunagawa. 2015. 'Over-expression of TFAM or twinkle increases mtDNA copy number and facilitates cardioprotection associated with limited mitochondrial oxidative stress', *PLoS One*, 10: e0119687.

Ikeuchi, M., H. Matsusaka, D. Kang, S. Matsushima, T. Ide, T. Kubota, T. Fujiwara, N. Hamasaki, A. Takeshita, K. Sunagawa, and H. Tsutsui. 2005. 'Over-expression of mitochondrial transcription factor a ameliorates mitochondrial deficiencies and cardiac failure after myocardial infarction', *Circulation*, 112: 683-90.

Ishihara, T., R. Ban-Ishihara, M. Maeda, Y. Matsunaga, A. Ichimura, S. Kyogoku, H. Aoki, S. Katada, K. Nakada, M. Nomura, N. Mizushima, K. Mihara, and N. Ishihara. 2015. 'Dynamics of mitochondrial DNA nucleoids regulated by mitochondrial fission is essential for maintenance of homogeneously active mitochondria during neonatal heart development', *Mol Cell Biol*, 35: 211-23.

Iyer, R. P., M. Jung, and M. L. Lindsey. 2016. 'MMP-9 signaling in the left ventricle following myocardial infarction', *Am J Physiol Heart Circ Physiol*, 311: H190-8.

Jagnandan, D., J. E. Church, B. Banfi, D. J. Stuehr, M. B. Marrero, and D. J. Fulton. 2007. 'Novel mechanism of activation of NADPH oxidase 5. calcium sensitization via phosphorylation', *J Biol Chem*, 282: 6494-507.

Kanazawa, A., Y. Nishio, A. Kashiwagi, H. Inagaki, R. Kikkawa, and K. Horiike. 2002. 'Reduced activity of mtTFA decreases the transcription in mitochondria isolated from diabetic rat heart', *Am J Physiol Endocrinol Metab*, 282: E778-85.

Kang, D., S. H. Kim, and N. Hamasaki. 2007. 'Mitochondrial transcription factor A (TFAM): roles in maintenance of mtDNA and cellular functions', *Mitochondrion*, 7: 39-44.

Kao, T. Y., Y. C. Chiu, W. C. Fang, C. W. Cheng, C. Y. Kuo, H. F. Juan, S. H. Wu, and A. Y. Lee. 2015. 'Mitochondrial Lon regulates apoptosis through the association with Hsp60-mtHsp70 complex', *Cell Death Dis*, 6: e1642.

Kawaguchi, M., I. Hay, B. Fetics, and D. A. Kass. 2003. 'Combined ventricular systolic and arterial stiffening in patients with heart failure and preserved ejection fraction: implications for systolic and diastolic reserve limitations', *Circulation*, 107: 714-20.

Kienhofer, J., D. J. Haussler, F. Ruckelshausen, E. Muessig, K. Weber, D. Pimentel, V. Ullrich, A. Burkle, and M. M. Bachschmid. 2009. 'Association of mitochondrial antioxidant enzymes with mitochondrial DNA as integral nucleoid constituents', *Faseb j*, 23: 2034-44.

Kim, S. C., J. P. Stice, L. Chen, J. S. Jung, S. Gupta, Y. Wang, G. Baumgarten, J. Trial, and A. A. Knowlton. 2009. 'Extracellular heat shock protein 60, cardiac myocytes, and apoptosis', *Circ Res*, 105: 1186-95.

Kudo-Sakamoto, Y., H. Akazawa, K. Ito, J. Takano, M. Yano, C. Yabumoto, A. T. Naito, T. Oka, J. K. Lee, Y. Sakata, J. Suzuki, T. C. Saido, and I. Komuro. 2014. 'Calpain-dependent cleavage of N-cadherin is involved in the progression of post-myocardial infarction remodeling', *J Biol Chem*, 289: 19408-19.

Kukat, C., K. M. Davies, C. A. Wurm, H. Spahr, N. A. Bonekamp, I. Kuhl, F. Joos, P. L. Polosa, C. B. Park, V. Posse, M. Falkenberg, S. Jakobs, W. Kuhlbrandt, and N. G. Larsson. 2015. 'Cross-strand binding of TFAM to a single mtDNA molecule forms the mitochondrial nucleoid', *Proc Natl Acad Sci U S A*.

Kukat, Christian, Christian A. Wurm, Henrik Spåhr, Maria Falkenberg, Nils-Göran Larsson, and Stefan Jakobs. 2011. 'Super-resolution microscopy reveals that mammalian mitochondrial nucleoids have a uniform size and frequently contain a single copy of mtDNA', *Proceedings of the National Academy of Sciences of the United States of America*, 108: 13534-39.

Kunkel, G. H., P. Chaturvedi, and S. C. Tyagi. 2015a. 'Resuscitation of a dead cardiomyocyte', *Heart Fail Rev*.

———. 2015b. 'Resuscitation of a dead cardiomyocyte', *Heart Fail Rev*, 20: 709-19.

———. 2016. 'Mitochondrial pathways to cardiac recovery: TFAM', *Heart Fail Rev*, 21: 499-517.

Lamparter, S., and B. Maisch. 2000. '[Significance of matrix metalloproteinases in cardiovascular diseases]', *Z Kardiol*, 89: 949-57.

Larsson, N. G., J. Wang, H. Wilhelmsson, A. Oldfors, P. Rustin, M. Lewandoski, G. S. Barsh, and D. A. Clayton. 1998. 'Mitochondrial transcription factor A is necessary for mtDNA maintenance and embryogenesis in mice', *Nat Genet*, 18: 231-6.

Lauritzen, K. H., L. Kleppa, J. M. Aronsen, L. Eide, H. Carlsen, O. P. Haugen, I. Sjaastad, A. Klungland, L. J. Rasmussen, H. Attramadal, J. Storm-Mathisen, and L. H. Bergersen. 2015. 'Impaired dynamics and function of mitochondria caused by mtDNA toxicity leads to heart failure', *Am J Physiol Heart Circ Physiol*: ajpheart.00253.2014.

Lebrecht, D., B. Setzer, U. P. Ketelsen, J. Haberstroh, and U. A. Walker. 2003. 'Time-dependent and tissue-specific accumulation of mtDNA and respiratory chain defects in chronic doxorubicin cardiomyopathy', *Circulation*, 108: 2423-9.

Li, D., X. Li, Y. Guan, and X. Guo. 2015. 'Mitofusin-2-mediated tethering of mitochondria and endoplasmic reticulum promotes cell cycle arrest of vascular smooth muscle cells in G0/G1 phase', *Acta Biochim Biophys Sin (Shanghai)*, 47: 441-50.

Li, L., W. E. Louch, S. A. Niederer, K. B. Andersson, G. Christensen, O. M. Sejersted, and N. P. Smith. 2011. 'Calcium dynamics in the ventricular myocytes of SERCA2 knockout mice: A modeling study', *Biophys J*, 100: 322-31.

Li, X., Y. Lan, Y. Wang, M. Nie, Y. Lu, and E. Zhao. 2017. 'Telmisartan suppresses cardiac hypertrophy by inhibiting cardiomyocyte apoptosis via the NFAT/ANP/BNP signaling pathway', *Mol Med Rep*, 15: 2574-82.

Li, Y., R. Si, Y. Feng, H. H. Chen, L. Zou, E. Wang, M. Zhang, H. S. Warren, D. E. Sosnovik, and W. Chao. 2011. 'Myocardial ischemia activates an injurious innate immune signaling via cardiac heat shock protein 60 and Toll-like receptor 4', *J Biol Chem*, 286: 31308-19.

Lipskaia, L., E. R. Chemaly, L. Hadri, A. M. Lompre, and R. J. Hajjar. 2010. 'Sarcoplasmic reticulum Ca(2+) ATPase as a therapeutic target for heart failure', *Expert Opin Biol Ther*, 10: 29-41.

Lu, Y. M., J. Huang, N. Shioda, K. Fukunaga, Y. Shirasaki, X. M. Li, and F. Han. 2011. 'CaMKIIdeltaB mediates aberrant NCX1 expression and the imbalance of NCX1/SERCA in transverse aortic constriction-induced failing heart', *PLoS One*, 6: e24724.

Lyon, A. R., M. L. Bannister, T. Collins, E. Pearce, A. H. Sepehripour, S. S. Dubb, E. Garcia, P. O'Gara, L. Liang, E. Kohlbrenner, R. J. Hajjar, N. S. Peters, P. A. Poole-Wilson, K. T. Macleod, and S. E. Harding. 2011. 'SERCA2a gene transfer decreases sarcoplasmic reticulum calcium leak and reduces ventricular arrhythmias in a model of chronic heart failure', *Circ Arrhythm Electrophysiol*, 4: 362-72.

Lyonnais, S., A. Tarres-Sole, A. Rubio-Cosials, A. Cuppari, R. Brito, J. Jaumot, R. Gargallo, M. Vilaseca, C. Silva, A. Granzhan, M. P. Teulade-Fichou, R. Eritja, and M. Sola. 2017. 'The human mitochondrial transcription factor A is a versatile G-quadruplex binding protein', *Sci Rep*, 7: 43992.

Ma, B., J. Yu, C. Xie, L. Sun, S. Lin, J. Ding, J. Luo, and H. Cai. 2015. 'Toll-Like Receptors Promote Mitochondrial Translocation of Nuclear Transcription Factor Nuclear Factor of Activated T-Cells in Prolonged Microglial Activation', *J Neurosci*, 35: 10799-814.

Mandal, A., C. L. Hoop, M. DeLucia, R. Kodali, V. E. Kagan, J. Ahn, and P. C. van der Wel. 2015. 'Structural Changes and Proapoptotic Peroxidase Activity of Cardiolipin-Bound Mitochondrial Cytochrome c', *Biophys J*, 109: 1873-84.

Maranzana, E., G. Barbero, A. I. Falasca, G. Lenaz, and M. L. Genova. 2013. 'Mitochondrial respiratory supercomplex association limits production of reactive oxygen species from complex I', *Antioxid Redox Signal*, 19: 1469-80.

Marshall, K. D., M. A. Edwards, M. Krenz, J. W. Davis, and C. P. Baines. 2014. 'Proteomic mapping of proteins released during necrosis and apoptosis from cultured neonatal cardiac myocytes', *Am J Physiol Cell Physiol*, 306: C639-47.

Matsushima, Y., R. Garesse, and L. S. Kaguni. 2004. 'Drosophila mitochondrial transcription factor B2 regulates mitochondrial DNA copy number and transcription in schneider cells', *J Biol Chem*, 279: 26900-5.

Mendelsohn, A. R., and J. W. Larrick. 2014. 'Partial reversal of skeletal muscle aging by restoration of normal NAD(+) levels', *Rejuvenation Res*, 17: 62-9.

Metodiev, M. D., N. Lesko, C. B. Park, Y. Camara, Y. Shi, R. Wibom, K. Hultenby, C. M. Gustafsson, and N. G. Larsson. 2009. 'Methylation of 12S rRNA is necessary for in vivo stability of the small subunit of the mammalian mitochondrial ribosome', *Cell Metab*, 9: 386-97.

Minematsu, H., M. J. Shin, A. B. Celil Aydemir, K. O. Kim, S. A. Nizami, G. J. Chung, and F. Y. Lee. 2011. 'Nuclear presence of nuclear factor of activated T cells (NFAT) c3 and c4 is required for Toll-like receptor-activated innate inflammatory response of monocytes/macrophages', *Cell Signal*, 23: 1785-93.

Mishra, P. K., S. Givvimani, V. Chavali, and S. C. Tyagi. 2013. 'Cardiac matrix: a clue for future therapy', *Biochim Biophys Acta*, 1832: 2271-6.

Mittal, B., A. Mishra, A. Srivastava, S. Kumar, and N. Garg. 2014. 'Matrix metalloproteinases in coronary artery disease', *Adv Clin Chem*, 64: 1-72.

Morozov, Y. I., K. Agaronyan, A. C. Cheung, M. Anikin, P. Cramer, and D. Temiakov. 2014. 'A novel intermediate in transcription initiation by human mitochondrial RNA polymerase', *Nucleic Acids Res*, 42: 3884-93.

Morozov, Y. I., A. V. Parshin, K. Agaronyan, A. C. Cheung, M. Anikin, P. Cramer, and D. Temiakov. 2015. 'A model for transcription initiation in human mitochondria', *Nucleic Acids Res*, 43: 3726-35.

Moshal, K. S., N. Metreveli, I. Frank, and S. C. Tyagi. 2008. 'Mitochondrial MMP activation, dysfunction and arrhythmogenesis in hyperhomocysteinemia', *Curr Vasc Pharmacol*, 6: 84-92.

Moshal, K. S., W. E. Rodriguez, U. Sen, and S. C. Tyagi. 2008. 'Targeted deletion of MMP-9 attenuates myocardial contractile dysfunction in heart failure', *Physiol Res*, 57: 379-84.

Moshal, K. S., M. Singh, U. Sen, D. S. Rosenberger, B. Henderson, N. Tyagi, H. Zhang, and S. C. Tyagi. 2006. 'Homocysteine-mediated activation and mitochondrial translocation of calpain regulates MMP-9 in MVEC', *Am J Physiol Heart Circ Physiol*, 291: H2825-35.

Moshal, K. S., S. M. Tipparaju, T. P. Vacek, M. Kumar, M. Singh, I. E. Frank, P. K. Patibandla, N. Tyagi, J. Rai, N. Metreveli, W. E. Rodriguez, M. T. Tseng, and S. C. Tyagi. 2008. 'Mitochondrial matrix metalloproteinase activation decreases myocyte contractility in hyperhomocysteinemia', *Am J Physiol Heart Circ Physiol*, 295: H890-7.

Moshal, K. S., N. Tyagi, V. Moss, B. Henderson, M. Steed, A. Ovechkin, G. M. Aru, and S. C. Tyagi. 2005. 'Early induction of matrix metalloproteinase-9 transduces signaling in human heart end stage failure', *J Cell Mol Med*, 9: 704-13.

Mozaffarian, D., E. J. Benjamin, A. S. Go, D. K. Arnett, M. J. Blaha, M. Cushman, S. R. Das, S. de Ferranti, J. P. Despres, H. J. Fullerton, V. J. Howard, M. D. Huffman, C. R. Isasi, M. C. Jimenez, S. E. Judd, B. M. Kissela, J. H. Lichtman, L. D. Lisabeth, S. Liu, R. H. Mackey, D. J. Magid, D. K. McGuire, E. R. Mohler, 3rd, C. S. Moy, P. Muntner, M. E. Mussolino, K. Nasir, R. W. Neumar, G. Nichol, L. Palaniappan, D. K. Pandey, M. J. Reeves, C. J. Rodriguez, W. Rosamond, P. D. Sorlie, J. Stein, A. Towfighi, T. N. Turan, S. S. Virani, D. Woo, R. W. Yeh, and M. B. Turner. 2016. 'Executive Summary: Heart Disease and Stroke Statistics--2016 Update: A Report From the American Heart Association', *Circulation*, 133: 447-54.

Mujumdar, V. S., L. M. Smiley, and S. C. Tyagi. 2001. 'Activation of matrix metalloproteinase dilates and decreases cardiac tensile strength', *Int J Cardiol*, 79: 277-86.

Muller, A. L., and N. S. Dhalla. 2012. 'Role of various proteases in cardiac remodeling and progression of heart failure', *Heart Fail Rev*, 17: 395-409.

Muller, A. L., D. Freed, L. Hryshko, and N. S. Dhalla. 2012. 'Implications of protease activation in cardiac dysfunction and development of genetic cardiomyopathy in hamsters', *Can J Physiol Pharmacol*, 90: 995-1004.

Müller, AlisonL, and NaranjanS Dhalla. 2012. 'Role of various proteases in cardiac remodeling and progression of heart failure', *Heart Fail Rev*, 17: 395-409.

Murphy, Michael P. 2009. 'How mitochondria produce reactive oxygen species', *Biochemical Journal*, 417: 1-13.

Naka, K. K., P. Vezyraki, A. Kalaitzakis, S. Zerikiotis, L. Michalis, and C. Angelidis. 2014. 'Hsp70 regulates the doxorubicin-mediated heart failure in Hsp70-transgenic mice', *Cell Stress Chaperones*, 19: 853-64.

Nakayama, H., K. Otsu, O. Yamaguchi, K. Nishida, M. O. Date, K. Hongo, Y. Kusakari, T. Toyofuku, S. Hikoso, K. Kashiwase, T. Takeda, Y. Matsumura, S. Kurihara, M. Hori, and M. Tada. 2003. 'Cardiac-specific over-expression of a high Ca2+ affinity mutant of SERCA2a attenuates in vivo pressure overload cardiac hypertrophy', *Faseb j*, 17: 61-3.

Nath, R., D. Kumar, T. Li, and P. K. Singal. 2000. 'Metallothioneins, oxidative stress and the cardiovascular system', *Toxicology*, 155: 17-26.

Okamoto, T., T. Akaike, T. Sawa, Y. Miyamoto, A. van der Vliet, and H. Maeda. 2001. 'Activation of matrix metalloproteinases by peroxynitrite-induced protein S-glutathiolation via disulfide S-oxide formation', *J Biol Chem*, 276: 29596-602.

Orrenius, S., V. Gogvadze, and B. Zhivotovsky. 2015. 'Calcium and mitochondria in the regulation of cell death', *Biochem Biophys Res Commun*, 460: 72-81.

Parameswaran, S., and R. K. Sharma. 2012. 'High molecular weight calmodulin-binding protein: 20 years onwards-a potential therapeutic calpain inhibitor', *Cardiovasc Drugs Ther*, 26: 321-30.

Park, W. J., and J. G. Oh. 2013. 'SERCA2a: a prime target for modulation of cardiac contractility during heart failure', *BMB Rep*, 46: 237-43.

Patterson, Cam, Andrea Portbury, Jonathan C. Schisler, and Monte S. Willis. 2011. 'Tear me down: Role of calpain in the development of cardiac ventricular hypertrophy', *Circ Res*, 109: 453-62.

Pearson-Stuttard, J., P. Bandosz, C. D. Rehm, J. Penalvo, L. Whitsel, T. Gaziano, Z. Conrad, P. Wilde, R. Micha, F. Lloyd-Williams, S. Capewell, D. Mozaffarian, and M. O'Flaherty. 2017. 'Reducing US cardiovascular disease burden and disparities through national and targeted dietary policies: A modelling study', *PLoS Med*, 14: e1002311.

Penny, W. F., and H. K. Hammond. 2017. 'Randomized Clinical Trials of Gene Transfer for Heart Failure with Reduced Ejection Fraction', *Hum Gene Ther*, 28: 378-84.

Perrin, C., C. Vergely, and L. Rochette. 2004. '[Calpains and cardiac diseases]', *Ann Cardiol Angeiol (Paris)*, 53: 259-66.

Pillai, V. B., A. Kanwal, Y. H. Fang, W. W. Sharp, S. Samant, J. Arbiser, and M. P. Gupta. 2017. 'Honokiol, an activator of Sirtuin-3 (SIRT3) preserves mitochondria and protects the heart from doxorubicin-induced cardiomyopathy in mice', *Oncotarget*, 8: 34082-98.

Pohjoismaki, J. L., and S. Goffart. 2017. 'The role of mitochondria in cardiac development and protection', *Free Radic Biol Med*, 106: 345-54.

Polyakova, V., S. Hein, S. Kostin, T. Ziegelhoeffer, and J. Schaper. 2004. 'Matrix metalloproteinases and their tissue inhibitors in pressure-overloaded human myocardium during heart failure progression', *J Am Coll Cardiol*, 44: 1609-18.

Polyakova, V., I. Loeffler, S. Hein, S. Miyagawa, I. Piotrowska, S. Dammer, J. Risteli, J. Schaper, and S. Kostin. 2011. 'Fibrosis in endstage human heart failure: severe changes in collagen metabolism and MMP/TIMP profiles', *Int J Cardiol*, 151: 18-33.

Prasad, A. M., and G. Inesi. 2012. 'Regulation and rate limiting mechanisms of Ca2+ ATPase (SERCA2) expression in cardiac myocytes', *Mol Cell Biochem*, 361: 85-96.

Prathipati, P., N. Metreveli, S. S. Nandi, S. C. Tyagi, and P. K. Mishra. 2016. 'Ablation of Matrix Metalloproteinase-9 Prevents Cardiomyocytes Contractile Dysfunction in Diabetics', *Front Physiol*, 7: 93.

Quijada, P., N. Hariharan, J. D. Cubillo, K. M. Bala, J. M. Emathinger, B. J. Wang, L. Ormachea, D. M. Bers, M. A. Sussman, and C. Poizat. 2015. 'Nuclear Calcium/Calmodulin-dependent Protein Kinase II Signaling Enhances Cardiac Progenitor Cell Survival and Cardiac Lineage Commitment', *J Biol Chem*, 290: 25411-26.

Quiros, P. M., T. Langer, and C. Lopez-Otin. 2015. 'New roles for mitochondrial proteases in health, ageing and disease', *Nat Rev Mol Cell Biol*, 16: 345-59.

Rezende, F., O. Lowe, V. Helfinger, K. K. Prior, M. Walter, S. Zukunft, I. Fleming, N. Weissmann, R. P. Brandes, and K. Schroder. 2015. 'Unchanged NADPH Oxidase Activity in Nox1-Nox2-Nox4 Triple Knockout Mice: What Do NADPH-Stimulated Chemiluminescence Assays Really Detect?', *Antioxid Redox Signal*.

Romanic, A. M., C. L. Burns-Kurtis, B. Gout, I. Berrebi-Bertrand, and E. H. Ohlstein. 2001. 'Matrix metalloproteinase expression in cardiac myocytes following myocardial infarction in the rabbit', *Life Sci*, 68: 799-814.

Russell, L. K., C. M. Mansfield, J. J. Lehman, A. Kovacs, M. Courtois, J. E. Saffitz, D. M. Medeiros, M. L. Valencik, J. A. McDonald, and D. P. Kelly. 2004. 'Cardiac-specific induction of the transcriptional coactivator peroxisome proliferator-activated receptor gamma coactivator-1alpha promotes mitochondrial biogenesis and reversible cardiomyopathy in a developmental stage-dependent manner', *Circ Res*, 94: 525-33.

Sakata, S., D. Lebeche, Y. Sakata, N. Sakata, E. R. Chemaly, L. Liang, C. Nakajima-Takenaka, T. Tsuji, N. Konishi, F. del Monte, R. J. Hajjar, and M. Takaki. 2007. 'Transcoronary gene transfer of SERCA2a increases coronary blood flow and decreases cardiomyocyte size in a type 2 diabetic rat model', *Am J Physiol Heart Circ Physiol*, 292: H1204-7.

Santos, J. M., M. Mishra, and R. A. Kowluru. 2014. 'Posttranslational modification of mitochondrial transcription factor A in impaired mitochondria biogenesis:

implications in diabetic retinopathy and metabolic memory phenomenon', *Exp Eye Res*, 121: 168-77.

Schwarz, K., N. Siddiqi, S. Singh, C. J. Neil, D. K. Dawson, and M. P. Frenneaux. 2014. 'The breathing heart - mitochondrial respiratory chain dysfunction in cardiac disease', *Int J Cardiol*, 171: 134-43.

Sciarretta, S., D. Yee, P. Ammann, N. Nagarajan, M. Volpe, G. Frati, and J. Sadoshima. 2015. 'Role of NADPH oxidase in the regulation of autophagy in cardiomyocytes', *Clin Sci (Lond)*, 128: 387-403.

Seidel-Rogol, B. L., V. McCulloch, and G. S. Shadel. 2003. 'Human mitochondrial transcription factor B1 methylates ribosomal RNA at a conserved stem-loop', *Nat Genet*, 33: 23-4.

Shintani-Ishida, K., and K. Yoshida. 2015. 'Mitochondrial m-calpain opens the mitochondrial permeability transition pore in ischemia-reperfusion', *Int J Cardiol*, 197: 26-32.

Shrout, T., D. W. Rudy, and M. T. Piascik. 2017. 'Hypertension update, JNC8 and beyond', *Curr Opin Pharmacol*, 33: 41-46.

Sikkel, M. B., C. Hayward, K. T. MacLeod, S. E. Harding, and A. R. Lyon. 2014. 'SERCA2a gene therapy in heart failure: an anti-arrhythmic positive inotrope', *Br J Pharmacol*, 171: 38-54.

Singh, R. B., S. P. Dandekar, V. Elimban, S. K. Gupta, and N. S. Dhalla. 2004. 'Role of proteases in the pathophysiology of cardiac disease', *Mol Cell Biochem*, 263: 241-56.

Siwik, D. A., P. J. Pagano, and W. S. Colucci. 2001. 'Oxidative stress regulates collagen synthesis and matrix metalloproteinase activity in cardiac fibroblasts', *Am J Physiol Cell Physiol*, 280: C53-60.

Siwik, D. A., J. D. Tzortzis, D. R. Pimental, D. L. Chang, P. J. Pagano, K. Singh, D. B. Sawyer, and W. S. Colucci. 1999. 'Inhibition of copper-zinc superoxide dismutase induces cell growth, hypertrophic phenotype, and apoptosis in neonatal rat cardiac myocytes in vitro', *Circ Res*, 85: 147-53.

Smith, M. A., and R. G. Schnellmann. 2012a. 'Calpains, mitochondria, and apoptosis', *Cardiovasc Res*, 96: 32-7.

———. 2012b. 'Mitochondrial calpain 10 is degraded by Lon protease after oxidant injury', *Arch Biochem Biophys*, 517: 144-52.

Song, K., Y. J. Nam, X. Luo, X. Qi, W. Tan, G. N. Huang, A. Acharya, C. L. Smith, M. D. Tallquist, E. G. Neilson, J. A. Hill, R. Bassel-Duby, and E. N. Olson. 2012. 'Heart repair by reprogramming non-myocytes with cardiac transcription factors', *Nature*, 485: 599-604.

Sonobe, T., T. Akiyama, C. K. Du, D. Y. Zhan, and M. Shirai. 2014. 'Contribution of calpain to myoglobin efflux from cardiomyocytes during ischaemia and after reperfusion in anaesthetized rats', *Acta Physiol (Oxf)*, 210: 823-31.

Sorescu, D., and K. K. Griendling. 2002. 'Reactive oxygen species, mitochondria, and NAD(P)H oxidases in the development and progression of heart failure', *Congest Heart Fail*, 8: 132-40.

Spinale, F. G., M. L. Coker, C. V. Thomas, J. D. Walker, R. Mukherjee, and L. Hebbar. 1998. 'Time-dependent changes in matrix metalloproteinase activity and expression during the progression of congestive heart failure: relation to ventricular and myocyte function', *Circ Res*, 82: 482-95.

Sreekumar, P. G., K. Ishikawa, C. Spee, H. H. Mehta, J. Wan, K. Yen, P. Cohen, R. Kannan, and D. R. Hinton. 2016. 'The Mitochondrial-Derived Peptide Humanin Protects RPE Cells From Oxidative Stress, Senescence, and Mitochondrial Dysfunction', *Invest Ophthalmol Vis Sci*, 57: 1238-53.

St John, J. C., A. Amaral, E. Bowles, J. F. Oliveira, R. Lloyd, M. Freitas, H. L. Gray, C. S. Navara, G. Oliveira, G. P. Schatten, E. Spikings, and J. Ramalho-Santos. 2006. 'The analysis of mitochondria and mitochondrial DNA in human embryonic stem cells', *Methods Mol Biol*, 331: 347-74.

Stammers, A. N., S. E. Susser, N. C. Hamm, M. W. Hlynsky, D. E. Kimber, D. S. Kehler, and T. A. Duhamel. 2015. 'The regulation of sarco(endo)plasmic reticulum calcium-ATPases (SERCA)', *Can J Physiol Pharmacol*, 93: 843-54.

Stokke, M. K., S. J. Briston, G. F. Jolle, I. Manzoor, W. E. Louch, L. Oyehaug, G. Christensen, D. A. Eisner, A. W. Trafford, O. M. Sejersted, and I. Sjaastad. 2011. 'Ca(2+) wave probability is determined by the balance between SERCA2-dependent Ca(2+) reuptake and threshold SR Ca(2+) content', *Cardiovasc Res*, 90: 503-12.

Stokke, M. K., K. Hougen, I. Sjaastad, W. E. Louch, S. J. Briston, U. H. Enger, K. B. Andersson, G. Christensen, D. A. Eisner, O. M. Sejersted, and A. W. Trafford. 2010. 'Reduced SERCA2 abundance decreases the propensity for Ca2+ wave development in ventricular myocytes', *Cardiovasc Res*, 86: 63-71.

Surovtseva, Y. V., and G. S. Shadel. 2013. 'Transcription-independent role for human mitochondrial RNA polymerase in mitochondrial ribosome biogenesis', *Nucleic Acids Res*, 41: 2479-88.

Suzuki, K., S. Hata, Y. Kawabata, and H. Sorimachi. 2004a. 'Structure, activation, and biology of calpain', *Diabetes*, 53 Suppl 1: S12-8.

Suzuki, Koichi, Shoji Hata, Yukiko Kawabata, and Hiroyuki Sorimachi. 2004b. 'Structure, Activation, and Biology of Calpain', *Diabetes*, 53: S12-S18.

Swift, F., C. Franzini-Armstrong, L. Oyehaug, U. H. Enger, K. B. Andersson, G. Christensen, O. M. Sejersted, and W. E. Louch. 2012. 'Extreme sarcoplasmic reticulum volume loss and compensatory T-tubule remodeling after SERCA2 knockout', *Proc Natl Acad Sci U S A*, 109: 3997-4001.

Takahashi, M., K. Tanonaka, H. Yoshida, M. Koshimizu, T. Daicho, R. Oikawa, and S. Takeo. 2006. 'Possible involvement of calpain activation in pathogenesis of chronic

heart failure after acute myocardial infarction', *J Cardiovasc Pharmacol*, 47: 413-21.

Takahashi, M., K. Tanonaka, H. Yoshida, M. Koshimizu, R. Oikawa, T. Daicho, and S. Takeo. 2005. 'Effects of angiotensin I-converting enzyme inhibitor and angiotensin II type 1 receptor blocker on the right ventricular sarcoglycans and dystrophin after left coronary artery ligation', *Eur J Pharmacol*, 522: 84-93.

Takaoka, H., G. Esposito, L. Mao, H. Suga, and H. A. Rockman. 2002. 'Heart size-independent analysis of myocardial function in murine pressure overload hypertrophy', *Am J Physiol Heart Circ Physiol*, 282: H2190-7.

Taneike, M., I. Mizote, T. Morita, T. Watanabe, S. Hikoso, O. Yamaguchi, T. Takeda, T. Oka, T. Tamai, J. Oyabu, T. Murakawa, H. Nakayama, K. Nishida, J. Takeda, N. Mochizuki, I. Komuro, and K. Otsu. 2011. 'Calpain protects the heart from hemodynamic stress', *J Biol Chem*, 286: 32170-7.

Thomas, R. R., S. M. Khan, R. M. Smigrodzki, I. G. Onyango, J. Dennis, O. M. Khan, F. R. Portelli, and J. P. Bennett, Jr. 2012. 'RhTFAM treatment stimulates mitochondrial oxidative metabolism and improves memory in aged mice', *Aging (Albany NY)*, 4: 620-35.

Tyagi, S. C. 1998. 'Dynamic role of extracellular matrix metalloproteinases in heart failure', *Cardiovasc Pathol*, 7: 153-9.

Undrovinas, A., V. A. Maltsev, and H. N. Sabbah. 2013. 'Calpain inhibition reduces amplitude and accelerates decay of the late sodium current in ventricular myocytes from dogs with chronic heart failure', *PLoS One*, 8: e54436.

Urmaliya, V., and G. Franchelli. 2017. 'A multidimensional sight on cardiac failure: uncovered from structural to molecular level', *Heart Fail Rev*, 22: 357-70.

Val-Blasco, A., M. J. Piedras, G. Ruiz-Hurtado, N. Suarez, P. Prieto, S. Gonzalez-Ramos, N. Gomez-Hurtado, C. Delgado, L. Pereira, G. Benito, C. Zaragoza, N. Domenech, M. G. Crespo-Leiro, D. Vasquez-Echeverri, G. Nunez, E. Lopez-Collazo, L. Bosca, and M. Fernandez-Velasco. 2017. 'Role of NOD1 in Heart Failure Progression via Regulation of Ca2+ Handling', *J Am Coll Cardiol*, 69: 423-33.

Vandewalle, A., E. Tourneur, M. Bens, C. Chassin, and C. Werts. 2014. 'Calcineurin/NFAT signaling and innate host defence: a role for NOD1-mediated phagocytic functions', *Cell Commun Signal*, 12: 8.

Veeraveedu, P. T., S. Sanada, K. Okuda, H. Y. Fu, T. Matsuzaki, R. Araki, M. Yamato, K. Yasuda, Y. Sakata, T. Yoshimoto, and T. Minamino. 2017. 'Ablation of IL-33 gene exacerbate myocardial remodeling in mice with heart failure induced by mechanical stress', *Biochem Pharmacol*, 138: 73-80.

Vega, R. B., J. L. Horton, and D. P. Kelly. 2015. 'Maintaining ancient organelles: mitochondrial biogenesis and maturation', *Circ Res*, 116: 1820-34.

Virbasius, J. V., and R. C. Scarpulla. 1994. 'Activation of the human mitochondrial transcription factor A gene by nuclear respiratory factors: a potential regulatory link

between nuclear and mitochondrial gene expression' in organelle biogenesis', *Proc Natl Acad Sci U S A*, 91: 1309-13.

Vu, T. H., and Z. Werb. 2000. 'Matrix metalloproteinases: effectors of development and normal physiology', *Genes Dev*, 14: 2123-33.

Wang, J. C., Y. Zhao, X. D. Li, N. N. Zhou, H. Sun, and Y. Y. Sun. 2012. 'Proteolysis by endogenous calpain I leads to the activation of calcineurin in human heart', *Clin Lab*, 58: 1145-52.

Wang, J., Q. Wang, L. J. Watson, S. P. Jones, and P. N. Epstein. 2011. 'Cardiac over-expression of 8-oxoguanine DNA glycosylase 1 protects mitochondrial DNA and reduces cardiac fibrosis following transaortic constriction', *Am J Physiol Heart Circ Physiol*, 301: H2073-80.

Wang, J., H. Wilhelmsson, C. Graff, H. Li, A. Oldfors, P. Rustin, J. C. Bruning, C. R. Kahn, D. A. Clayton, G. S. Barsh, P. Thoren, and N. G. Larsson. 1999. 'Dilated cardiomyopathy and atrioventricular conduction blocks induced by heart-specific inactivation of mitochondrial DNA gene expression', *Nat Genet*, 21: 133-7.

Wanichawan, Pi   mthanya, Tandekile Lubelwana Hafver, Kjetil Hodne, Jan Magnus Aronsen, Ida Gjervold Lunde, Bjørn Dalhus, Marianne Lunde, Heidi Kvaløy, William Edward Louch, Theis Tønnessen, Ivar Sjaastad, Ole Mathias Sejersted, and Cathrine Rein Carlson. 2014. 'Molecular Basis of Calpain Cleavage and Inactivation of the Sodium-Calcium Exchanger 1 in Heart Failure', *J Biol Chem*, 289: 33984-98.

Watanabe, A., M. Arai, N. Koitabashi, K. Niwano, Y. Ohyama, Y. Yamada, N. Kato, and M. Kurabayashi. 2011. 'Mitochondrial transcription factors TFAM and TFB2M regulate Serca2 gene transcription', *Cardiovasc Res*, 90: 57-67.

Weber, K. T., Y. Sun, S. C. Tyagi, and J. P. Cleutjens. 1994. 'Collagen network of the myocardium: function, structural remodeling and regulatory mechanisms', *J Mol Cell Cardiol*, 26: 279-92.

Wei, C. C., Y. Chen, L. C. Powell, J. Zheng, K. Shi, W. E. Bradley, P. C. Powell, S. Ahmad, C. M. Ferrario, and L. J. Dell'Italia. 2012. 'Cardiac kallikrein-kinin system is up-regulated in chronic volume overload and mediates an inflammatory induced collagen loss', *PLoS One*, 7: e40110.

Wei, M., Z. Li, L. Xiao, and Z. Yang. 2015. 'Effects of ROS-relative NF-kappaB signaling on high glucose-induced TLR4 and MCP-1 expression in podocyte injury', *Mol Immunol*.

Williams, C. R., and J. L. Gooch. 2014. 'Calcineurin Abeta regulates NADPH oxidase (Nox) expression and activity via nuclear factor of activated T cells (NFAT) in response to high glucose', *J Biol Chem*, 289: 4896-905.

Xin, W., X. Li, X. Lu, K. Niu, and J. Cai. 2011. 'Improved cardiac function after sarcoplasmic reticulum Ca(2+)-ATPase gene transfer in a heart failure model induced by chronic myocardial ischaemia', *Acta Cardiol*, 66: 57-64.

Xu, S., M. Zhong, L. Zhang, Y. Wang, Z. Zhou, Y. Hao, W. Zhang, X. Yang, A. Wei, L. Pei, and Z. Yu. 2009. 'Over-expression of TFAM protects mitochondria against beta-amyloid-induced oxidative damage in SH-SY5Y cells', *Febs j*, 276: 3800-9.

Yang, D., S. Ma, Y. Tan, D. Li, B. Tang, X. Zhang, M. Sun, and Y. Yang. 2010. 'Increased expression of calpain and elevated activity of calcineurin in the myocardium of patients with congestive heart failure', *Int J Mol Med*, 26: 159-64.

Yue, R., X. Xia, J. Jiang, D. Yang, Y. Han, X. Chen, Y. Cai, L. Li, W. E. Wang, and C. Zeng. 2015. 'Mitochondrial DNA Oxidative Damage Contributes to Cardiomyocyte Ischemia/Reperfusion-Injury in Rats: Cardioprotective Role of Lycopene', *J Cell Physiol*.

Yoshino, M., A. Naka, Y. Sakamoto, A. Shibasaki, M. Toh, S. Tsukamoto, K. Kondo, and K. Iida. 2015. 'Dietary isoflavone daidzein promotes Tfam expression that increases mitochondrial biogenesis in C2C12 muscle cells', *J Nutr Biochem*, 26: 1193-9.

Zhao, M., H. Guo, J. Chen, M. Fujino, H. Ito, K. Takahashi, F. Abe, M. Nakajima, T. Tanaka, J. Wang, H. Huang, S. Zheng, M. Hei, J. Li, S. Huang, J. Li, X. Ma, Y. Chen, L. Zhao, J. Zhuang, P. Zhu, and X. K. Li. 2015. '5-aminolevulinic acid combined with sodium ferrous citrate ameliorates H2O2-induced cardiomyocyte hypertrophy via activation of the MAPK/Nrf2/HO-1 pathway', *Am J Physiol Cell Physiol*, 308: C665-72.

Zsebo, K., A. Yaroshinsky, J. J. Rudy, K. Wagner, B. Greenberg, M. Jessup, and R. J. Hajjar. 2014. 'Long-term effects of AAV1/SERCA2a gene transfer in patients with severe heart failure: analysis of recurrent cardiovascular events and mortality', *Circ Res*, 114: 101-8.

CURRICULUM VITAE

George H. Kunkel, MS

Ph.D. Candidate /NIH Fellow
Suresh C. Tyagi Laboratory
University of Louisville, School of Medicine
Department of Physiology
(502) 996-1707 / ghkunk01@louisville.edu

EDUCATION

University of Louisville School of Medicine
Department of Physiology
Ph.D. Physiology
Expected Graduation date: August 2017

University of Louisville School of Medicine
Department of Physiology
M.S. Physiology & Biophysics
Graduated: May 2016

St. John's University
Department of Biology
B.S. Biology (Cum Laude); Physics Minor
Graduated: May 2014

RESEARCH EXPERIENCE

University of Louisville, Louisville KY
Department of Physiology

Suresh C. Tyagi Cardiovascular Remodeling Laboratory
National Institute of Health, Ruth L. Kirschstein Pre-doctoral Research Fellow
Grant #: 1F31HL132527-01

Mentor: Suresh C. Tyagi, Ph.D.
Ph.D. Candidate/NIH Fellow
(July 2016-Present)

Project: TFAM's Protective Role in Cardiomyocyte Stability

- o *In Vitro* Aims:
- Focus: Investigating Mitochondrial Transcription Factor A (TFAM) role in Cardiomyocyte stability. Assessed via lipofectamine transfection of TFAM over-expression vector and CRISPR-cas9 TFAM knockdown vector in HL-1 cardiomyocytes. Molecular analysis of TFAM, NFAT, SERCA2a, Lon protease, Calpain 1, and MMP 9 followed.
- **Kunkel GH**, Theilen N, Nair R, Tyagi SC "Mechanisms of TFAM Mediated Cardiomyocyte Protection" Can J Physiol Pharmocol. (July 2017)
- **Kunkel GH**, Chaturvedi P, Tyagi SC. 2016 "Mitochondrial Pathways to Cardiac Recovery: TFAM" Heart Fail Rev (June 2016)

    o *In Vivo* Aims:
- Focus: Investigating the effects of heart failure surgery model "Aortic Banding" (TAC) on TFAM transgenic mice (TFAM-TG).
- Mastered thoracic surgical procedure TAC in mice.
- UofL/Kleinert Surgery Institute Microsurgery Certificate (May 2017)
- Analyzing cardiovascular effects of the surgical procedure on mouse models via assays: Echocardiography, heart rate (HR), blood pressure, histology and immunohistochemistry (IHC).

Ph.D. Student/IPIBS Fellow
(August 2014 – June 2016)
- Focus: Interaction of Calpains and Matrix-metalloproteinases (MMP's) in cardiomyopathies utilizing mitochondrial interventions.
- Published two review articles focused on cardiomyocyte protease activity
- Present annually at two conferences; national conference (Experimental Biology Conference), regional conference (American Physiological Society – Kentucky Chapter Meeting)
- Investigate the relationship between calpain and matrix metalloproteinase activity and Ca^{2+} mishandling/ROS production in cardiomyopathies
- Analysis of protein and RNA content via isolation methods from cardiomyocytes
- Practicing ex-vivo cardiomyocyte isolation from cardiac tissue

St. John's University, Queens NY
Department of Biology
(January 2012- May 2014)

Irvin N. Hirshfield Laboratory
Undergraduate Student Researcher
Mentor: Irvin N. Hirshfield, Ph.D.
- Focus: Antibiotic treatment of Polymixin B to E.coli mutant IH9 (resistant to acid and hydrogen peroxide)
- Analyzed growth and antibiotic treatment resistance of E.coli small colony variants IH3 & IH9
- Tested for membrane permeability of E.coli mutants (IH3 & IH9)
- Three unpublished research articles for undergraduate research credit (15 page min.)

Baylor College of Medicine Houston, TX
Division of Thrombosis Research
(Summer 2013)

Miguel A. Cruz Laboratory
SMART Summer Student Researcher
Mentor: Miguel Cruz, Ph.D.
- Biochemical studies focused on mapping the binding site of Vimentin to the Von Willenbrand Factor (VWF)
- Conducted Thrombosis research on the functional aspects of VWF binding platelets upon vimentin interaction with A2 domain
- Analyzed Vimentin/VWF interaction via ELISA assays and Western Blotting
- Oral presentation at Baylor College of Medicine Summer Symposium
- Unpublished research article (McNair Scholars requirement, 20 pages)

SCIENTIFIC PUBLICATIONS
- **Kunkel GH**, Theilen N, Nair R, Tyagi SC "Mechanisms of TFAM Mediated Cardiomyocyte Protection" Can J Physiol (July 2017)
- Familtseva A, Jeremic N, **Kunkel GH**, Tyagi SC. 2016 "Folate and Methionine Cycle in the epigenome of hyertension via TOLL- Like Receptor 4" Am J Physiol (April 2017)
- Theilen N, **Kunkel GH**, Tyagi SC "The Role of Exercise and TFAM in Skeletal Muscle Atrophy" 2016 J Cell Physiol. (Dec. 2016)
- Familtseva A, Chaturvedi P, Kalani A, Jeremic N, Metreveli N, **Kunkel GH**, Tyagi SC. 2016 "Toll-like Receptor 4 Mutation Suppresses Hyperhomocysteinemia- Induced Hypertension" Am J Physiol Cell Physiol AJP (Aug 2016)
- **Kunkel GH**, Chaturvedi P, Tyagi SC. 2016 "Mitochondrial Pathways to Cardiac Recovery: TFAM" Heart Fail Rev (May 2016)
- **Kunkel GH**, Chaturvedi P, Tyagi SC. 2015 "Resuscitation of a Dead Cardiomyocyte" Heart Fail Rev (Nov 2015)
- **Kunkel GH**, Chaturvedi P, Tyagi SC. 2015. "Epigenetic Revival of a Dead Cardiomyocyte through mitochondrial interventions" BioMol Concepts (Aug 2015)
- Chaturvedi P, **Kunkel GH,** Familsteva A, Tyagi SC. 2016 "Exercise mitigates calpain 1 induced cardiac dysfunction through PCP-4 in diabetes role" Mol Cell Biochem (In Press)

ABSTRACTS & POSTERS
- Experimental Biology Conference (2015, 2016)
- American Physiological Society-Kentucky Chapter Meeting (2015,2016)
- Research Louisville (2015)
- SACNAS Conference (2015, 2016)
- International Academy of Cardiovascular Sciences – Young Investigators Forum (2015)
- American Physiological Society – Kentucky Chapter Meeting (2015)
- Baylor College of Medicine "SMART" summer program (2013)

ORAL PRESENTATIONS
- Invited Speaker: American Physiological Society-KY Chapter Cardiovascular Scientific Meeting (2017)
- Invited Speaker: St. John's University Biology Department Research Seminar (2015)
- STJ Biology Honor Society (2013 & 2014)
- McNair Scholars National Research Conference (2014)

GRANTS
- Graduate Student SACNAS Travel Scholarship (October 2016)
- Ruth L. Kirschstein NIH Pre-doctoral Fellowship (July 2016-present)
- IPIBS Graduate Research Fellowship (August 2014 – June 2016)
- UofL, School of Med. IPIBS Travel Grant for SACNAS conference (2015)
- UofL, Dpt. Physiology & Biophysics Travel Grant for EB conference (2015, 2016)
- Graduate Student Council Travel Grant (2015, 2016)
- McNair Scholars Stipend for Summer Research (2013)
- NIH – NHLBI for Baylor College of Medicine Summer Research (2013)

AWARDS & MEMBERSHIP
- Experimental Biology Travel Award (2017)

- APS-KY Scientific Meeting Awarded "Meritorious Graduate Student Oral Presentation Award" at Western Kentucky University (2017)
- Acknowledged in "Trainee Spotlight" on UofL School of Medicine website http://louisville.edu/medicine/grad-postdoc (June 2016-October 2016)
- Appointed Graduate Student Officer on UofL School of Medicine Diversity Committee (2016 – present)
- Co-founder/Vice President: UofL SACNAS Chapter (Graduate Organization) (2015 – present)
- St. John's University (STJ) Biology Gold Key Honorable Mention (2014)
- Member of American Physiological Society (2014 – present)
- McNair Scholars Research Program (2012 – 2014)
- Member of American Society of Microbiology (2013)
- Founder/President of St. John's U. Chapter of Phi Sigma National Biological Sciences Honor Society (2013)
- Founder: Glen Oaks Volunteer Ambulance Corp. (GOVAC) - STJ Biology Honor Society (BHS) Emergency Medical Technician connection program (2013)
- Founder: Tutoring Affiliation between BHS and Biology & Chemistry departments (2013)
- Inducted Member of Sigma Pi Sigma National Physics Honor Society (2012)
- Member of STJ Society of Physics Students (2011)
- Deans List recipient (2011 – 2014)
- St. John's University Academic Scholarship (2010)
- Vincent O'Connor Leadership Award (2009)
- St. Francis Preparatory High School Leadership Scholarship (2009 – 2010)
- St. Francis Preparatory High School Academic Scholarship (2006 – 2010)

SKILLS
- Radnoti Perfusion: Cardiomyocyte Isolation
- RNA & Protein Isolation
- Western Blotting
- PCR
- Cell Culture
- Ultrasound/Echocardiography
- Surgical Techniques (Mouse & Rat Model)
- UofL/Kleinert Surgery Institute Microsurgery Certificate (May 2017)
- Nationally Certified EKG Technician (2011 – 2015)
- Nationally Certified Phlebotomist (2011 – 2015)
- New York State Certified Emergency Medical Technician (EMT) (2010 –present)
- CPR/First Aid Instructor (2011 – 2012)

MENTORED STUDENTS
- Nicholas Theilen, M.S. (PhD Student)
- Rohit Nair (MS Student): Graduated August 2016
- Christopher Kunkel, B.S. (Summer Student – 2017)

EXTRACURRICULAR ACTIVITIES
- UofL Graduate School (IPIBS) Recruiter (2015-present)
- Member of Black Knights Men's Hockey Team (2016-present)
- EMT – Glen Oaks Volunteer Ambulance Corp. (2011 - 2014)
- Founded/Managed (BHS) Hayden Nichols Fundraiser (2014)
- Team leader for Breast Cancer Walk Team STJ – BHS (2014)

- Interviewer for GOVAC – BHS connection program (2013)
- Director BHS tutoring (2013)
- Tutor: General & Organic Chemistry (2013 – 2014)
- Emergency Center Assistant (Texas Children's Hospital) (2013)
- Phlebotomy Teachers Assistant, Queens borough community College (2/2011 – 8/2011)
- CPR & First Aid Instructor, St. Francis Prep. (9/2010 – 5/2011)
- Volunteer, Little Neck Nursing Home (2007 – 2009)

LITERARY PUBLICATIONS

- Kunkel, G. H., & Ozuna, H. (2017, January 2). Graduate Students Attend SACNAS Conference. *UofL Diversity Newsletter*.